

Investigation on New Tertiary *P*-Chirogenic Di(triaryl phosphines)

Dissertation

zur

Erlangung des akademischen Grades
doctor rerum naturalium (Dr. rer. nat.)
am Leibniz-Institut für Katalyse
der Mathematisch-Naturwissenschaftlichen Fakultät
der Universität Rostock

vorgelegt von

M. Sc. Katharina Rumpel, geb. am 23.06.1992 in Perleberg
aus Dessau-Roßlau

Dessau-Roßlau, 17.11.2018



Dieses Werk ist lizenziert unter einer
Creative Commons Namensnennung - Nicht kommerziell - Keine Bearbeitungen 4.0
International Lizenz.

Gutachter:

Prof. Dr. Armin Börner, Leibniz-Institut für Katalyse, Universität Rostock

Prof. Dr. Sylvain Jugé, Université de Bourgogne-Franche-Comté, ICMUB Institut de Chimie
Moléculaire

Jahr der Einreichung: 2018

Jahr der Verteidigung: 2019

Danksagung

An dieser Stelle möchte ich mich herzlich bei allen bedanken, ohne die die Fertigstellung dieser Arbeit nicht möglich gewesen wäre.

Mein besonderer Dank gilt Prof. Armin Börner, der mich nicht nur herzlich in seinem Arbeitskreis aufgenommen und mir ein spannendes Themengebiet für die Promotion aufgezeigt hat, sondern mir auch ein sorgsamer Doktorvater war, der stets ein offenes Ohr für Fragen und Probleme hatte.

Ein herzlicher Dank gilt meinem Themenleiter Dr. Jens Holz und meiner lieben Kollegen Gudrun Wenzel, die mir sowohl bei fachlichen Problemen als auch im Labor immer mit Rat und Tat zur Seite standen. Beide sorgten immer für eine herzliche und entspannte Arbeitsatmosphäre, in der ich mich sehr wohl gefühlt habe.

J'adresse mes plus sincères remerciements au Pr. Sylvain Jugé qui m'a accueillie dans son groupe de travail pour trois mois. Merci beaucoup pour le soutien dans toutes les démarches administratives et aussi pour les excursions géniales qui m'ont permis de découvrir la belle Bourgogne.

Gleichfalls gebührt mein Dank den technischen Mitarbeitern des Leibniz-Instituts für Katalyse für die Anfertigung der analytischen Daten. Besonders bedanken möchte ich mich für die Unterstützung von Dr. Anke Spannenberg, Dr. Christine Fischer, Dr. Dirk Michalik und Dr. Wolfgang Baumann für Hilfestellungen bei der Problemlösung hinsichtlich Röntgenstrukturanalyse, Massenspektrometrie beziehungsweise NMR-Spektroskopie.

Herzlich bedanken möchte ich mich auch bei meinen Eltern und Großeltern für die liebevolle Unterstützung sowohl finanziell als auch mit aufmunternden Worten und Gesten. Durch euch habe ich den Optimismus nie verloren und konnte schwierige Zeiten schnell hinter mir lassen.

Abschließend möchte ich mich bei Dr. David Kuhrt für die Kraft, den Beistand und die Liebe in beschwerlichen Zeiten bedanken. Auch bei starkem Seegang bist du mein Fels in der Brandung und passt auf, dass ich nicht untergehe. Danke.

Contents

List of Figures	5
List of Schemes	6
List of Tables	8
1. Introduction	9
1.1 Tertiary Phosphines in Asymmetric Catalysis	10
1.2 Steric and Electronic Effects of Tertiary Phosphine Ligands	11
1.3 Tertiary Phosphine Ligands with Asymmetric Phosphorus.....	14
1.3.1 Inversion Barrier of Tertiary Phosphines	14
1.3.2 Synthesis of Tertiary <i>P</i> -Chirogenic Phosphines.....	16
1.3.3 Chiral Biaryl Backbones	32
2. Investigation of <i>P</i> -Chirogenic Di(triaryl phosphines).....	39
2.1 Aim of the investigations.....	40
2.2 Results and Discussion	43
2.2.1 Synthesis of <i>P</i> -Chirogenic Triaryl phosphines with a DPE-Backbone.....	43
2.2.2 Asymmetric Catalysis with DPEphos ligands.....	47
2.2.3 Synthesis of <i>P</i> -Chirogenic Triarylphosphines with a DBFphos-Backbone	53
2.2.4 Asymmetric Catalysis with DBFphos Ligands	54
2.2.5 Investigation on the Epimerisation Behaviour of <i>P</i> -Chirogenic Di(triaryl phosphines).....	58
2.3 Conclusion	74
3. Synthesis of <i>P</i> -Chirogenic Di(triaryl phosphines) with Additional Axial Chirality	76
3.1 Aim of the investigations.....	77
3.2 Results and Discussion	78
3.3 Conclusion	93
4. Experimental Data	94
4.1 General Information	i
4.2 Synthesis and Analytic Data	iii
5. Abbreviations.....	xxxvi
Word abbreviations	xxxvi
Chemicals and Elements	xxxvi
Units and Symbols	xxxvii
6. References	xxxix

List of Figures

Figure 1: Tolman's cone angle Θ model (left) and natural bite angle β model (right).	12
Figure 2: Coordination modes of Rh(I)-alkene-hydride complexes.	13
Figure 3: Inversion of phosphines via a planar transition state.	14
Figure 4: Chiral auxiliaries used for resolution of racemic phosphines.	20
Figure 5: Common ferrocenyl phosphines.	31
Figure 6: Common "privileged ligands".	40
Figure 7: Common chelating triaryl phosphines.	41
Figure 8: <i>P</i> -chirogenic Xantphos derivatives.	43
Figure 9: Molecular structure of $\text{Pd}_2(\mu_2\text{-Cl})_2(\mu_2\text{-77a})$ -complex in the solid state.	57
Figure 10: Geminally diaurated aryl bridged by a dibenzofuran backbone 79 and DBFphos-chelated copper iodide nanocluster 80.	58
Figure 11: Epimerization of (1 <i>S</i> ,1' <i>S</i>)-(2,7-di- <i>t</i> -butyl-9,9-dimethyl-9H-xanthene-4,5-diyl)di((2-ethoxy)-phenyl phosphine) (66a).	62
Figure 12: ^{31}P NMR Spectra of 66a (CDCl_3) recorded at different temperatures (Table 10).	64
Figure 13: ^1H NMR spectra of 66a (CDCl_3) recorded at different temperatures (Table 10).	65
Figure 14: ^1H NMR of 68a' (CDCl_3).	67
Figure 15: Temperature ^{31}P NMR study of 68a' (CDCl_3).	67
Figure 16: Plausible coordination modes of borane to 60a.	69
Figure 17: ^{31}P NMR spectra (CDCl_3) of 68a and 68a' after thermal treatment (55 °C).	71
Figure 18: ^{31}P NMR spectra (CDCl_3) of 77a and 77a' after thermal treatment (50 °C).	72
Figure 19: Reaction of (1 <i>S</i> ,1' <i>S</i>)-(9,9-dimethyl-9H-xanthene-4,5-diyl)di(arylphenyl phosphine) (65) with BH_3 .	73
Figure 20: Products after the reaction of 16d with 2,2'-dilithiated binaphthyl.	79
Figure 21: Comparison of ^{13}C NMR spectra of 87a and 87a' (CDCl_3).	82
Figure 22: ^{13}C NMR (CDCl_3) of 87b,c.	83
Figure 23: ^{31}P NMR spectrum (CDCl_3) of the raw product of the synthesis of (<i>R</i>)-(1-iodonaphthalen-1-yl)(2-methoxyphenyl)-(phenyl)phosphine borane (96).	86
Figure 24: Molecular structure of the "wrong" isomer 100b in the solid state.	87
Figure 25: Molecular structure of 101 in the solid state.	88
Figure 26: ^{31}P NMR spectrum (CDCl_3) of the raw product (red) after reduction of 101 with PMHS and $\text{Ti}(\text{O}i\text{Pr})_4$.	92

List of Schemes

Scheme 1: Rh-catalysed asymmetric hydrogenation of α -phenyl acrylic acid developed by Knowles.	10
Scheme 2: Asymmetric hydrogenation of an unsaturated prochiral amino acid by Dang and Kagan using (<i>S,S</i>)-DIOP as chiral ligand.	10
Scheme 3: Resolution of the racemic mixture of ethylmethylphenylphosphine oxide by Meisenheimer and Lichtenstadt in 1911.	18
Scheme 4: Resolution of racemic <i>t</i> butylphenylphosphinous acid (4) with enantiopure ephedrine and cinchonine.	19
Scheme 5: Stereoselective synthesis of <i>P</i> -chirogenic phosphines by using (-)-menthol as chiral auxiliary suggested by Mislow and Cram.	20
Scheme 6: Synthesis of CAMP, PAMP and DIPAMP by Knowles.	21
Scheme 7: Resolution of racemates with help of transition metal complexes.	22
Scheme 8: Dynamic resolution of secondary phosphine boranes.	23
Scheme 9: Direct enantioselective synthesis of <i>P</i> -chirogenic aminophosphine boranes 15 using (-)-ephedrine.	24
Scheme 10: Stereochemistry of the ring opening reaction of oxazaphospholidine 14.	25
Scheme 11: Acidic methanolysis of the ephedrine unit.	25
Scheme 12: Synthesis of optically pure tertiary phosphines 18	26
Scheme 13: Synthesis of secondary and tertiary phosphines via enantiopure chlorophosphines.	26
Scheme 14: Synthesis of phosphine oxides 23 in high enantiomeric purity by using (-)-ephedrine.	27
Scheme 15: Direct stereoselective synthesis of DIPAMP with a camphor derivative.	28
Scheme 16: Synthesis of chiral tertiary phosphine boranes from dimethylarylphosphine borane 29.	29
Scheme 17: Synthesis of BisP* from dimethylarylphosphine borane.	29
Scheme 18: Synthesis of MiniPHOS from dimethylarylphosphine borane 29.	29
Scheme 19: Synthesis of unsymmetrical BisP* 37.	30
Scheme 20: Synthesis of enantiopure ferrocenyl phosphines from Ugi's amine (38).	31
Scheme 21: Atropisomerism of biphenyl compounds.	32
Scheme 22: Synthesis of <i>P</i> -chirogenic binaphthyl monophosphines 42 by Hamada and Buchwald.	33
Scheme 23: Separation of diastereomeric binaphthyl monophosphines 42a,b by Hamada and Buchwald.	34
Scheme 24: Synthesis of atropisomeric diphosphine ligands by Cereghetti et al.	34
Scheme 25: Synthesis of bisphosphine ligands with two chirogenic <i>P</i> -centres and two atropisomeric BINAP units by Zhang et al.	35
Scheme 26: Synthesis of phosphine-phosphites by Pizzano et al.	35
Scheme 27: Synthesis of <i>P</i> -chirogenic BINAP bisulphide analogues 55 by Gilheany et al.	36
Scheme 28: Synthesis of atropisomeric biphenyl diphosphine dioxide (<i>S</i> _a , <i>S</i> _P , <i>S</i> _P)-(+)-61 due to Pietrusiewicz et al.	37
Scheme 29: Synthesis of BipheP* due to Imamoto et al.	37
Scheme 30: BASF menthol-process.	42
Scheme 31: Synthesis of (aryl)methyl-(phenylphosphinite)-boranes 16a-e.	44
Scheme 32: Synthesis of the DPE-derivatives 68.	45
Scheme 33: Hydrogenation of citral to citronellal.	47
Scheme 34: Asymmetric hydrogenation of isophorone 70 to chiral ketone 71 and alcohol 72.	48
Scheme 35: Asymmetric allylation of dimethyl malonate (74) with (<i>E</i>)-1,3-diphenylallyl acetate (73).	51
Scheme 36: Synthesis of DBFphos derivatives 77.	53

Scheme 37: Pyramidal inversion of triaryl phosphines via a planar transition state.....	59
Scheme 38: Protection of DPEphos- and DBFphos derivatives with BH ₃ -groups.	66
Scheme 39: Migration of the borane group in (<i>S</i>)- <i>o</i> -anisylmethylphenyl phosphine-borane found by Imamoto and working group.	69
Scheme 40: Envisaged synthesis of BINAP-Derivatives 81 with the (-)-ephedrine methodology.	78
Scheme 41: Postulated mechanism of the formation of 82 and 83.	79
Scheme 42: Postulated mechanism of the formation of 84.	80
Scheme 43: Synthesis of enantiopure <i>m</i> -anisylarylphenyl phosphine (85).	80
Scheme 44: Synthesis of aryl(2-iodo-3-methoxyphenyl)(phenyl)phosphine borane (86).	81
Scheme 45: Synthesis of enantiopure <i>m</i> -anisylarylphenylphosphine oxide (87) using H ₂ O ₂	81
Scheme 46: Synthesis of enantiopure <i>m</i> -anisylarylphenylphosphine oxide (23) using <i>m</i> -CPBA.	82
Scheme 47: Synthesis of aryl(2-iodo-3-methoxyphenyl)(phenyl)phosphine oxide (24).	82
Scheme 48: Synthesis of 1,2-diiodo naphthalene (91).	84
Scheme 49: Synthesis of 2-anisylphenyl phosphine borane (94).	84
Scheme 50: Synthesis of (<i>R</i>)-(1-iodonaphthalen-1-yl)(2-methoxyphenyl)(phenyl)phosphine borane (96a) and its regioisomer 96b.	85
Scheme 51: Removal of the borane group from derivatives 96.	86
Scheme 52: Oxidation of 27.	87
Scheme 53: Application of 100a for the Ullmann coupling.	88
Scheme 54: Exemplary investigations of the reduction of the <i>P</i> -chirogenic compound 101.....	89
Scheme 55: Reduction of 101 with PMHS and Ti(O <i>i</i> Pr) ₄	92

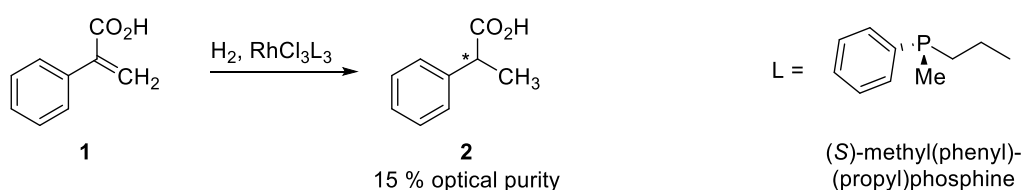
List of Tables

Table 1: Yield of compound 10 with different substituents.	44
Table 2: Ratio of mono- and disubstitution of the DPE-backbone.	46
Table 3: Asymmetric hydrogenation of isophorone ^a	49
Table 4: Asymmetric hydrogenation of isophorone (70) in dependence on the solvent ^a	50
Table 5: Asymmetric allylation of dimethyl malonate 74 with (<i>E</i>)-1,3-diphenylallyl acetate (73) ^a	52
Table 6: Conversion and yield of the synthesis of DBFphos derivatives.	54
Table 7: Asymmetric hydrogenation of isophorone by utilisation of DBFphos ligands.	55
Table 8: Asymmetric allylation of dimethyl malonate (74) with (<i>E</i>)-1,3-diphenylallyl acetate (73) ^a . ..	56
Table 9: Alteration of stereochemistry in di(triaryl phosphines) over the time at room temperature	60
Table 10: NMR Investigations on temperature dependency of inversion at the <i>P</i> -centre of di(triaryl phosphines).	63
Table 11: Ratio of 68a' isomers at different temperatures determined by quantitative ³¹ P NMR.	68
Table 12: Results of the asymmetric hydrogenation of isophorone ^a in dependence on the protection of the phosphorus with BH ₃	74
Table 13: Results of the exemplary investigations of the reduction of the <i>P</i> -stereogenic compound 102.	90

1. Introduction

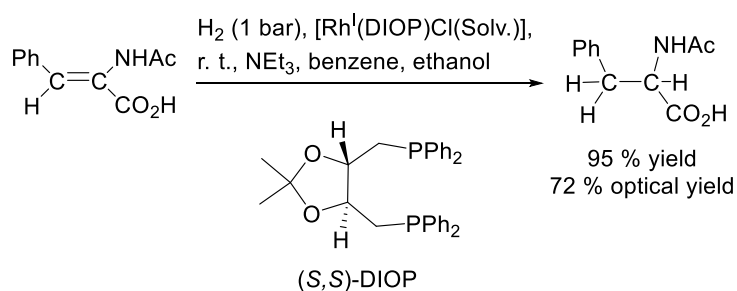
1.1 Tertiary Phosphines in Asymmetric Catalysis

In 1968, the first homogeneously catalysed asymmetric hydrogenation of olefins with rhodium complexes bearing chiral, monodentate tertiary phosphine ligands was performed by Knowles and Horner independently of one another.^{1,2}



Scheme 1: Rh-catalysed asymmetric hydrogenation of α -phenyl acrylic acid developed by Knowles.

They synthesised (*S*)-methyl(phenyl)(propyl)phosphine and tested it as a ligand in the Rh-catalysed asymmetric hydrogenation of e. g. α -phenyl acrylic acid **1** (Scheme 1). The optical purity of the resulting hydratropic acid (**2**) was only about 15 %, but it was the start of a new era of catalytic chemistry. Three years later, Dang and Kagan achieved a real breakthrough by using other prochiral substrates like α -acetamidocinnamic acid (Figure 1).³



Scheme 2: Asymmetric hydrogenation of an unsaturated prochiral amino acid by Dang and Kagan using (*S,S*)-DIOP as chiral ligand.

As a precatalyst $[\text{Rh}(\text{DIOP})\text{Cl}(\text{Solvent})]$ was used. An optical purity of up to 72 % in the product resulted (Scheme 2). DIOP was the first bidentate C_2 -chiral diphosphine ligand. It

results from the modification of tartaric acid derivatives, which can be gained from the chiral pool.

Originating from this discovery, a huge library of chiral bidentate phosphine ligands was synthesised and studied in detail. The chirality of the ligands can be based on different elements of symmetry, e. g. chirogenic carbon atoms or axial chirality. A major challenge is also the synthesis of chirogenic *P*-centres.

1.2 Steric and Electronic Effects of Tertiary Phosphine Ligands

The steric and electronic characteristics of ligands are the key to regulate the activity and selectivity of their catalytically active complexes. Different σ -donor- und π -acceptor properties of ligands can influence the electron density of metal centres, which has a great impact on the binding force between the substrate and the central atom.

In 1967, Strohmeier and Müller showed, how to determine the relative π -acceptor strength at the P-atom in ligands, which are coordinated to mono substituted metal carbonyls.⁴ They investigated several carbonyl complexes in respect to their C=O-stretching vibration with IR spectroscopy and sorted them by increasing wave numbers ν in a table. They gave evidence that the relative π -acceptor strength at the P-atom increases by increasing number of electronegative substituents. They organised the substituents as follows (π -acceptor strength increases; R = alkyl):

Class:	I	< II	< III	< IV	< V	< VI
Type:	PR ₃	< P(C ₆ H ₅) ₃	< PCl(C ₆ H ₅) ₂	< PCl ₂ (C ₆ H ₅)	< PCl ₃	< PF ₃

In 1970, Tolman disclosed another methodology to determine the σ -donor- und π -acceptor properties of ligands.^{5,6} He used IR spectroscopic investigations on [Ni(CO)₃L] complexes in CH₂Cl₂, in which the A₁ vibrational band of the carbonyl is examined in respect to the ligand L. P(*t*Bu)₃ was selected as the most basic phosphine of this series, which absorbs at a frequency of 2056.1 cm⁻¹. In dependence of this value, Tolman established the following equation:

Equation 1

$$\nu_{CO}(A_1) = 2056,1 + \sum_{i=1}^3 \chi_i \text{ cm}^{-1}$$

In Equation 1, the substituent parameter χ_i describes the electronical properties of the substituent R of the trivalent phosphine $\text{PR}^1\text{R}^2\text{R}^3$. The sum of all three substituent parameters equals the Tolman basicity of the phosphine. When χ is small, the substituent is considered as a strong σ -donor. Strong π -acceptors are characterised by high χ -values. The advantage of this model is the ability to estimate the π -acceptor strength of ligands in relation to other ligands, even if the real values are not known.

The strength of the bond between ligand and metal centre is not the only impact on the reaction at the catalyst complex. By using sterically demanding ligands, the substrate can be shielded from the central atom or can be adjusted in a defined orientation when it comes to coordination. In regard to polydentate ligands, the geometry of coordination plays an important role in catalysis.

There are simple parameters which describe steric properties of ligands and help to find simple correlations. Tolman developed in 1970 the model of the cone angle Θ , which characterises the steric hindrance of ligands.^{6,7} The cone angle Θ is defined as the angle which spans between the outer atom shells of the phosphorus substituents and the metal centre, whereas the metal-phosphorus-distance is fixed to 2.28 Å, which is known as the average P-Ni-distance.

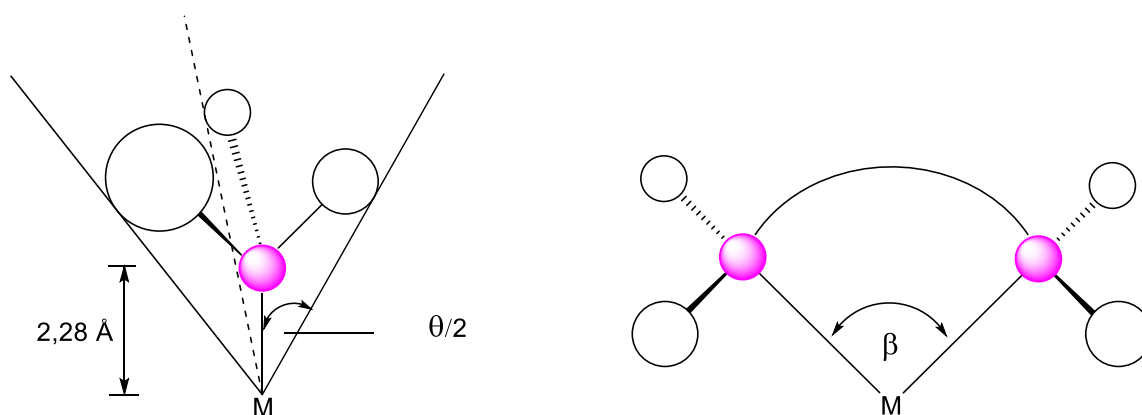


Figure 1: Tolman's cone angle Θ model (left) and natural bite angle β model (right).

1. Introduction

1.2 Steric and Electronic Effects of Tertiary Phosphine Ligands

The cone angle model (Figure 1) can also be applied on complexes of other transition metals, qualitatively, but there are also some limitations. To calculate the real bond length, van-der-Waals radii are used, but molecule characteristics can differ from that. Another limiting aspect is that the Tolman cone angle can reproduce values exclusively for spherical substituents like PMe_3 and $\text{P}(t\text{Bu})_3$. It cannot illustrate exactly different substituents or planar rings which can rotate. In these cases, the calculated cone angles differ strongly from that determined by crystal structure analysis.

The natural bite angle β is another model often used to describe the steric hindrance of polydentate ligands (Figure 1). It was developed by Casey and Whiteker in 1990.⁸ The natural bite angle P-M-P is defined as the favoured chelation angle of the ligand, which only depends on the backbone of the ligand but not on the metal valence angle. The flexibility of a ligand indicates the possible range of the bite angles which can be reached by an energetic impact of less than 3 kcal/mol originating from the calculated natural bite angle.⁹ The coordination geometry of a catalytically active complex can be controlled by the bite angle of a chelating ligand. This is how the ligand can actively affect the regioselectivity of catalytic reactions, which was proved in 1992 by Casey and his working group using Rh-complexes for hydroformylation.¹⁰ They found that bidentate diphosphines can coordinate in apical or equatorial position of the trigonal bipyramid of a Rh(I)-alkene-hydride complex. Ligands with natural bite angles of approximately 90° stabilise the apical-equatorial position, whereas larger bite angles of approximately 120° favour the equatorial-equatorial coordination mode. Different coordination modes at the metal atom affect the regioselectivity of the hydroformylation in respect to its *n*-selectivity. Bite angles about 120° increase the *n*-selectivity, whereas bite angles about 90° lead to the *iso*-product.

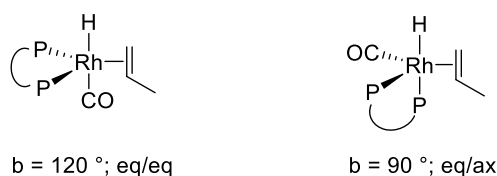


Figure 2: Coordination modes of Rh(I)-alkene-hydride complexes.

Also the model of the natural bite angle has some limitations. As mentioned before, the natural bite angle of a ligand owns a flexibility range depending on its backbone and electronic or steric effects of other ligands coordinated on the same metal centre. The actual bite angle correlates

nicely to the natural bite angle only if the other co-ligands are very small like H, CO and alkenes.

1.3 Tertiary Phosphine Ligands with Asymmetric Phosphorus

Tertiary phosphines generate pyramidal structures which consist of a central P-atom bearing three substituents and a lone pair of electrons. If all three substituents at the phosphorus are different, the phosphine is called *P*-chirogenic or *P*-stereogenic.

1.3.1 Inversion Barrier of Tertiary Phosphines

Ammonia and amines have low inversion barriers of 5-10 kcal/mol and tend easily toward stereoisomerisation. Therefore, only under special circumstances amines with three different substituents are configurationally stable. In contrast, *P*-chirogenic phosphines have a much higher inversion barrier of around 30 kcal/mol, which allows the isolation of single enantiomers.¹¹

The higher inversion barrier at phosphorus in contrast to nitrogen is caused by the lower electronegativity of phosphorus.¹² Murrell and his co-workers explained, that phosphorus has a greater lone pair *s* character due to the lower electronegativity in terms of differential hydrogen 1s-central atom *ns* and *np* overlap.^{12,13} For second-row elements like nitrogen, the 1s-2s overlap is significantly greater than the 1s-2p overlap. That leads to a large *s* character in the bonding orbitals and thus to a stronger *p* character of the lone pair. In contrast, the reduced electronegativity of the third-row elements like phosphorus supports the 1s-3p overlap with respect to 1s-3s which promotes the *p* character of the bonds and the *s* character of the lone pair.

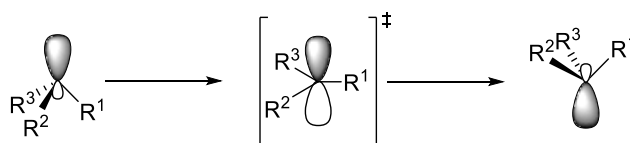


Figure 3: Inversion of phosphines via a planar transition state.

1. Introduction

1.3 Tertiary Phosphine Ligands with Asymmetric Phosphorus

To invert the phosphine, a planar transition state must be passed (see above). This transition state is characterised by a pure p character of the lone pair and a strong s character of the bonding orbitals. To achieve this state, the phosphine requires more energy than the amine because the amine already provides similar conditions in respect to the transition state.

Other impacts on the value of the inversion barrier are the electronegativity of the substituents, their steric hindrance, conjugation, lone pair electrons of the substituents and the angle between substituent-metal centre-substituent.

The effect of different effects on the inversion barrier can be shown by the example of alkyl vs. aryl substituents. Alkyl groups with sp^3 -hybridised carbon-atoms are less electronegative than aryl groups with sp^2 -hybridised carbons. Levin established the rule that the higher the electronegativity of the substituent, the higher is the inversion barrier.¹² Therefore, aryl groups should increase the s character of the lone pair of the central atom and thus rise the inversion barrier in comparison to alkyl substituents.

In contrast, it was proven that by a growing number of aryl substituents at the phosphorus the inversion barrier decreases. To show this trend, Baechler and Mislow calculated the free activation energy needed to invert tertiary phosphines.¹⁴ The inversion barrier ($\Delta G^\ddagger_{\text{inv}}$) of trialkyl phosphines is about 36 kcal/mol, that of dialkyl aryl phosphines is about 33 kcal/mol and that of alkyl diaryl phosphines is about 30 kcal/mol. To follow this trend, triaryl phosphines, which are in the focus of this work, should have even lower inversion barriers.

This anomaly can be explained by different effects. It can be assumed that a conjugation of the lone electron-pair of phosphorus and π -orbital(s) of the adjacent aryl ring(s) occurs.¹⁵ The pyramidal structure of the phosphine is flattened due to energetically advantageous interactions between the orbitals. This condition is close to the transition state therefore the needed energy to overcome the inversion barrier is lower. The same effect was described for pyramidal inversion at the *P*-centre with adjacent double bonds like in acyl phosphines or phospholes.¹⁶

Also the steric influence of bulky substituents can enhance the inversion of the steric centre. It was found, that tris(2,6-diisopropylphenyl)phosphine has a lower inversion barrier (only 37.5 kJ/mol)¹⁷ than it was calculated in the literature for triphenyl phosphine.¹⁸

These effects seem to exceed the rule of electronegativity; therefore, the inversion barrier decreases by an increasing number of aryl substituents at the phosphorus.

This effect can be a reason why in some special cases of triaryl phosphines, which have been investigated in this work, racemisation takes place at room temperature or at moderate heating. Until now, there are no experimental data or calculations which prove this statement. Therefore, in the context of this work some long-term temperature NMR stability tests of the triaryl phosphines were conducted.

1.3.2 Synthesis of Tertiary *P*-Chirogenic Phosphines

1.3.2.1 Protection and Deprotection of *P*-Chirogenic Phosphines

Since the synthesis of the first asymmetric organophosphorus compounds in the last century, and by using them as ligands in metal catalysed asymmetric reactions, the demand for efficient synthetic routes increased continuously, not only in academic research but also in industrial applications. There were various methodologies published to get access to these compounds.¹⁹ In the first years after their discovery resolution of racemates were dominant in obtaining enantiopure compounds, but later on, also the use of chiral auxiliaries made the stereoselective synthesis of asymmetric phosphorus compounds possible.

The most important families of phosphine derivatives in this regard are their oxides and boranes, respectively. Oxygen and borane are used as protective groups to prevent inversions of the *P*-centre or, in case of boranes, undesirable oxidation. In the following section, the interconversions between phosphines and phosphine oxides and boranes are discussed.

1.3.2.1.1 Phosphines, Phosphine Oxides and Sulphides

Secondary and tertiary phosphine oxides were applied as classical precursors to *P*-chirogenic phosphines until they were (partially) supplanted by phosphine boranes, which are easy to handle due to their air and moisture stability as well as due to their configurational stability even at high temperatures.^{19d} There are various methodologies to oxidise phosphines, but the most typical reagents are peroxo reagents such as H₂O₂, *t*BuOOH and *m*-CPBA.²⁰ Phosphines can also react readily with oxygen from air, but often impure products yield.²¹ Reacting

1. Introduction

1.3 Tertiary Phosphine Ligands with Asymmetric Phosphorus

P-chirogenic phosphines with halogens or pseudohalogens in water lead also to phosphine oxides but with inverted *P*-centres.²²

To reduce phosphine oxides very strong oxophiles and harsh conditions are needed due to the high stability of the P=O group. Frequently silanes like HSiCl₃, PhSiH₃ and PMHS together with amines or hydrides like LiAlH₄ are used.²¹ Depending on the reducing agent, the reduction occurs under retention or inversion of the chirogenic phosphorus centre. Often the reduction may lead to a loss of enantiopurity or can even give racemic mixtures of the chiral phosphine.

Similar to phosphine oxides, many phosphine sulphides can be found in the literature, but their use in *P*-chirogenic chemistry is rather seldom. Phosphine sulphides are prepared easily by reacting phosphines with elemental sulphur. With *P*-chirogenic phosphines this reaction proceeds under retention of the configuration.²³

The reduction of phosphine sulphides proceeds stereoselectively with hexachlorodisilane and Raney nickel.^{19d}

1.3.2.1.2 Phosphines and Phosphine Boranes

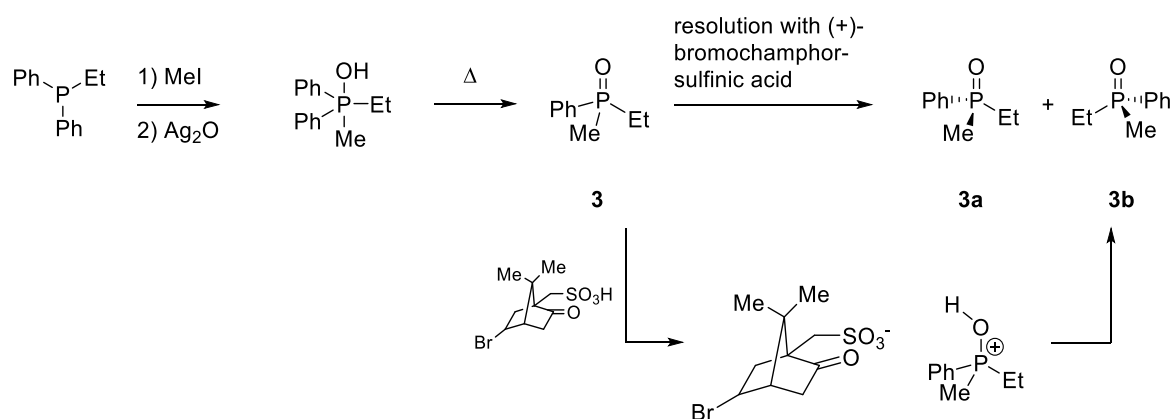
Since the work of Imamoto and his co-workers in 1990, the importance of phosphine boranes as intermediates for the synthesis of *P*-chirogenic phosphines increased continuously.^{19d,24} Today, BH₃ is mostly used as the protection group of phosphines to inhibit oxidation or isomerisation. Due to the low polarity and polarizability of the P-B and B-H bonds, the reactivity of this protection group is very low, making phosphine boranes very easy to handle and purify.

The preparation of phosphine boranes proceeds normally by direct reaction of the phosphine with borane complexed to Lewis bases like BH₃·thf or BH₃·SMe₂.^{19d} In particular BH₃·SMe₂ reacts quantitatively with phosphines. These reactions proceed under retention of the configuration at the chiral *P*-centre.

The popularity of phosphine boranes is due to their easy removal of the protective group. Amines like diethylamine,²⁵ TMEDA,²⁶ pyrrolidines,²⁷ morpholine²⁸ and DABCO²⁹ or alcohols are used as borane acceptors. The reactions proceed normally at room temperature or at moderate heat and with retention of the configuration at the *P*-centre.

1.3.2.2 Resolution of Racemic or Diastereomeric Mixtures

To obtain enantiopure or diastereomerically pure phosphines, several methodologies were developed over the years. In the beginning, the most important method was classical resolution of racemic compounds by formation of diastereomers from chiral auxiliaries. The disadvantages of this procedure are the search for suitable auxiliaries or metal complexes for the resolution process and laborious recrystallisation or chromatographic separation.



Scheme 3: Resolution of the racemic mixture of ethylmethylphenylphosphine oxide by Meisenheimer and Lichtenstadt in 1911.

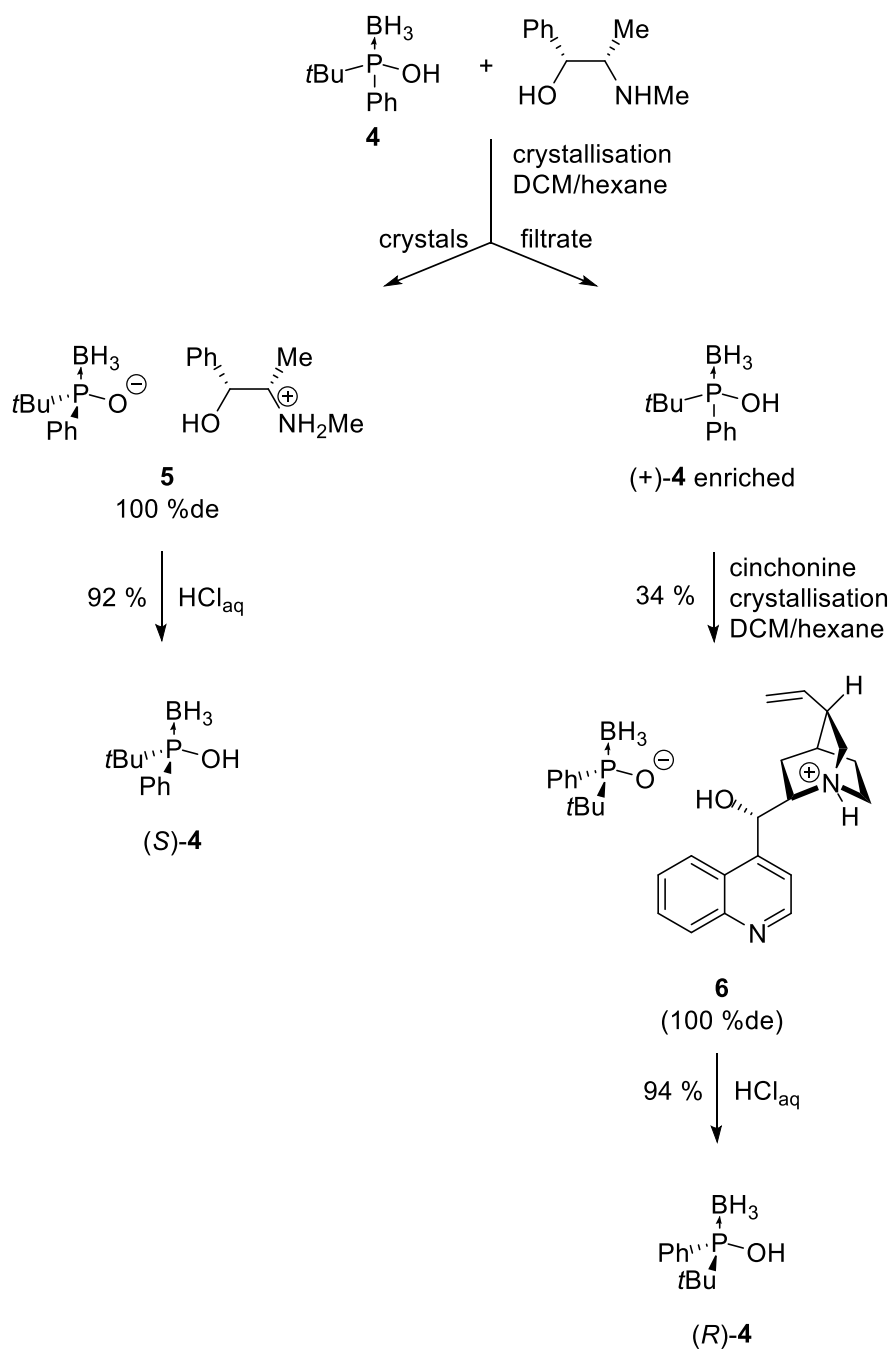
The first researchers who published a method to resolve a racemic mixture of ethylmethylphenylphosphine oxide (3) were Meisenheimer and Lichtenstadt in 1911.³⁰ They added (+)-bromocamphorsulfonic acid to the racemic phosphine oxide 3. The chiral auxiliary protonates the weakly basic phosphoryl group to build a diastereomeric salt. The diastereoisomers were separated by crystallisation from EtOAc and EtOAc/diethyl ether (Scheme 3).

In an exemplarily manner for resolution of phosphine boranes, Scheme 4 shows the resolution of racemic *t*-butylphenylphosphinous acid (4) with enantiomerically pure ephedrine and cinchonine, respectively, as chiral auxiliaries.³¹ It is obvious that the phosphine must possess a protic group for this resolution method. The acid provides a proton which is attracted by a weakly basic chiral auxiliary. Also in this case, a diastereomeric salt (5, 6) is created which can be resolved by crystallisation.

1. Introduction

1.3 Tertiary Phosphine Ligands with Asymmetric Phosphorus

In both cases, the resolution is based on ionic interactions which means on the formation of salts. There are also some cases (see below) in which the chiral auxiliary binds covalently at the phosphine. The covalent bond has to be cleaved after the separation. Therefore, different phosphines require various chiral auxiliaries. Some of the most important auxiliaries are listed in Figure 4.



Scheme 4: Resolution of racemic *t*butylphenylphosphinous acid (**4**) with enantiopure ephedrine and cinchonine.

1. Introduction

1.3 Tertiary Phosphine Ligands with Asymmetric Phosphorus

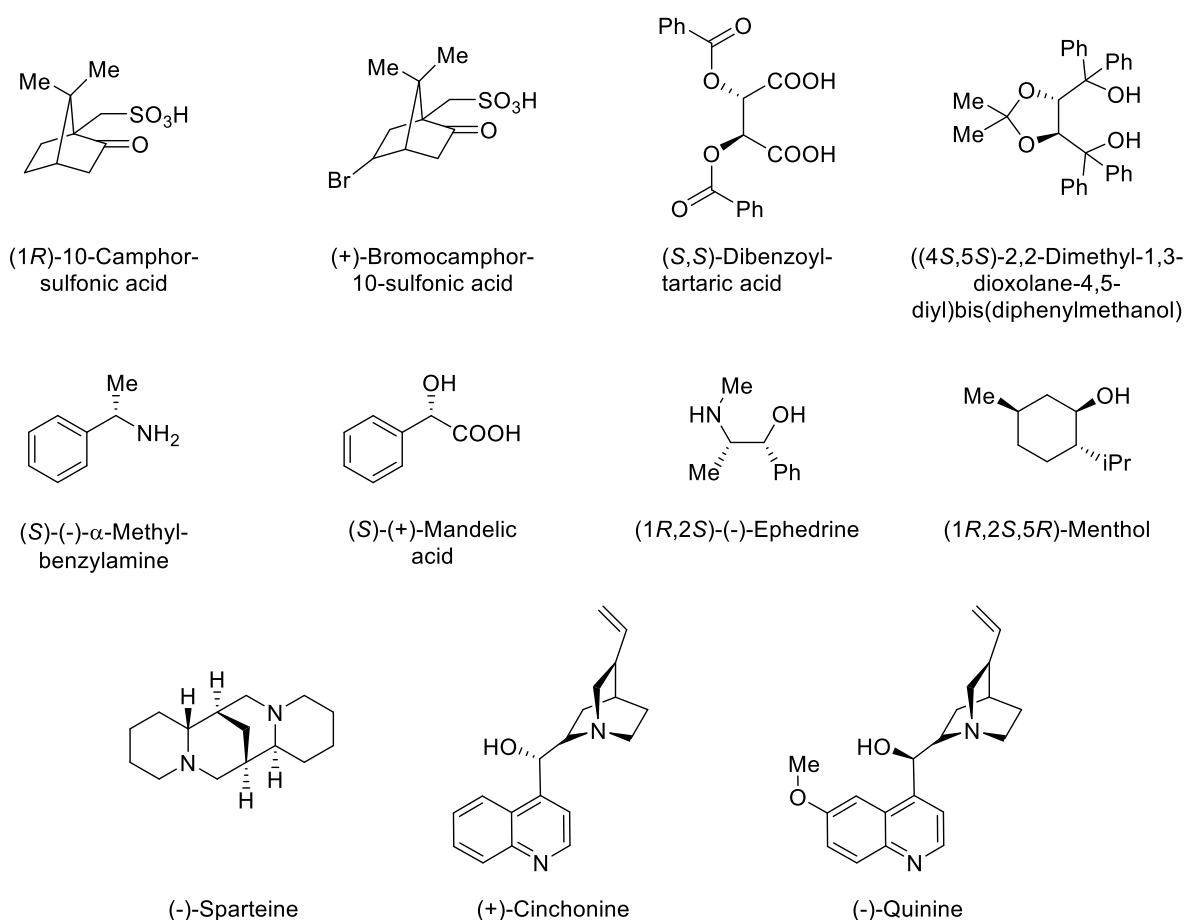
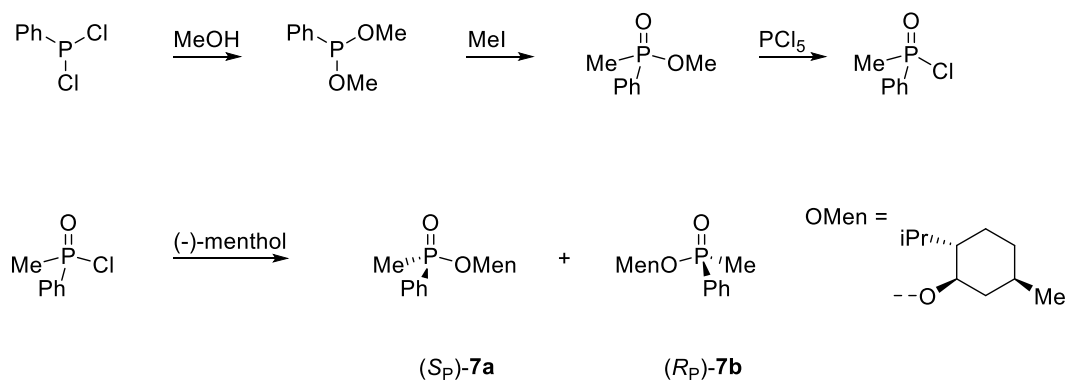


Figure 4: Chiral auxiliaries used for resolution of racemic phosphines.

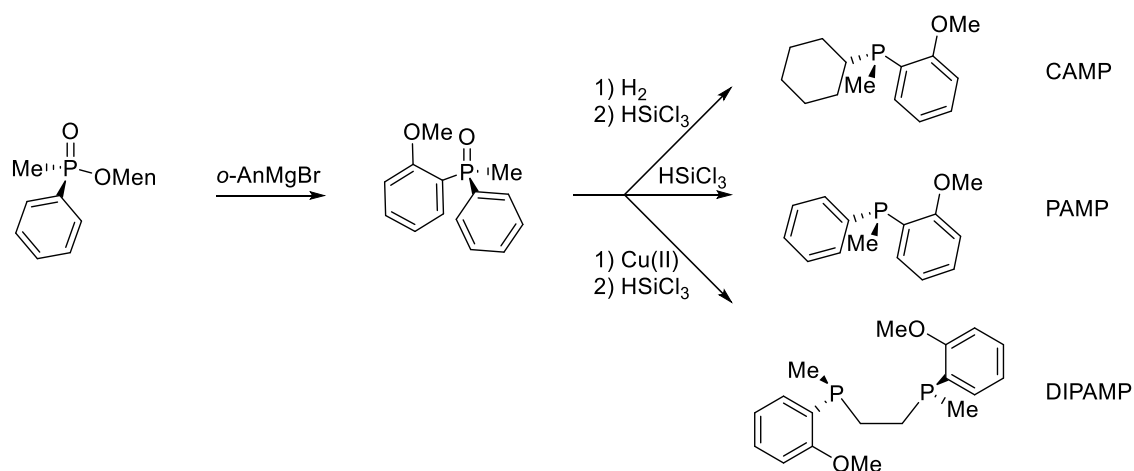
At the end of the 1960s, the working groups of Mislow³² and Cram,³³ independently of each other, published a methodology of stereoselective synthesis of *P*-chirogenic phosphines by using (-)-menthol as chiral auxiliary (Scheme 5).



Scheme 5: Stereoselective synthesis of *P*-chirogenic phosphines by using (-)-menthol as chiral auxiliary suggested by Mislow and Cram.

1.3 Tertiary Phosphine Ligands with Asymmetric Phosphorus

The application of (-)-menthol as chiral auxiliary for the synthesis of enantiopure phosphines was a breakthrough in the history of asymmetric homogeneous catalysis. With its help, Knowles and his working group synthesised *o*-anisylmethylphenylphosphine (PAMP) and *o*-anisylcyclohexylmethylphenylphosphine (CAMP) (Scheme 6) which were subsequently applied in the rhodium catalysed asymmetric hydrogenation of α -acylaminoacrylic acids. PAMP and CAMP were proved to be appropriate ligands for rhodium(I) in the asymmetric hydrogenation, because optical purities of 58 % and 88 %, respectively, were induced in the chiral product.^{34,35} These were the first man-made catalysts with enzymelike selectivity. Knowles' second-generation ligand was the chelating diphosphine ligand DIPAMP which was also synthesised according to Mislow's procedure and which found its application in the commercial L-DOPA process due to its excellent enantioselectivity of 95 %ee.^{36,37}

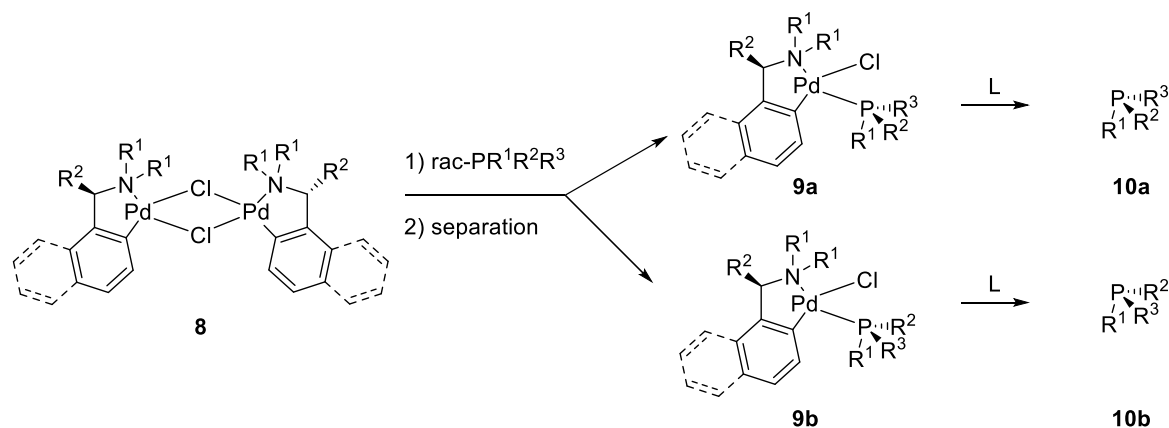


Scheme 6: Synthesis of CAMP, PAMP and DIPAMP by Knowles.

Not only chiral non-metal auxiliaries can be used to support resolution of racemates, but also enantiopure transition metal complexes. For the most common procedure chlorobridged dimeric palladacycles **8** are used (Scheme 7).³⁸

1. Introduction

1.3 Tertiary Phosphine Ligands with Asymmetric Phosphorus



Scheme 7: Resolution of racemates with help of transition metal complexes.

In the first step of the synthesis, the palladium dimer splits in its monochloro complexes. The racemic phosphines coordinate to the palladium centre to form diastereomeric complexes **9a,b**, which can be separated by fractional crystallisation or column chromatography. To liberate the enantiopure phosphines, strongly coordinating ligands (L) like cyanide or dppe are added to form insoluble complexes.³⁸ The released *P*-chirogenic phosphines **10a,b** remain in solution and can be separated from the insoluble precipitation easily.

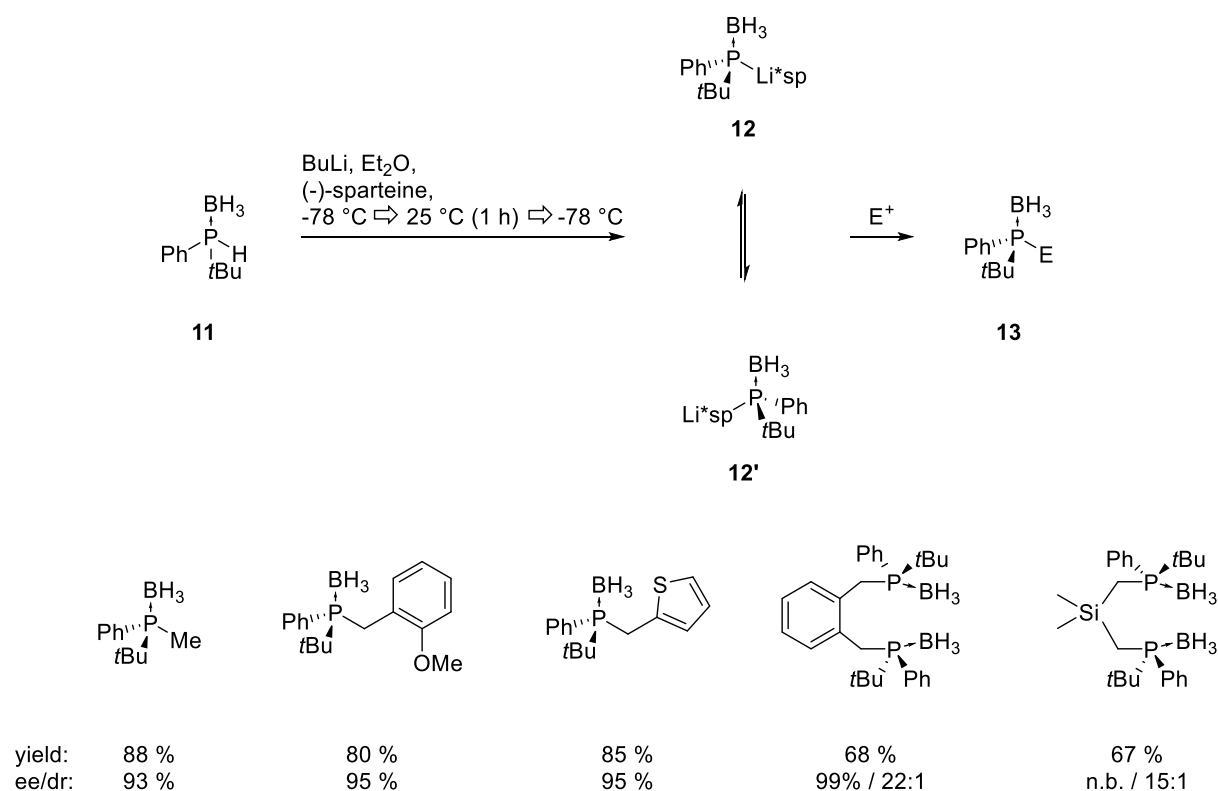
This procedure turned out to be effective not only for monophosphines but also for bi- or polydentate phosphines.

1.3.2.3 Direct Resolution by Chromatographic Methodologies

In the early days of the synthesis of *P*-chirogenic compounds the optical purity was estimated by optical rotation or integration of NMR signals of diastereomeric adducts. Today, the enantiomeric excess of phosphine oxides, boranes or sulphides is often determined by chiral HPLC. Preparative HPLC proceeds under similar conditions and can be used to separate racemates in gram or even larger scale.^{19d} In spite of being extremely time-efficient, this method is used rarely due to economic reasons such as acquisition costs for the special apparatus or columns and the requirement of large volumes of solvents. Nevertheless, preparative HPLC is sometimes used for the resolution of several phosphine oxides due to a lack of other appropriate synthetic routes.^{19a}

1.3.2.4 Dynamic Resolution of Secondary Phosphine Boranes

Wolfe and Livinghouse published a methodology to synthesise *P*-chirogenic phosphine boranes by dynamic resolution in 1998.³⁹ Starting from racemic *t*butylphenylphosphine borane (**11**) the deprotonation of the secondary phosphine was realised by the reaction with *n*BuLi in Et₂O at -78 °C in the presence of (-)-sparteine (sp) to obtain **12/12'**. This mixture was warmed to 25 °C and stirred for one hour. After cooling the solution to -78 °C again followed by quenching the reaction with electrophilic alkyl or aryl halides (E-X) the corresponding tertiary phosphine borane could be obtained in good yields. Some examples of the synthesised compounds **13** are shown in the scheme below. Through this dynamic thermodynamic control enantiomeric excess of 95 % could be realised.^{39,40}



Scheme 8: Dynamic resolution of secondary phosphine boranes.

The stereoselectivity of the reaction depends on the temperature and the time of the reaction.⁴⁰ Furthermore, the enantioselectivities can be controlled by the thermodynamic equilibration of **12** and **12'**. The metallation and the final electrophilic quenching were performed at -78 °C. At this temperature both diastereomers **12** and **12'** cannot convert into each other although **12**

appears to be more stable. The equilibration step needs higher temperatures: the reaction at 0 °C for 30 minutes afforded 35 %ee, whereas at 25 °C for 1 hour the product yielded with 95 %ee.

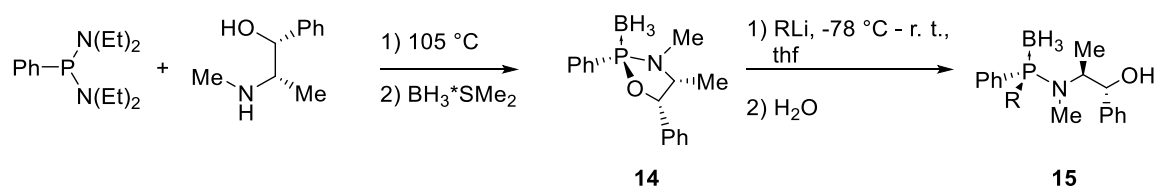
39

1.3.2.5 Direct Enantioselective Synthesis of *P*-Chirogenic Phosphines Using Chiral Auxiliaries

The above-mentioned methodologies are appropriate ways to get enantiopure *P*-chirogenic compounds and are still used nowadays in some cases. A great disadvantage of these procedures is that in all cases two or more different species are prepared although often only one is required. To avoid the undesirable waste of material, the knowledge of direct stereoselective synthesis of *P*-chirogenic phosphines with the assistance of chiral auxiliaries increased more and more over the past 60 years.

1.3.2.5.1 (-)-Ephedrine as Chiral Auxiliary for the Enantioselective Synthesis of *P*-Chirogenic Phosphines

In 1990 Jugé and co-workers developed an versatile methodology to obtain *P*-chirogenic phosphines directly by taking benefit from the effect that alkoxy groups can be nucleophilically substituted with high stereoselectivity at the phosphorus.²⁵ Di(diethylamino)phenyl phosphine reacted with (-)-ephedrine to the diastereomerically pure compound **14**. In the second step, the ring of oxazaphospholidine **14** was opened which gives the aminophosphine **15** with high diastereoselectivity (92/8 = 84 %de; Scheme 9).

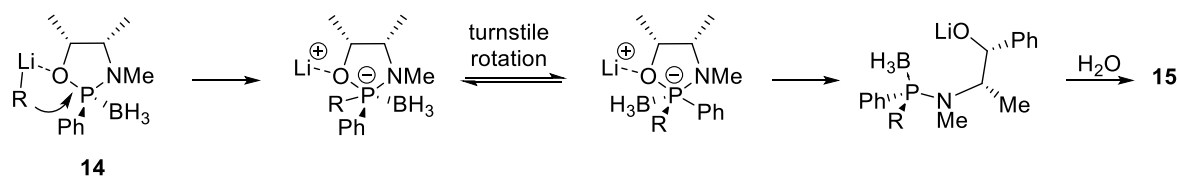


Scheme 9: Direct enantioselective synthesis of *P*-chirogenic aminophosphine boranes **15** using (-)-ephedrine.

1. Introduction

1.3 Tertiary Phosphine Ligands with Asymmetric Phosphorus

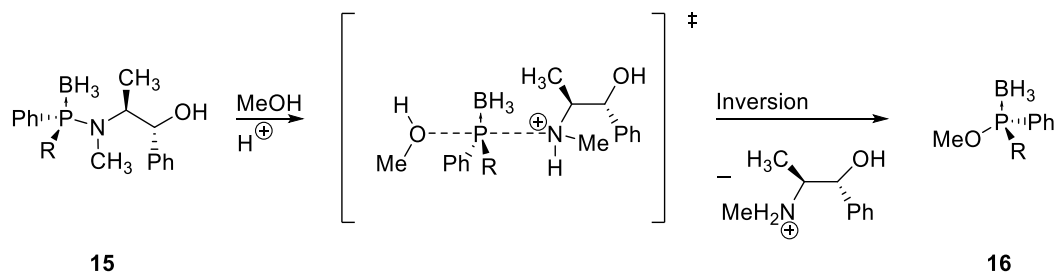
The dominant stereochemistry can be rationalized by the nucleophilic attack of an organolithium reagent at the P-O-bond which occurs from the less hindered site (Scheme 10).⁴¹ The attack does not happen at the NMe group due to its steric hindrance. In this manner the P-O-bond is weakened. Subsequently the alkyl or aryl group R was introduced into the molecule from the same site.



Scheme 10: Stereochemistry of the ring opening reaction of oxazaphospholidine **14**.

The postulated mechanism requires the creation of a pentacoordinated phosphorus-intermediate which is able to initiate a so-called turnstile rotation which brings the P-O-bond in an apical situation.^{19c} By a P-O-bond cleavage a lithium salt is formed which can be reacted to compound **15** by hydrolysis and under retention of the configuration at the *P*-centre. Notably, to achieve an inverse stereochemistry at the *P*-centre, an isomerisation of the pentacoordinated phosphorus-intermediate would be required. The supposed mechanism therefore would involve a Berry pseudorotation which does not proceed favourably through a five membered ring with an O-P-N-angle of 90 °.

The steering ephedrine unit of the ring opening product **15** was substituted via acidic methanolysis eventually.^{25,41} During this reaction the P-N-bond was cleaved and ephedrine was substituted by a methoxy group. This reaction proceeded with excellent yields and under inversion of the *P*-centre by a S_N2-mechanism (Scheme 11).



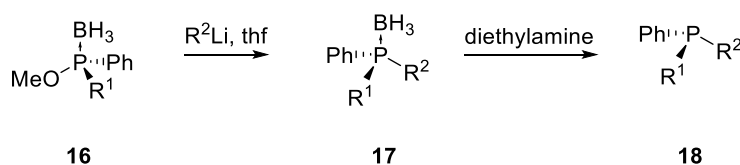
Scheme 11: Acidic methanolysis of the ephedrine unit.

1. Introduction

1.3 Tertiary Phosphine Ligands with Asymmetric Phosphorus

In the next step the methyl phosphinite **16** was reacted with alkyl or aryl lithium to achieve optically pure phosphine boranes **17**. This reaction proceeded also under inversion of the stereocentre (Scheme 12).

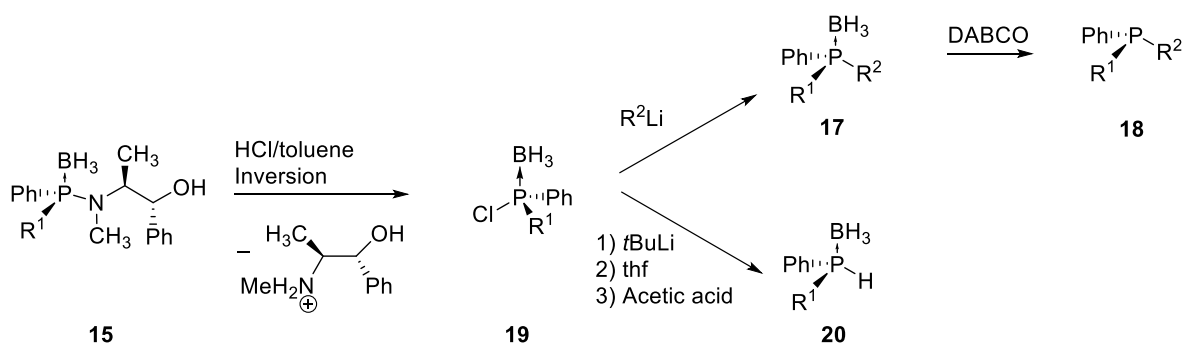
To use the phosphine as a ligand finally, the BH_3 -decomplexation was conducted under mild conditions with diethylamine without loss of optical purity (Scheme 12).^{25,41}



Scheme 12: Synthesis of optically pure tertiary phosphines **18**

The (-)-ephedrine methodology turned out to be quite general for a large variety of substituents achieving good yields and stereoselectivity.

Instead following the acidic methanolysis of the (-)-ephedrine methodology, one can obtain enantiopure phosphines also via *P*-stereogenic chlorophosphine boranes **19** (Scheme 13). Here, the P-N-bond of the aminophosphine borane **15** was cleaved by the reaction in a toluene solution of gaseous HCl under inversion of the *P*-centre.^{42,43,44} Since *P*-chirogenic chlorophosphines are not configurationally stable and racemise slowly at room temperature, the chlorophosphines should not be stored for a long time and should therefore react directly with organolithium reagents to obtain phosphine boranes **17**.^{19c,e} Via *P*-stereogenic chlorophosphine boranes **19** secondary phosphine boranes **20** can be derived also by reacting with *t*BuLi first and acetic acid, subsequently, at temperatures at -85°C .⁴⁵

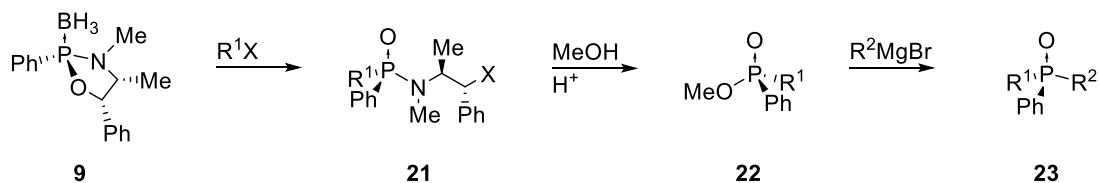


Scheme 13: Synthesis of secondary and tertiary phosphines via enantiopure chlorophosphines.

1. Introduction

1.3 Tertiary Phosphine Ligands with Asymmetric Phosphorus

(-)-Ephedrine can also be used to synthesise phosphine oxides in high enantiomeric purity, like Jugé and his working group demonstrated in 1989.⁴⁶ They started with oxazaphospholidine **14** and reacted it with alkyl halide R^1X ($R^1 = \text{Me, Et, Pr, PhCH}_2$; $X = \text{Cl, I, Br}$) to obtain the phosphine amides **21** by Michaelis Arbuzov rearrangement (Scheme 14).



Scheme 14: Synthesis of phosphine oxides **23** in high enantiomeric purity by using (-)-ephedrine.

After final acidic methanolysis which proceeded under inversion of the *P*-centre, a second aryl substituent was introduced using aryl magnesium bromide. An enantiomeric excess of about 95 % could be observed.

1.3.2.5.2 Camphor Derivatives as Chiral Auxiliary for the Enantioselective Synthesis of *P*-Chirogenic Phosphines

Corey and co-workers developed a methodology for the direct stereoselective synthesis of phosphines such as DIPAMP using camphor derivative **24** (Scheme 15).⁴⁷

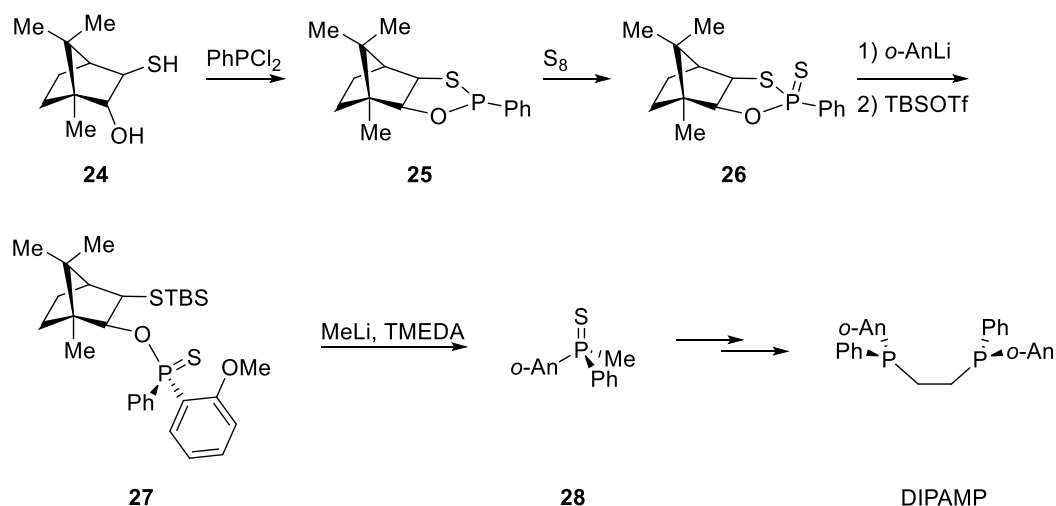
The stereoinductor was reacted with dichlorophenylphosphine to obtain oxathiaphospholidine **25** stereospecifically. Afterwards sulphur was introduced as a protection group by the reaction with elemental sulphur. The ring opening of the thiophosphosphonate **26** proceeded by treatment of **26** with *o*-anisyllithium and *t*butyldimethylsilyl triflate (TBSOTf). Subsequently, thiophosphinate **27** was converted into the enantiopure tertiary phosphine sulphide **28** by the assistance of MeLi and tetramethylethylenediamine (TMEDA). The enantiomeric excess of **28** was determined to be >99 %.

The oxidative coupling of **28** and subsequently desulphurisation yielded (*R,R*)-DIPAMP in >99 %ee.

1. Introduction

1.3 Tertiary Phosphine Ligands with Asymmetric Phosphorus

There are some further methodologies of direct synthesis of enantiopure phosphines from chiral auxiliaries described in literature, but in contrast to the methods described above, they are of lower relevance.



Scheme 15: Direct stereoselective synthesis of DIPAMP with a camphor derivative.

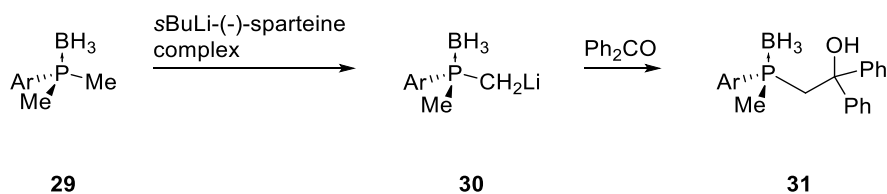
1.3.2.6 Enantioselective Deprotonation Using Chiral Bases

There are various studies that show that the deprotonation of methyl phosphine oxides^{48,49} or methyl phosphine boranes^{24,50} can easily proceed through the application of strong bases like LDA or $s\text{BuLi}$. The electron-withdrawing properties of the oxo or borane group causes the high acidity of the methyl group. The deprotonated methyl group acts as a strong nucleophile which can be reacted with electrophiles to give α -functionalised products.

Evans and his working group published in 1995 a methodology to synthesise chiral tertiary phosphine boranes **31** from dimethylarylphosphine borane **29** ($\text{Ar} = \text{phenyl}, o\text{-anisyl}, o\text{-tolyl}, 1\text{-naphthyl}$) via selective deprotonation with a $s\text{BuLi}$ -(-)-sparteine complex (Scheme 16).⁵¹

1. Introduction

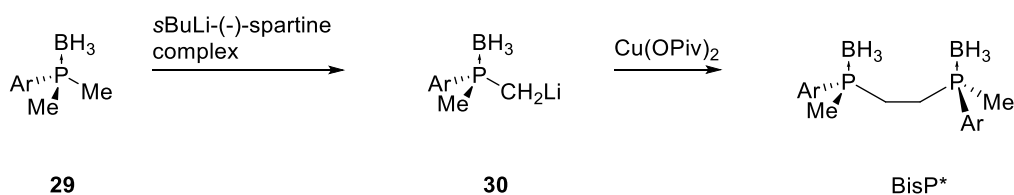
1.3 Tertiary Phosphine Ligands with Asymmetric Phosphorus



Scheme 16: Synthesis of chiral tertiary phosphine boranes from dimethylarylphosphine borane **29**.

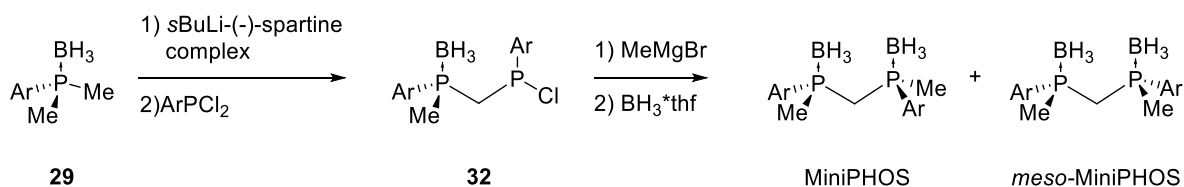
Subsequently, **30** was treated with benzophenone and compound **31** could be obtained in yields and enantiomeric excesses above 80 %.

This methodology could also be applied to synthesise bidentate tertiary phosphines like BisP* or MiniPHOS (Scheme 17 and 18). Evans used copper(II) pivalate for the oxidative coupling of compound **30**. BisP* could be enantioenriched by recrystallisation from ethyl acetate and hexane to achieve enantioselectivities of >99 %.



Scheme 17: Synthesis of BisP* from dimethylarylphosphine borane.

MiniPHOS was designed by Imamoto and Yamanoi in 1999.⁵² They also started from dimethylarylphosphine borane and treated it with the sBuLi(-)-sparteine complex and ArPCl₂, subsequently (Scheme 18). In the final step, the chlorophosphine **32** was converted with MeMgBr and BH₃ to achieve the optically active MiniPHOS and its *meso*-form in a 1:1 ratio.



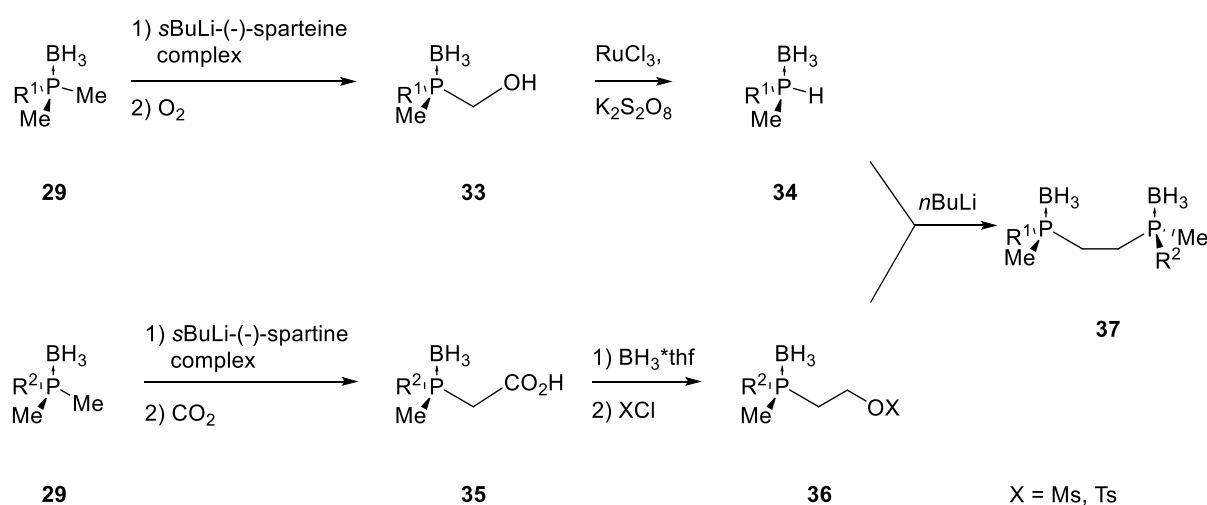
Scheme 18: Synthesis of MiniPHOS from dimethylarylphosphine borane **29**.

1. Introduction

1.3 Tertiary Phosphine Ligands with Asymmetric Phosphorus

MiniPHOS could be separated by from its *meso*-form by recrystallisation from methanol or ethanol.

Enantioselective deprotonation using chiral bases is not only a way to synthesise C_2 -symmetric bidentate phosphines but also diphosphines with two different *P*-centres. Imamoto and his working group published in 2001 a preparative route where an enantiopure secondary phosphine⁵³ and a tertiary phosphine⁵⁴ bearing an alkyl group with a good leaving group were coupled (Scheme 19). The secondary phosphine borane **34** was synthesised from **29** via deprotonation with the *s*BuLi(-)-sparteine complex. Molecular oxygen was used as electrophile to introduce a hydroxy group. The P-C bond was cleaved by oxidative degradation of the primary alcohol using Ru(III)-catalysed oxidation with $K_2S_2O_8$. The second intermediate **36** was produced in a similar way using CO_2 instead of molecular oxygen in the first step. The carboxylic acid of compound **35** was then reduced with $BH_3 \cdot thf$ and reacted with TsCl or MsCl to achieve **36** bearing a good leaving group. In a last step the intermediates **34** and **36** were coupled to unsymmetrical BisP* **37** in quantitative yields and with high enantioselectivities >97 %.



Scheme 19: Synthesis of unsymmetrical BisP* **37**.

1.3.2.7 Chiral Ferrocenyl Phosphines

Chiral diphosphine ligands with a ferrocene backbone are known to be highly active and enantioselective in various transition metal catalysed reactions.⁵⁵ There are various structurally different types of chiral ferrocenyl phosphines but the most common ones are Josiphos⁵⁶, Taniaphos⁵⁷, Mandyphos⁵⁸, Walphos⁵⁹, TRAP⁶⁰ and BoPhoz⁶¹ (Figure 5). They are commercially available and often used in homogeneous asymmetric catalysis.

1. Introduction

1.3 Tertiary Phosphine Ligands with Asymmetric Phosphorus

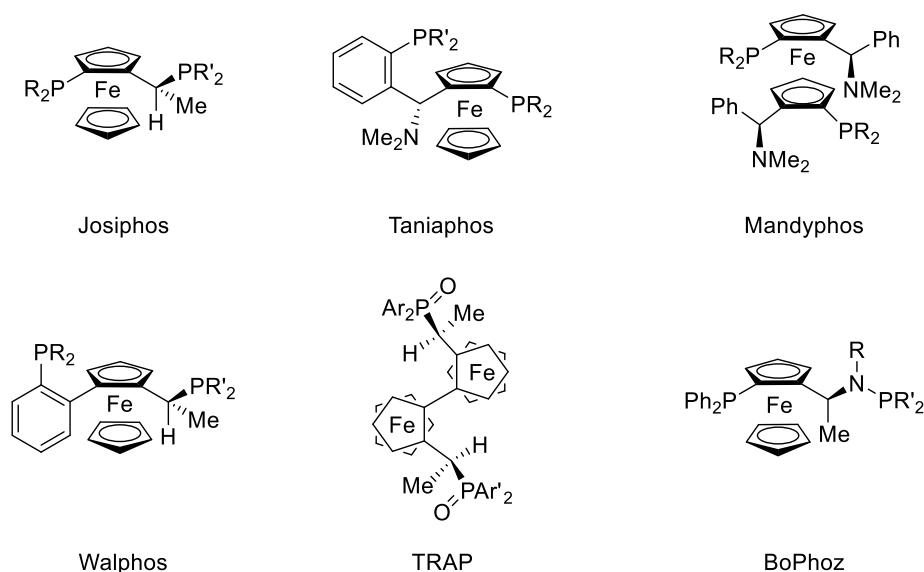
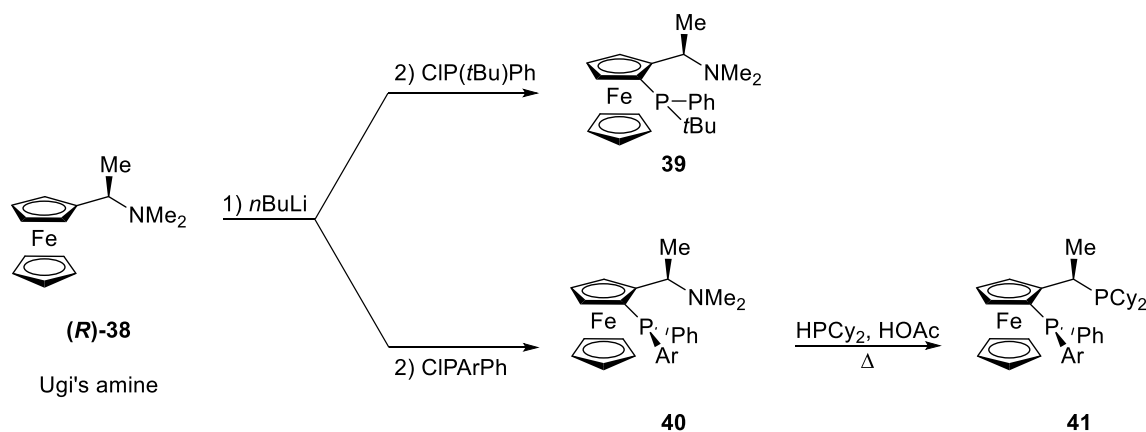


Figure 5: Common ferrocenyl phosphines.

Often those ferrocene containing structures can be synthesised by standard methods for the preparation of *P*-stereogenic compounds as shown in the procedures above.^{19d} But, there are also interesting routes where enantiopure ferrocenyl units are coupled with racemic or achiral phosphorus fragments and subsequent resolution of diastereomers is needed.

The ferrocenyl fragment is chiral when it is *o*-substituted. Moreover, there are many examples in which the side chains bear additional chiral carbon atoms.⁵⁵ A common starting point of the procedure to achieve chiral ferrocenyl phosphines is the well-known Ugi's amine (**38**).^{62,63} Cullen and his working group developed a diastereoselective *ortho*-lithiation of **38** (Scheme 20).⁶² By reacting with racemic $ClP(tBu)Ph$ compound **39** was obtained as a single diastereoisomer.



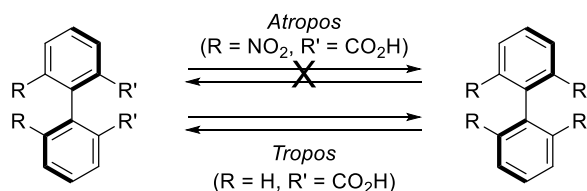
Scheme 20: Synthesis of enantiopure ferrocenyl phosphines from Ugi's amine (**38**).

Togni and co-workers transferred the *ortho*-lithiated species of **38** with ClPArPh into the epimers **40**, which could be separated by column chromatography (Scheme 20).⁶³ To obtain a diphosphine structure, **40** was treated with HPCy₂ under acidic conditions. The nucleophilic substitution occurred at the carbon bearing the dimethylamino group. NMe₂ was replaced by PCy₂ to yield the *P*-stereogenic ferrocenyl diphosphine **41**.

1.3.3 Chiral Biaryl Backbones

As shown in the sections above, chirality of the ligands can be incorporated into the metal complex by different elements of chirality, e. g. by chirogenic carbon centres or axial chirality. A particular challenge represents the use of *P*-chirogenic centres. Considering the great variety of such ligands, it is not astonishing that in the literature numerous hybrid ligands can be found containing chirogenic phosphorus and carbon centres. In contrast, ligands possessing both *P*-chirogenic centres as well as axial chirality are rare.¹⁹

A special case of axial chirality is the so-called atropisomerism. Atropisomeric compounds are rotamers whose rotation occurs at a C-C-single bond (Scheme 21). Their rotation is restricted due to bulky substituents; therefore they can be isolated as single conformers.



Scheme 21: Atropisomerism of biphenyl compounds.

The word atropisomer derives from the Greek word Atropos (‘ατροπος’ = ‘she who cannot be turned’).⁶⁴ The Greek mythology says that Atropos is one of the three sisters Moirai who are the personification of the inescapable destiny of man. Atropos cuts the thread of a man’s life with her shears after their sisters Klotho and Lachesis have spun and measured its length, respectively. The cut of Atropos is absolutely unalterable and therefore the dynamic behaviour of molecules with a chiral axis is described as ‘tropos’ for free rotation and ‘atropos’ for restricted rotation.

At the beginning of the 21st century, chemists started to investigate ligands by combining different symmetry elements in one molecule. They hoped to affect more easily the asymmetric

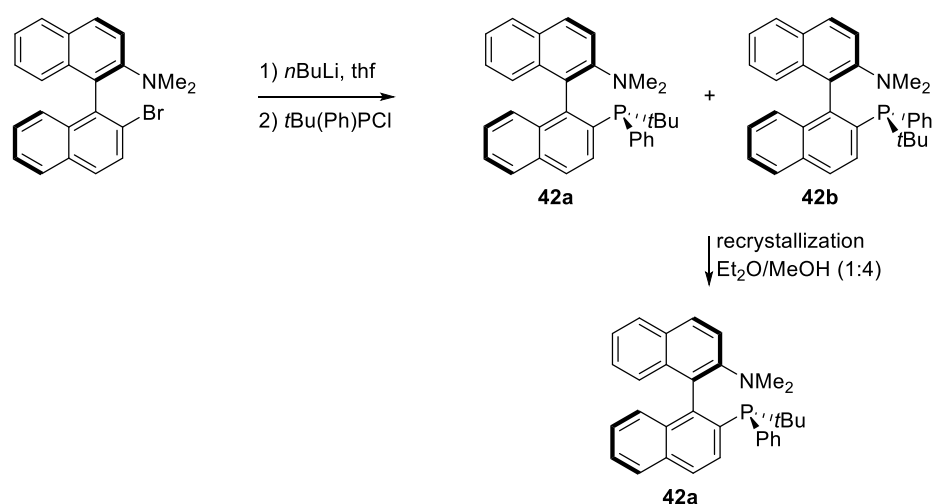
1. Introduction

1.3 Tertiary Phosphine Ligands with Asymmetric Phosphorus

catalytic system which could lead to an increase of enantiomeric excess and turnover frequencies. Furthermore, it could help to develop a better comprehension of important factors in ligand design and chirality transfer.

1.3.3.1 Monodentate Tertiary *P*-Chirogenic Phosphines with Additional Axial Chirality

The first who published monodentate phosphines combining both a chirogenic *P*-centre and atropisomerism were Hamada and Buchwald in 2002.⁶⁵ In the first step (*R*)-2-bromo-2'-*N,N*-(dimethylamino)-1,1'-binaphthyl was submitted to a lithium-halogen exchange with *n*BuLi (Scheme 22). Subsequent addition of the *P*-chirogenic chlorophosphine gave the diastereomeric products **42a** and **42b** which could be separated by recrystallisation. The isolated yield of (*R,R*)-(+)-**42a** was 12 %.

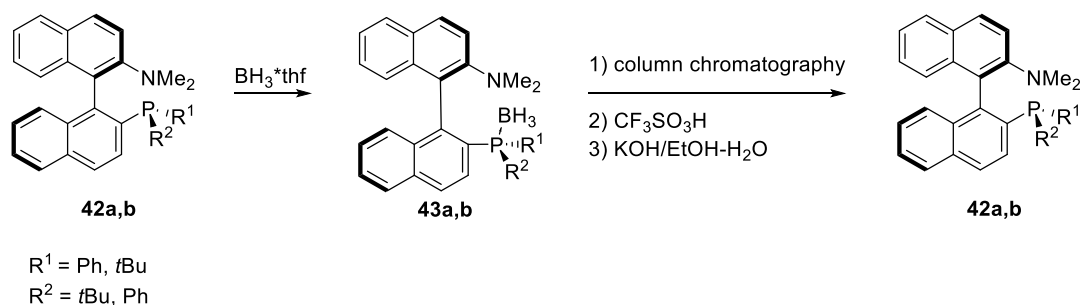


Scheme 22: Synthesis of *P*-chirogenic binaphthyl monophosphines **42** by Hamada and Buchwald.

The other diastereomer could be obtained by addition of BH₃*thf to the mother liquor resulting from the recrystallisation of (*R,R*)-**42a** to get the phosphine-borane-adducts **43a,b** (Scheme 23). These diastereomers could be likewise separated by column chromatography to afford additionally 11 % of (*R,R*)-**42a** (23 % overall yield) and 16 % of (*R,S*)-**42b**.

1. Introduction

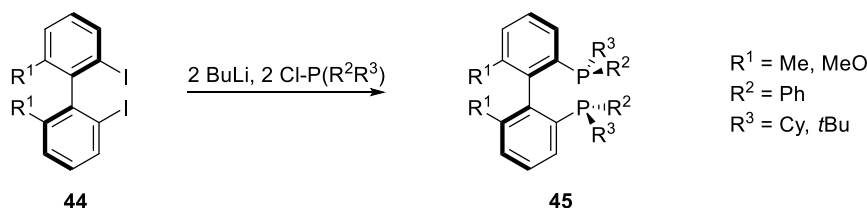
1.3 Tertiary Phosphine Ligands with Asymmetric Phosphorus



Scheme 23: Separation of diastereomeric binaphthyl monophosphines **42a,b** by Hamada and Buchwald.

1.3.3.2 Bidentate Tertiary *P*-Chirogenic Phosphines with Additional Axial Chirality

There are only a few examples of phosphines containing two *P*-chirogenic centres together with axial chirality. Cereghetti et al. published in 1996 the synthesis of a phosphine which bears such two elements of chirality (Scheme 24).⁶⁶ For the synthesis, the enantiomerically pure 6,6'-dimethyl- or 6,6'-dimethoxy-2,2'-diiodo-1,1'-diphenyl (**44**) was dilithiated and treated afterwards with racemic chlorophosphines at -70 °C. As substituents of the chlorophosphines phenyl, cyclohexyl or *t*butyl groups were used. The reaction was realised in yields of 60-80 %. Full retention of the axial chirality was noted. The resulting diastereomers were separated by column chromatography and crystallised from EtOAc/MeOH.



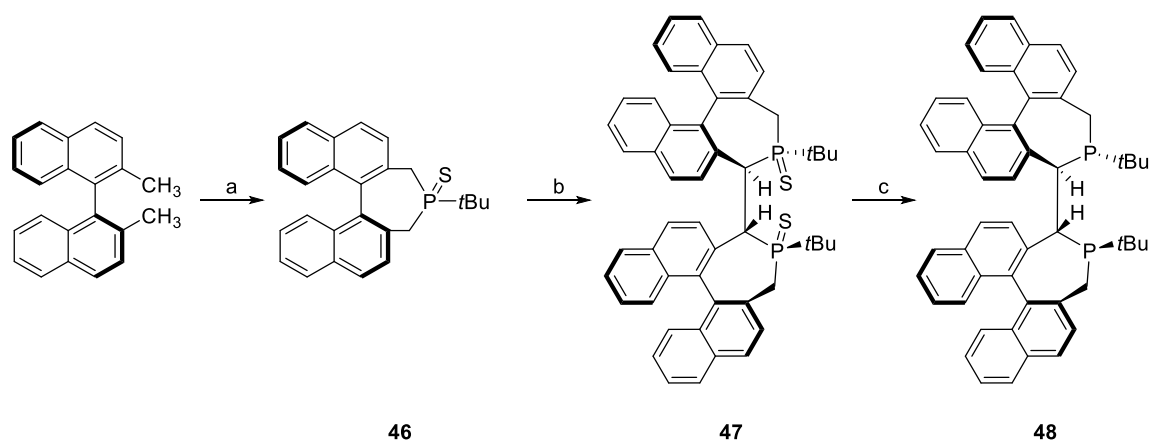
Scheme 24: Synthesis of atropisomeric diphosphine ligands by Cereghetti et al.

Zhang and co-workers published in 2003 the synthesis of bisphosphines with two chirogenic *P*-centres and two atropisomeric BINAP units (Scheme 25).⁶⁷ After dilithiation of 2,2'-dimethylbinaphthyl with *n*BuLi/TMEDA, the *t*BuP-unit was introduced by employing *t*BuPCl₂. Addition of elemental sulphur provided the relevant binaphthophosphine sulphide **46**. With the assistance of *t*BuLi/TMEDA compound **46** was deprotonated and subsequently coupled in

1. Introduction

1.3 Tertiary Phosphine Ligands with Asymmetric Phosphorus

a CuCl_2 mediated reaction yielding the enantiopure compound **47**. The latter could be desulphurised using hexachlorodisilane to give **48**.

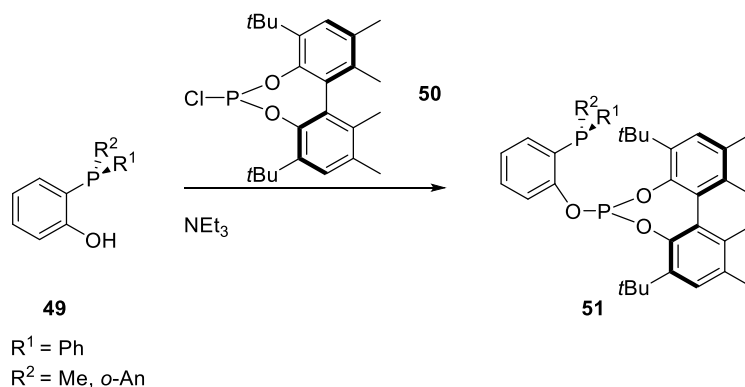


a) 1. $n\text{BuLi/TMEDA}$, Et_2O ; 2. $t\text{BuPCl}_2$, S_8 , thf ; b) $t\text{BuLi/TMEDA}$, hexamethyl phosphoramide/ thf , CuCl_2 ; c) Si_2Cl_6 , benzene.

Scheme 25: Synthesis of bisphosphepine ligands with two chirogenic *P*-centres and two atropisomeric BINAP units by Zhang et al.

Compound **48** was tested in the Rh-catalysed asymmetric hydrogenation of methyl (*Z*)- β -aryl- β -(acetylamino)acrylates. Independently from the electronic properties of diverse aryl substituents, the enantiomeric excess of the products was nearly exclusive more than 99 %.

In 2007, the working group of Pizzano published the synthesis of phosphine-phosphites with one *P*-chirogenic centre as well as one centre of axial chirality (Scheme 26).⁶⁸ In their protocol (2-hydroxyphenyl)phosphine (**49**) was treated with (*R*)-3,3'-di-*t*-butyl-5,5',6,6'-tetramethyl-2,2'-bisphenoxyphosphorous chloride (**50**) in the presence of NEt_3 . Compound **51** was isolated by column chromatography.



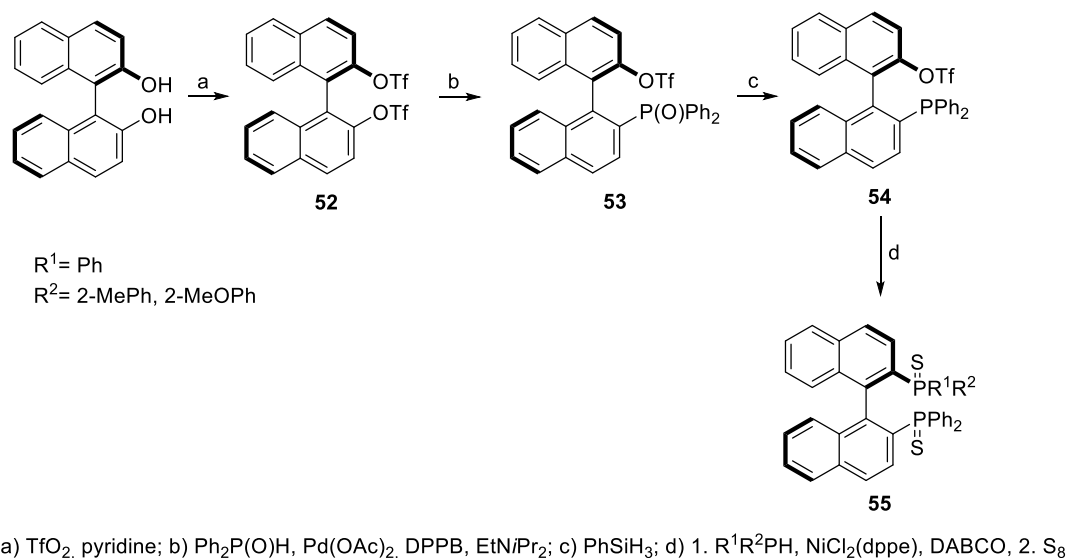
Scheme 26: Synthesis of phosphine-phosphites by Pizzano et al.

1. Introduction

1.3 Tertiary Phosphine Ligands with Asymmetric Phosphorus

The hybrid ligand **51** was tested in some hydroformylation reactions and provided *iso/n*-ratios of 98/2 and ee values up to 43 % for styrene and *iso/n*-ratios of 94/6 and ee values up to 23 % for allyl cyanide.⁶⁹

The synthesis of *P*-chirogenic BINAP bisulfide analogues was published in 2011 by Gilheany and colleagues (Scheme 27).⁷⁰ Enantiomerically pure (*R*)-BINOL was reacted with triflic anhydride in the presence of a base to give bis-triflate **52**. To introduce one diphenylphosphine oxide unit, Pd(OAc)₂ was used as coupling catalyst. In the next step, the phosphine oxide was reduced with PhSiH₃ to “provide space for the subsequent nickel catalysed coupling” of R¹R²PH with triflate **54**. To obtain the *P*-chirogenic BINAP bisulphide analogues the crude products were treated directly with elemental sulphur. Compounds **55** received were purified and the diastereomers were separated by column chromatography.



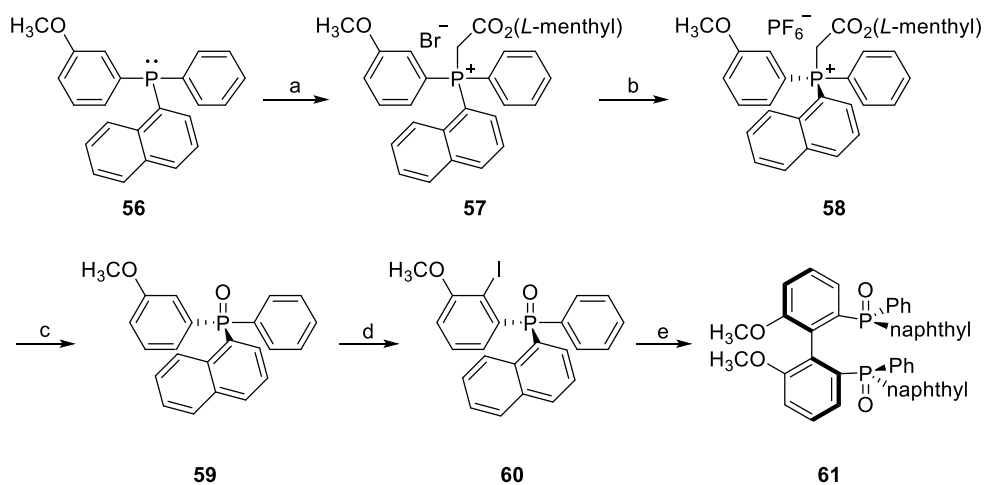
Scheme 27: Synthesis of *P*-chirogenic BINAP bisulphide analogues **55** by Gilheany et al.

In 2010, the group of Pietrusiewicz published the synthesis of atropisomeric biphenyl diphosphine dioxide **61** via an asymmetric Ullmann coupling (Scheme 28).⁷¹ They started their synthetic route with a racemic triaryl phosphine **56** which was reacted with *L*-menthyl bromoacetate to give a mixture of two epimers of phosphonium bromides **57**. After replacement of the bromide anion by hexafluorophosphate, enantiomerically pure (*S*)-**58** could be obtained by recrystallisation. After removal of the chiral auxiliary *L*-menthyl acetate by Wittig-reaction (which proceeded under retention of the configuration at the *P*-centre), the enantiopure product **59** was *ortho*-lithiated by reaction with LDA at -78 °C. The lithiated species was treated with

1. Introduction

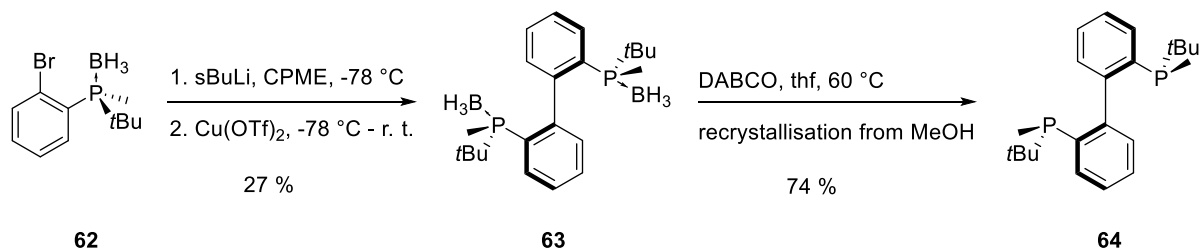
1.3 Tertiary Phosphine Ligands with Asymmetric Phosphorus

iodine to give the aryl iodine **60**. The latter was coupled under Ullmann conditions to afford the atropisomeric biphenyl diphosphine dioxide (S_a, S_P, S_P)-(+)-**61** with 27 % yield.



Scheme 28: Synthesis of atropisomeric biphenyl diphosphine dioxide (S_a, S_P, S_P)-(+)-**61** due to Pietrusiewicz et al.

In 2018, Imamoto and co-workers published a new ligand called BipheP* **64** which consists of a biphenyl backbone and two chirogenic *P*-centres in 2,2'-position.⁷²



Scheme 29: Synthesis of BipheP* due to Imamoto et al.

As a starting material, they used enantiopure (*R*)-2-bromophenyl(*t*butyl)(methyl)phosphine borane (**62**) which was treated with *s*BuLi. In the second step, $\text{Cu}(\text{OTf})_2$ was applied at -78°C to perform the homocoupling. After deprotection of the phosphorus with DABCO, they obtained (*R,R*)-2,2'-bis((*t*butyl)(methyl)phosphino)biphenyl (BipheP*, **64**). The phosphine exists as a single diastereomer in respect to the bulky substituents which restrict the rotation around the C-C-bond between the phenyl rings. Diphosphine **64** provided high yields and

1. Introduction

1.3 Tertiary Phosphine Ligands with Asymmetric Phosphorus

enantioselectivities (up to 97 %) in Rh-catalysed hydrogenations of various prochiral methyl (*Z*)-2-acetamido-3-arylacrylates.

2. Investigation of *P*-Chirogenic Di(triaryl phosphines)

2.1 Aim of the investigations

Since the breakthrough in asymmetric hydrogenation of Dang and Kagan in 1971 with the first bidentate C₂-chiral diphosphine DIOP used as a ligand in Rh-complexes, a broad variation of bidentate phosphines was created and studied intensively. These phosphines should be cost-effective and producible in milligram to kilogram scale. Furthermore, they should be variable in their structure, bind sufficiently strong to the metal centre and provide high activity and selectivity in the catalytic transformation. Some of these so-called “privileged ligands”,¹⁹ are shown in the figure below, provide in several catalytic applications excellent enantioselectivities and high productivity.

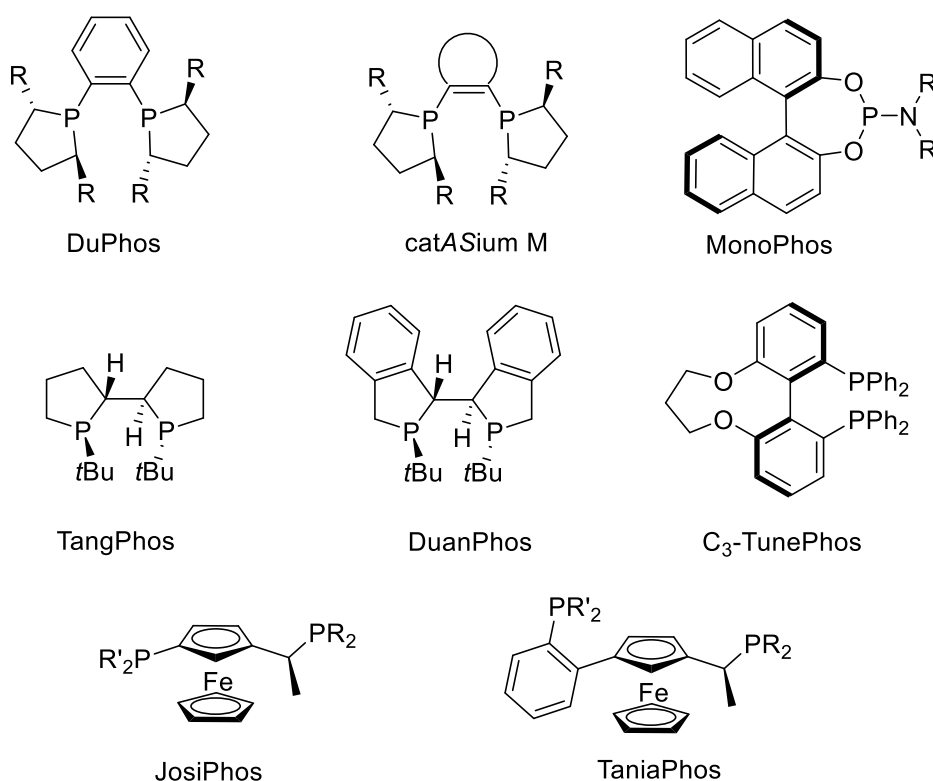


Figure 6: Common "privileged ligands".

There are numerous other chelating diphosphines such as DiPAMP, BINAP, 1,1'-di(diphenylphosphino)ferrocen, Xantphos and DPEphos which are of great interest. DiPAMP and BINAP are *P*-chirogenic and axially chiral, respectively. In contrast to these chiral compounds, 1,1'-di(diphenylphosphino)ferrocen, Xantphos and DPEphos are achiral. However, all these compounds have one thing in common: They possess triaryl phosphine units. These triaryl phosphines are nearly resistant to oxidation by air and therefore easy to handle.

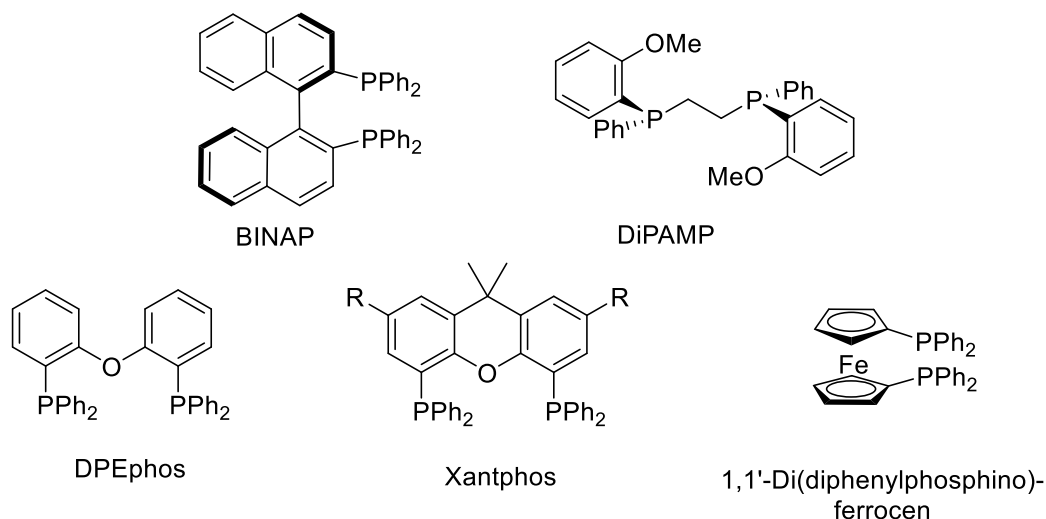


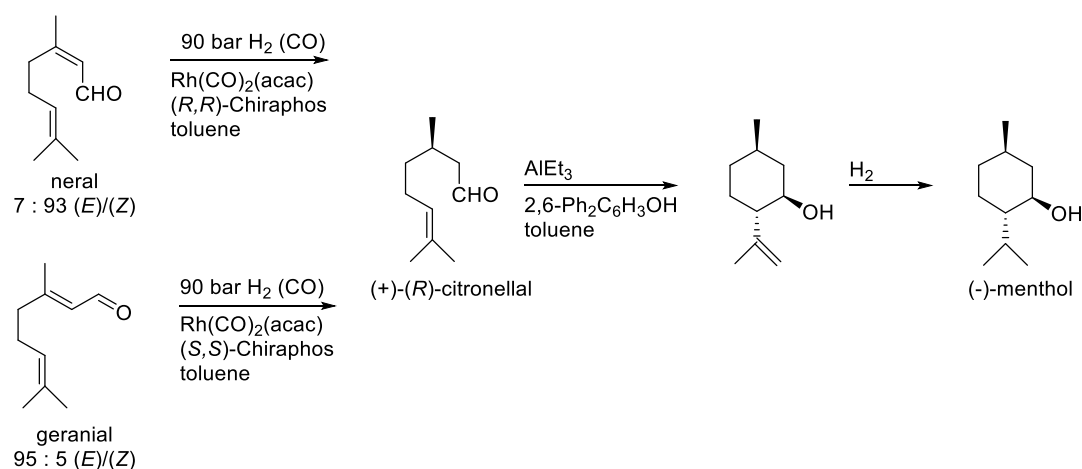
Figure 7: Common chelating triaryl phosphines.

The applications of the named achiral phosphines are limited in catalysis. DPEphos and Xantphos provide rigid backbones which generate large bite angles in respect to the coordination to the metal centre. The natural bite angles of DPEphos and Xantphos amount 102 ° and 112 °, respectively, whereat the angles exhibit certain flexibility. As mentioned in Chapter 1.2, the natural bite angle influences the coordination geometry of catalytically active complexes. This defined coordination modus can stabilise or destabilise catalyst-substrate intermediates and therefore support the significant reaction step. Bite angles about 120 ° as typically for Xantphos derivatives increase the *n*-selectivity in hydroformylation reactions, whereas bite angles about 90 ° lead to the *iso*-product.⁹

A further interesting property of DPEphos and Xantphos is shown in the presence of an ether group in the compounds. The oxygen in the diphosphines provides an additional (potential hemilabile) coordinating atom able to interact with the transition metal.

A former research project of the working group had the aim to synthesise citronellal selectively from citral (neral/geranial). Actually, the BASF SE uses (*R*)-citronellal as starting material for the menthol-synthesis. (*R*)-Citronellal can be synthesised via asymmetric hydrogenation of citral (mixture of neral and geranial) in the presence of a Rh-Chiraphos catalyst. It is remarkable that the reaction only proceeds quantitatively with small amounts of CO during the generation of the active catalyst species as well as during the catalysis itself (Scheme 30). The reaction generates an enantiomeric excess of about 83 %. The presence of toxic and relatively expensive carbon monoxide requires supplementary technological effort and additional safety measures.

It was shown in our research group, that the α,β -located double bond in the starting material citral could be hydrogenated selectively under mild conditions in the absence of CO by using Xantphos or DPEphos as ligands.⁷³ The advantages of the usage of Xantphos or DPEphos are not only the prevention of additional safety devices during operation due to the avoidance of CO but also the milder reaction conditions in respect to pressure (1-25 bar) and temperature (25 °C). Under these reaction conditions, citronellal was produced with more than 90 % yield and side reactions, such as the formation of citronellol as secondary product of the aldehyde reduction, could be inhibited effectively.



Scheme 30: BASF menthol-process.

At this point the following question arose: Is it possible to convert Xantphos or DPEphos into chiral compounds to allow subsequently the catalytic synthesis of enantiomerically enriched (*R*)-citronellal.

Two options could lead to this aim: Either chiral substituents will be introduced into the backbone of these molecules or into the substituents of the phosphorus, or the chirality could be installed directly at the phosphorus atom as a *P*-chirogenic derivative. Since the chiral substituents in the backbone would be located in a very remote distance to the active centre at the metal atom, this manipulation of the molecules seemed not to be as effective for the enantioselective hydrogenation as the introduction of chirality into the phosphorus unit.

Therefore, we decided to replace the PPh₂- by PPh(Ar)-groups. The presence of three different aryl groups directly at the active reaction centre promises a high selectivity of the reaction in dependence of the substitution pattern of the aromatic ring.

At the beginning we started with the synthesis and application of Xantphos derivatives (Figure 8). The *P*-chirogenic groups consist of a phenyl group and another substituted aryl group beside the xanthene backbone as the third aromatic substituent at phosphorus atom.^{74,75}

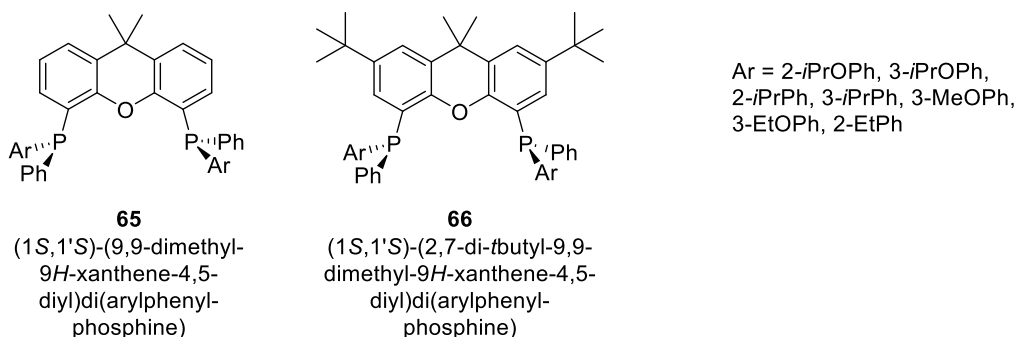


Figure 8: *P*-chirogenic Xantphos derivatives.

Finally, it could be shown that the application of such *P*-chirogenic Xantphos derivatives as ligands in the asymmetric hydrogenation of neral yielded only enantioselectivities up to 30%.⁷⁶

In continuation, the work was focused on the synthesis and application of DPEphos- and DBFphos derivatives.

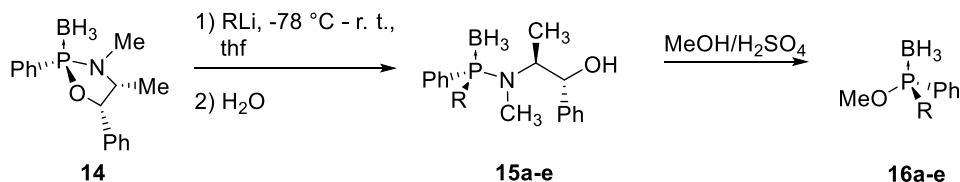
Furthermore, to examine the racemisation behaviour of such triaryl phosphine derivatives at ambient or enhanced temperatures some long-term temperature NMR stability tests of these phosphines were carried out.

2.2 Results and Discussion

2.2.1 Synthesis of *P*-Chirogenic Triaryl phosphines with a DPE-Backbone

Since diphenyl ether (DPE) is quite similar to xanthene, regarding the structure of two phenyl rings connected by an ether group, it was decided to synthesise *P*-chirogenic Xantphos analogues bearing the DPE structure. The unique feature of DPE is the flexibility of this molecule due to the ether bridge.

Thus, several (aryl)methyl-(phenylphosphinite)-borane adducts **16a-e** were synthesised based on the (-)-ephedrine methodology developed by Jugé and co-workers (Chapter 1.3.2.5.1) (Scheme 31).²⁵



Scheme 31: Synthesis of (aryl)methyl-(phenylphosphinite)-boranes **16a-e**.

The first step was the ring opening of 1,3,2-oxazaphospholidine in which an aryl group was introduced stereoselectively into the phospholidine **14**. Compounds **15a-e** were formed with retention of the configuration at the *P*-centre. By NMR investigations, it was found that products **15** were formed diastereomerically pure and in good to excellent yields (Table 1). Subsequently, the aminophosphines **15** were cleaved by acidic methanolysis. The reaction proceeded under the inversion of the *P*-centre. Compounds of type **16** were obtained in enantiopure state and in good to excellent yields (Table 1). Different aryl lithium groups were chosen to broaden the scope of the ligand family and to study the electronic and steric influence during the catalytic reactions.

Table 1: Yield of compound **10** with different substituents.

Product	R	15		16	
		Yield	%de ^a	Yield	%ee ^b
a	2-EtOPh	81 %	100	79 %	>99
b	3-EtOPh	90 %	100	83 %	>98
c	4-EtOPh	71 %	100	79 %	>99
d	3-MeOPh	93 %	100	79 %	>98
e	3- <i>i</i> PrOPh	88 %	100	85 %	>99

a) Estimated by quant. ³¹P NMR. b) Estimated by chiral HPLC.

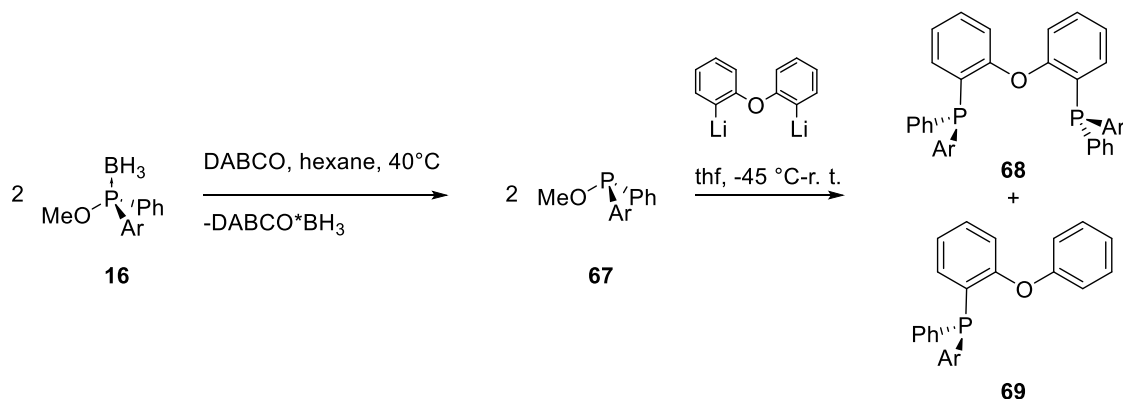
Due to Jugé's methodology, the third aryl group can be readily introduced into the phosphinite borane by the reaction of **16** with alkyl or aryl lithium.²⁵ Since the phenyl groups of DPE provide free rotation of the backbone, the first intention was to introduce the two P-units as

borane adducts. Provided that the phenyl rings of DPE can turn the P-groups into opposite directions of the molecule, the bulky substituents of the phosphorus units should not interfere with each other.

Unexpectedly, it was found that the reaction of the dilithiated DPE with two equivalents of BH₃-protected chiral methyl phosphinites (such as **16**) failed.

Therefore, it was necessary to remove the BH₃-protection group of the phosphinite borane with DABCO prior to the introduction of the phosphinite units into the DPE backbone (Scheme 32).

Afterwards, the free phosphinite **67** was treated with the dilithiated DPE. After hydrolysis, two species were found in the raw product: The mono- and the di-substituted DPE-derivative **68** and **69**.



Scheme 32: Synthesis of the DPE-derivatives **68**.

It is interesting to note, that although phosphinite **67** was added in an excess of 2.2 equivalents in relation to the DPE, there was a high percentage of mono-substituted product (Table 2). The remaining phosphinite **67** stayed unchanged and could be identified by NMR in the raw reaction mixture.

It is noteworthy, that the yield of mono-substituted product **69** increased with the increase of bulkiness of the substituent in ortho position (3-MeOPh < 3-EtOPh < 3-*i*PrOPh). Also the substitution pattern in the aryl group affected the conversion to mono- or di-product. The ratio between **68** and **69** decreased with increasing distance of the substituents (2-EtOPh < 3-EtOPh < 4-EtOPh).

Table 2: Ratio of mono- and disubstitution of the DPE-backbone.

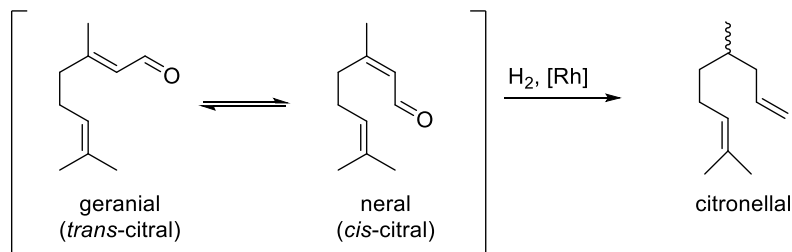
Ar	Conversion to 68 ^a	Conversion to 69 ^a	Yield 68 ^b
a 2-EtOPh	44 %	23 %	41 % (90 %)
b 3-EtOPh	39 %	9 %	30 % (94 %)
c 4-EtOPh	67 %	8 %	21 % (97 %)
d 3-MeOPh	69 %	15 %	47 % (94 %)
e 3- <i>i</i> PrOPh	37 %	25 %	22 % (96 %)

^aRatios were estimated by quant.³¹P NMR. ^bRatio of **68** after column chromatography in parenthesis, estimated by quant.³¹P NMR.

Since the polarity of the mono- and di-product is quite similar, a separation of both phosphines via column chromatography or crystallisation could not be completely achieved. The purity of the disubstituted product **68** varied between 90 to 97 % (Table 2). Nevertheless, the products were used as ligands in a subsequent asymmetric catalysis to determine their productivity and selectivity since the NMR spectra showed that the compounds **68a-e** were diastereomerically pure.

2.2.2 Asymmetric Catalysis with DPEphos ligands

Previous experiments showed that the asymmetric hydrogenation of neral/geranial to citronellal with *P*-chirogenic Xantphos derivatives resulted in fairly good conversions but did only provide poor enantiomeric excesses up to 22 % (Scheme 33).⁷⁵



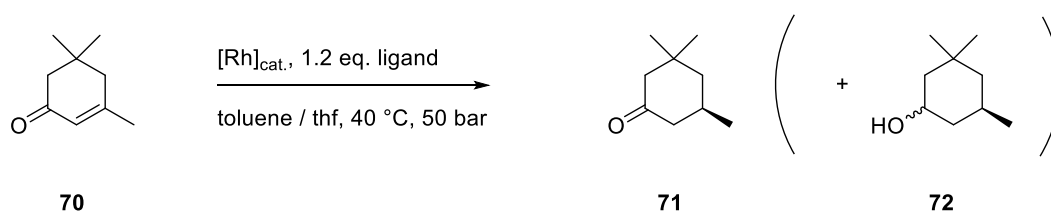
Scheme 33: Hydrogenation of citral to citronellal.

Citral is a configurationally flexible α,β -unsaturated aldehyde with an additional double bond. Due to the enhanced reactivity of the molecule, the isomerisation between neral and geranial is promoted. The different geometrical isomers of citral may lead to the formation of opposite enantiomers of citronellal in the asymmetric hydrogenation. Due to this facile transition between α,β -unsaturated aldehydes, the asymmetric hydrogenation of citral may proceed with low enantioselectivity finally.

As a result of these investigations, other substrates were used to examine the stereodifferentiating properties of the DPEphos derivatives. The Rh-catalysed asymmetric hydrogenation of isophorone and the Pd-catalysed asymmetric allylation of dimethyl malonate with DPEphos ligands were studied as alternatives.

2.2.2.1 Rh-Catalysed Asymmetric Hydrogenation of Isophorone with DPEphos Ligands

To investigate the stereodifferentiating properties of the DPEphos derivatives, they were screened as ligands in asymmetric hydrogenation of isophorone (**70**, Scheme 34).



Scheme 34: Asymmetric hydrogenation of isophorone **70** to chiral ketone **71** and alcohol **72**.

Not only the stereoselectivity but also the chemoselectivity of the reaction is a particular challenge for the hydrogenation of **70**, since the substrate bears besides the C=C double bond a carbonyl group. Only the C=C double bond should react with hydrogen while the carbonyl group should be untouched.

Two types of Rh-precursors were tested for the reaction: Rh(acac)(cod) (acac = acetylacetonate, cod = 1,5-cyclooctadiene) and Rh(acac)(CO)₂ (Table 3).

By using Rh(acac)(cod) as precursor for the hydrogenation reaction, the conversion was almost quantitatively independent on the solvent. Only with ligand **68b** in toluene the conversion amounted only 88 % of **71**. Nevertheless, no noteworthy enantiomeric excesses could be determined in this catalytic reaction. Rh(acac)(CO)₂ seemed to be a better choice. Even though the conversion varies between 0 - 100 %, an enantiomeric excess of up to 59 % could be realised. The reactions using toluene as solvent gave superior results in comparison to the use of thf. Noteworthy, the best results in terms of stereoselectivity gave ligands with ortho substituted aryl groups like Ar = 2-MeOPh, 2-EtOPh. The enantiomeric excess decreased by increasing distance between phosphorus and the additional substituent of the aryl group. Whereas the 2-MeOPh-ligand induced an enantiomeric excess of 59 % in toluene and with the Rh(acac)(CO)₂-precursor, the 3- and 4-MeOPh-ligands afforded only 6 and 1 %, respectively. The same phenomenon could be observed by using ligands with EtOPh-substituents. Whereas the 2-EtOPh-ligand yielded an enantiomeric excess of 27 % in toluene and with the Rh(acac)(CO)₂-precursor, both, the 3- and 4-EtOPh-ligands, generated only 3 %.

Table 3: Asymmetric hydrogenation of isophorone^a.

Ligand (Ar)	Solvent	Rh(acac)(cod)		Rh(acac)(CO) ₂	
		Conversion [%] ^b	ee of 71 [%] ^c	Conversion [%] ^b	ee of 71 [%] ^c
68a (2-EtOPh)	toluene	100 (>99)	1 (<i>S</i>)	26 (>99)	27 (<i>S</i>)
68a (2-EtOPh)	thf	100 (>99)	1 (<i>S</i>)	59 (>99)	5 (<i>S</i>)
68b (3-EtOPh)	toluene	88 (>99)	1 (<i>S</i>)	60 (>99)	3 (<i>S</i>)
68b (3-EtOPh)	thf	100 (>99)	2 (<i>S</i>)	0	0
68c (4-EtOPh)	toluene	100 (>99)	1 (<i>S</i>)	51 (>99)	3 (<i>S</i>)
68c (4-EtOPh)	thf	100 (>99)	2 (<i>S</i>)	13 (>99)	1 (<i>S</i>)
68d (3-MeOPh)	toluene	100 (>99)	1 (<i>S</i>)	63 (>99)	6 (<i>S</i>)
68d (3-MeOPh)	thf	100 (>99)	1 (<i>S</i>)	0	0
68e (3- <i>i</i> PrOPh)	toluene	100 (>99)	1 (<i>S</i>)	59 (>99)	1 (<i>S</i>)
68e (3- <i>i</i> PrOPh)	thf	100 (>99)	3 (<i>S</i>)	0	0
68f^d (2-MeOPh)	toluene	8 (>99)	10 (<i>S</i>)	100 (>99) ^e	59 (<i>S</i>)
68f^d (2-MeOPh)	thf	5 (>99)	3 (<i>S</i>)	97 (>99) ^e	51 (<i>S</i>)
68g^d (4-MeOPh)	toluene	100 (93)	1 (<i>R</i>)	10 (>99) ^e	1 (<i>S</i>)
68g^d (4-MeOPh)	thf	100 (78)	1 (<i>R</i>)	10 (>99) ^g	2 (<i>R</i>)
65a^d (2-MeOPh)	toluene	100 (70) ^g	9 (<i>R</i>)	100 (81) ^f	85 (<i>S</i>)
65a^d (2-MeOPh)	thf	100 (75) ^e	9 (<i>R</i>)	100 (97) ^e	84 (<i>S</i>)
65b^d (2-MePh)	toluene	70 (98)	50 (<i>S</i>)	100 (>99) ^e	96 (<i>S</i>)
65b^d (2-MePh)	thf	85 (97)	37 (<i>S</i>)	100 (>99) ^e	97 (<i>S</i>)

^aConditions: 1 mmol of isophorone (138.2 mg), 5 μmol of [Rh], 6 μmol of ligand, 3 ml of solvent, 40 °C, 50 bar, 15 h. ^bDetermined by NMR. The portions of ketone **71** are given in parenthesis. ^cEstimated by GC. ^dSee reference 75,76. ^eHydrogenation time 4 h. ^fHydrogenation time 20 h. ^gHydrogenation time 8 h.

In order to investigate the influence of the solvent on the asymmetric hydrogenation of isophorone, **68a** was used as model ligand, since it gave the best performance in this system. The catalysis was performed as described before, but using different solvents (Table 4).

Table 4: Asymmetric hydrogenation of isophorone (**70**) in dependence on the solvent^a.

Solvent	Rh(acac)(CO) ₂		Rh(acac)(cod)	
	Conversion [%] ^b	ee of 71 [%] ^c	Conversion [%] ^b	ee of 71 [%] ^c
toluene	100 (>99)	1 (<i>S</i>)	26 (>99)	27 (<i>S</i>)
DCM	100 (>99)	1 (<i>S</i>)	12 (>99)	5 (<i>S</i>)
thf	100 (>99)	1 (<i>S</i>)	59 (>99)	5 (<i>S</i>)
AcOEt	100 (>99)	2 (<i>S</i>)	51 (>99)	4 (<i>S</i>)
EtOH	100 (>99)	1 (<i>S</i>)	6 (>99)	8 (<i>S</i>)
MeOH	100 (>99)	1 (<i>S</i>)	11 (>99)	2 (<i>S</i>)

^aConditions: 1 mmol of isophorone (138.2 mg), 5 μmol of [Rh], 6 μmol of ligand, 3 ml of solvent, 40 °C, 50 bar. ^bDetermined by NMR. The portions of ketone **71** are given in parenthesis. ^cEstimated by GC.

Rh(acac)(cod) as metal source provided full conversions independent on the solvent. With Rh(acac)(CO)₂ much lower conversion rates yielded (between 6 % in ethanol and 59 % in thf).

Whereas the conversion rate was the highest with Rh(acac)(cod), this metal source provided only racemic mixtures of the ketone. Rh(acac)(CO)₂ supported the asymmetric transformation and gave slightly higher enantiomeric excesses (between 2 % in methanol and 27 %) in toluene.

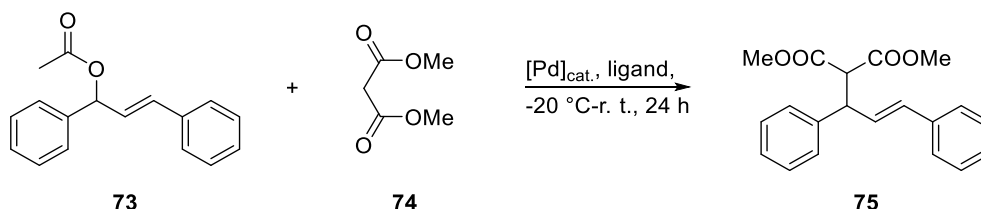
In conclusion, *P*-chirogenic DPEphos seems not to be an appropriate ligand for Rh-catalysed asymmetric hydrogenation of isophorone under our tested conditions. Despite of high conversions with Rh(acac)(cod), the enantiomeric excesses were poor in both catalytic systems in any kind of solvent. Nevertheless, it was found that the formation of ketone **71** was favoured (>99 % in the product) in comparison to the alcohol **72**. Therefore, the regioselectivity of the asymmetric hydrogenation with these DPEphos–ligands was nearly perfect.

Apparently, the lack of stereoselectivity resulted from the flexibility of the back bone of the DPEphos derivatives which could affect the resulting bite angle in the metal complex. In case of a large bite angle the coordination to the metal may be weaker. This situation destabilises the coordination geometry at the catalyst and accelerates isomerisation reactions.⁹ The differences between the stability of the major or minor product nearly vanish and the system does not differentiate the stereoselectivity of the final product.

In comparison to the results with DPEphos ligands it was found, that Xantphos derivatives induce higher enantioselectivities.⁷⁵ Ligand **65a** incorporated in Rh(acac)(CO)₂ gave conversions up to 97 % and enantioselectivities of 96 %. Xantphos ligands possessed a rigid xanthene backbone which seemed to enhance the coordination to the metal and therefore the stereodiscriminating properties of the hydrogenation catalyst.

2.2.2.2 Pd-Catalysed Asymmetric Allylation of Dimethyl malonate with DPEphos Ligands

As a second application of the enantiopure DPEphos derivatives **68** the Pd-catalysed asymmetric allylation of dimethyl malonate (**74**) with (*E*)-1,3-diphenylallyl acetate (**73**) was investigated.



Scheme 35: Asymmetric allylation of dimethyl malonate (**74**) with (*E*)-1,3-diphenylallyl acetate (**73**).

The allylation reaction proceeded under basic conditions at -20 °C to room temperature in 1,2-dichloroethane. Pd(dba)₂ served as metal source in this catalytic system. The product dimethyl (*E*)-2-(1,3-diphenylallyl)malonate (**75**) was isolated by column chromatography. The enantiomeric excess was estimated by chiral HPLC-methods.

Table 5: Asymmetric allylation of dimethyl malonate **74** with (*E*)-1,3-diphenylallyl acetate (**73**)^a.

Ligand (Ar)	yield [%] ^b	ee of 75 [%] ^c
68a (2-EtOPh)	87	64 (<i>R</i>)
68b (3-EtOPh)	84	36 (<i>R</i>)
68c (4-EtOPh)	84	16 (<i>S</i>)
68d (3-MeOPh)	60	29 (<i>R</i>)
68e (3- <i>i</i> PrOPh)	6	33 (<i>R</i>)
68f ^d (2-MeOPh)	89	82 (<i>R</i>)
68g ^d (4-MeOPh)	86	6 (<i>S</i>)
68h ^d (2- <i>i</i> PrOPh)	83	34 (<i>R</i>)
65a ^d (2-MeOPh)	92	93 (<i>R</i>)
65b ^d (2-MePh)	82	90 (<i>R</i>)

^aConditions: 1 mmol of dimethyl malonate **74** (132 mg), 1 mmol of (*E*)-1,3-diphenylallyl acetate (**73**), 0.2 mmol of lithium acetate (13 mg), 5 ml 1,2-dichloroethane, 1 mmol *N,O*-bis(trimethylsilyl)acetamide (203 mg), 10 μmol of Pd(dba)₂ (5.75 mg) and 10 μmol of ligand.

^bDetermined by NMR. ^cEstimated by chiral HPLC. ^dSee reference 75.

By the application of DPEphos derivatives **68** as ligands in most cases good to excellent yields (between 83 to 89 %) could be obtained. Only **68d** and **68e** gave yields of 60 % and 6 %, respectively. The stereoselectivity of this reaction depends on the substituent at the P-aryl group. By shifting the substituent from *ortho*- via *meta*- to *para*-position the enantiomeric purity of **75** decreased. As Table 5 shows, for the MeO-substituent at the aryl ring, the enantiomeric excess of the product **75** dropped from 82 % to 29 and 6 %, respectively. A similar trend could be seen for ligands bearing EtOPh- and *i*PrOPh-substituents. It is noteworthy, that the DPEphos with aryl substituents in 2- and 3-position yielded the (*R*)-enantiomer of **75**, whereas the *para*-substituted derivatives provided predominantly the (*S*)-enantiomeric product.

In comparison to the DPEphos ligands **68**, the Xantphos derivatives **65** provided higher enantioselectivities. **65b** yielded 92 % of **75** with 93 %ee in contrast to **68f** which allowed a yield of 89 % and an enantiomeric excess of 82 % (*R*).

2.2.3 Synthesis of *P*-Chirogenic Triarylphosphines with a DBFphos-Backbone

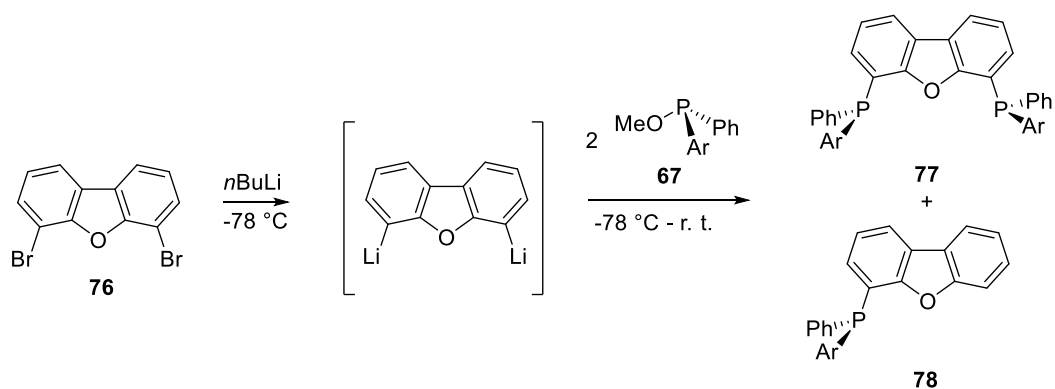
Since the DPE-backbone is rather flexible, another xanthene-like molecule - dibenzofuran - which possesses an ether group between the phenyl groups and a C-C-bridge to stabilise the steric of the backbone was employed as a backbone for the formation of *P*-stereogenic DBFphos derivatives **77**. It was assumed that such DBFphos derivatives could be rigid enough to provide high stereoselectivity in asymmetric catalysis.

4,6-Dibromodibenzo[b,d]furan was used as starting material to couple the phosphinites **16** in *ortho*-position of the fused rings. Since the distance between the *ortho*-positions is spread due to the furan structure in the middle, we speculated, that the simultaneous introduction of two phosphinite BH₃-adducts **16** into the backbone could be possible.

In contrast, it was found, that no reaction took place at all. The pure phosphinite BH₃-adduct **16** was recovered. Not even the mono-substituted DBFphos was formed.

Therefore, it was decided to remove the BH₃-group of the methyl phosphinite **16** first, to enhance the conversion with the dilithiated DBF (Scheme 36)

The synthesis of these diphosphines proceeded analogously to the procedure for the synthesis of the DPEphos derivatives **68**.



Scheme 36: Synthesis of DBFphos derivatives **77**.

Table 6: Conversion and yield of the synthesis of DBFphos derivatives.

Ar	Conversion to 77 ^a	Conversion to 78 ^a	Yield 77 ^b
a 2-EtOPh	75.4 %	5.4 %	56 % (94 %)
b 3-EtOPh	92.8 %	7.2 %	80% (96 %)
c 2-MeOPh	94.3 %	5.7 %	70 % (98 %)

^aEstimated with quant. ³¹P NMR. ^bRatio of **77** after column chromatography in parenthesis, estimated by quant. ³¹P NMR.

Product **77** could be obtained in diastereomerically pure form in moderate yield (Table 6). Likewise to the results with the DPEphos derivatives, by synthesis of the DBFphos derivatives a small amount of mono-substituted product **78** was formed. Since products **77** and **78** are quite similar with respect to polarity, the products could not be separated accurately by column chromatography or crystallisation.

The diphosphines **77** were tested in Rh-catalysed asymmetric hydrogenation of isophorone and Pd-catalysed asymmetric allylation of dimethyl malonate.

2.2.4 Asymmetric Catalysis with DBFphos Ligands

2.2.4.1 Rh-Catalysed Asymmetric Hydrogenation of Isophorone with DBFphos Ligands

To investigate the stereodifferentiating properties of the DBFphos derivatives, they were applied as ligands in the Rh-catalysed asymmetric hydrogenation of isophorone (**70**) (Scheme 34).

In Table 7 it can be seen that DBFphos derivatives used as ligands in the asymmetric hydrogenation provided conversions of 23-100 % with Rh(acac)(cod) as metal source and yields of 0-75 % using Rh(acac)(CO)₂. The stereoselectivity of the hydrogenation was poor. With both precatalysts the ketone **71** was formed in a nearly racemic manner. The only exception was the hydrogenation of isophorone employing Rh(acac)(CO)₂ in thf with **77a** as ligand. At a good conversion rate of 75 %, 24 %ee could be achieved, which was the best result in this series. Under the same conditions, ligand **77b** provided only a racemate. These results followed the same trend as found with the DPEphos ligands in Chapter 2.2.2. If the distance

between the P-atom and the substituent at the aryl group increased, the stereoselectivity of the asymmetric hydrogenation decreased.

Table 7: Asymmetric hydrogenation of isophorone by utilisation of DBFphos ligands.

Ligand (R)	Solvent	t [h]	Rh(acac)(cod)		Rh(acac)(CO) ₂	
			Conversion [%] ^b	ee of 71 [%] ^c	Conversion [%] ^b	ee of 71 [%] ^c
77a (2-EtOPh)	toluene	15	23 (>99)	2 (<i>S</i>)	0	0
77a (2-EtOPh)	thf	6	30 (>99)	2 (<i>S</i>)	75 (>99)	24 (<i>S</i>)
77b (3-EtOPh)	toluene	15	100 (>99)	1 (<i>S</i>)	4 (>99)	0
77b (3-EtOPh)	thf	6	100 (>99)	0	0	0

^aConditions: 1 mmol of isophorone (138.2 mg), 5 μmol of [Rh], 6 μmol of ligand, 3 ml of solvent, 40 °C, 50 bar. ^bDetermined by NMR. The portions of ketone **71** are given in parenthesis. ^cEstimated by GC.

In conclusion, obviously DBFphos derivatives were not appropriate ligands for Rh-catalysed asymmetric hydrogenation of isophorone. Despite of high conversions with Rh(acac)(cod) as metal source, the enantiomeric excesses were poor with both catalytic systems.

2.2.4.2 Pd-Catalysed Asymmetric Allylation of Dimethylmalonate with DBFphos Ligands

The above described DBFphos derivatives were also investigated in the asymmetric allylation of dimethyl malonate (**74**) with (*E*)-1,3-diphenylallyl acetate (**73**) (Scheme 6).

Table 8: Asymmetric allylation of dimethyl malonate (**74**) with (*E*)-1,3-diphenylallyl acetate (**73**)^a.

Ligand (R)	yield [%]	ee of 75 [%] ^b
77a (2-EtOPh)	78	11 (<i>S</i>)
77b (3-EtOPh)	88	1 (<i>S</i>)

^aConditions: 1 mmol of dimethyl malonate (132 mg), 1 mmol of (*E*)-1,3-diphenylallyl acetate, 0.2 mmol of lithium acetate (13 mg), 1 mmol *N,O*-bis(trimethylsilyl)acetamide (203 mg), 10 μ mol of Pd(dba)₂ (5.75 mg) and 10 μ mol of ligand. ^bEstimated by chiral HPLC.

The asymmetric allylation of dimethyl malonate proceeded with good yields (78 - 88 %). The ee-values were poor and amounted only 1-11 %. This also followed the same trend as found in the asymmetric hydrogenation. It can be concluded that transition from the *ortho*-substituted derivative to the *meta*-substituted one means decreasing of enantioselectivity.

The lack of stereoselectivity by utilisation of DBFphos derivatives as ligands in catalytic systems can be explained by the wide bite angle provided by the DBF backbone. The distance between the phosphorus atoms is too large (**77a**, x-ray structural analysis⁷⁵: P-P: 5.6/5.9 Å), so that the metal, in this case rhodium or palladium, does not coordinate as expected to the ligand.

To prove this theory, a crystal structure of a DBFphos derivative coordinating to a metal was required. Thus, **77a** was reacted with Pd(NCMe)₂Cl₂. Orange crystals were obtained and analysed by x-ray structural analysis (Figure 9).

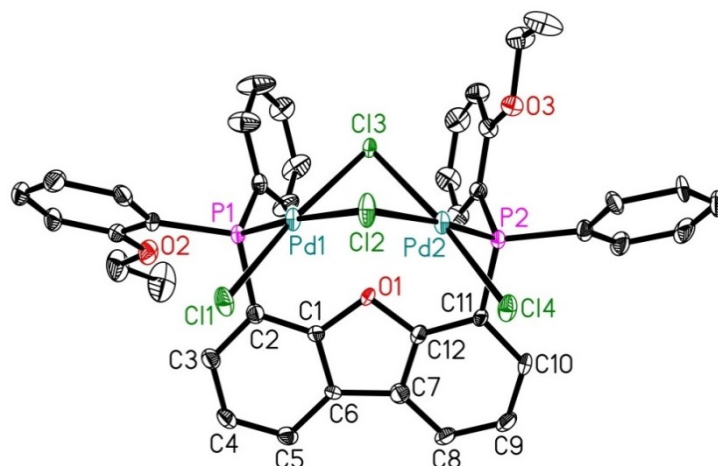


Figure 9: Molecular structure of $\text{Pd}_2(\mu_2\text{-Cl})_2(\mu_2\text{-77a})$ -complex in the solid state.

Displacement ellipsoids correspond to 30 % probability. Hydrogen atoms and co-crystallised solvent (CH_2Cl_2) are omitted for clarity. Selected interatomic distances [Å]: P1-Pd1, 2.2343(19); P2-Pd2, 2.2218(18); Pd1-Pd2, 2.9939(4); Cl1-Pd1, 2.2970(19), Cl2-Pd1, 2.4221(18), Cl2-Pd2, 2.4299(17); Cl3-Pd2, 2.3537(15); Cl3-Pd1, 2.3597(16), Cl4-Pd2, 2.3015(19). Selected angles [°]: Cl3-Pd2-Pd1, 50.65(4); Cl2-Pd2-Pd1, 51.78(5); P1-Pd1-Pd2, 123.70(5); P2-Pd2-Pd1, 124.37(5).

The crystal structure of the $\text{Pd}_2(\mu_2\text{-Cl})_2(\mu_2\text{-77a})$ -complex shows unexpectedly, that the DBFphos ligand built a dinuclear complex with Pd. This could explain why the stereoselectivity of the product **71** or **75** were lower with DBFphos ligands **77** compared with the results found with Xantphos derivatives **65**. In the literature, various Pd-Xantphos-complexes are described, which display Xantphos coordinating to only one Pd-centre.⁷⁷ This condition seems to enhance the stereoselectivity of the asymmetric catalysis.

There are only a few examples of DBFphos-metal-complexes in the literature, where the structure has been determined. Depending on the coordinating metal, mono- or dinuclear DBFphos-complexes exist.

For Ru,⁷⁸ Re⁷⁹ and Os⁸⁰ mononuclear complexes were found. Noteworthy, not only phosphorus, but also the oxygen coordinates to the metal which seems to stabilise the mononuclear structure. The bite angles of DBFphos in these complexes range from 150 to 160 °.

Dinuclear complexes have been observed for geminally disubstituted aryls where gold atoms are bridged by a dibenzofuran backbone⁸¹ **79** and for DBFphos chelated copper iodide nanoclusters⁸² **80** (Figure 10).

In the gold complex **79**, the metal atoms are not only bridged by an aryl-unit and a diphosphine ligand but do also make direct interactions between each other, whereas the metals in the DBFphos chelated copper iodide nanoclusters **80** and in the $\text{Pd}_2(\mu_2\text{-Cl})_2(\mu_2\text{-68a})$ -complex described above are linked by halogen bridges.

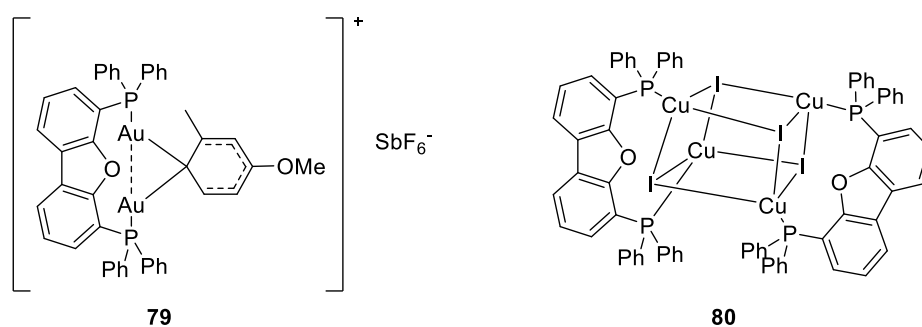
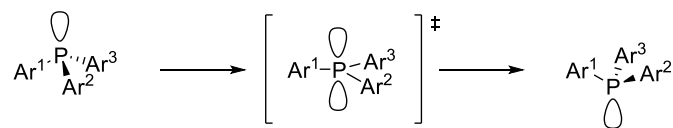


Figure 10: Geminally disubstituted aryl bridged by a dibenzofuran backbone **79** and DBFphos-chelated copper iodide nanocluster **80**.

2.2.5 Investigation on the Epimerisation Behaviour of *P*-Chirogenic Di(triaryl phosphines)

P-Chirogenic phosphines possess an inversion barrier of circa 30 kcal/mol, which allows the isolation of single enantiomers.¹¹ By increasing number of aryl substituents, the inversion barrier decreases. Baechler and Mislow have shown this trend by the calculation of the free activation energy needed to invert tertiary phosphines.¹⁴ Whereas the inversion barrier ($\Delta G^\ddagger_{\text{inv}}$) of trialkyl phosphines is about 36 kcal/mol, alkyldiarylphosphines invert by the impact of circa 30 kcal/mol. Following this trend, the inversion barrier of triarylphosphines should be even lower but nevertheless high enough to isolate single enantiomers at room temperature.



Scheme 37: Pyramidal inversion of triaryl phosphines via a planar transition state.

In contrast to the assumption that di(triaryl phosphines) are stable at room temperature, it was found that the Xantphos, DPEphos and DBFphos derivatives slowly epimerise forming a mixture of (*S,S*)-, (*R,R*)- and (*R,S*)-isomers over the time due to thermic (storage under inert atmosphere at room temperature) and/or catalytic (e. g. impurities like silica from column chromatography) effects (Table 9).

Table 9: Alteration of stereochemistry in di(triaryl phosphines) over the time at room temperature

Entry	Backbone	R	Separation method	Time [month]	chiral/achiral new ^a	chiral/achiral after ageing ^a
1	DMX	2-Naphthyl	Crystallisation	23	100/0	100/0
2	DMX	2-Naphthyl	Column	27	100/0	67/21 ^b
3	DMX	2-Anisyl	Crystallisation	12	100/0	100/0
4	DMX	2-Tolyl	Crystallisation	6	100/0	100/0
5	DMX	2-EtOPh	Column	3	97/3	90/10
6	<i>t</i> Bu-DMX	1-Naphthyl	Column	4	100/0	94/6
7	<i>t</i> Bu-DMX	2-Naphthyl	Crystallisation	26	100/0	100/0
8	<i>t</i> Bu-DMX	2-EtPh	Column	9	95/5	95/5
9	<i>t</i> Bu-DMX	4-Tolyl	Column	9	100/0	69/13 ^b
10	<i>t</i> Bu-DMX	2-EtOPh	Column	9	100/0	80/14 ^b
11	DPE	2-Tolyl	Crystallisation	28	100/0	100/0
12	DPE	2-Naphthyl	Crystallisation	36	100/0	100/0
13	DPE	4-Anisyl	Column	26	100/0	55/45
14	DPE	2-EtOPh	Column	2	97/3	91/9
15	DBF	2-EtOPh	Column	4	95/5	71/29

^aDetermined by NMR. ^bAdditional impurities such as oxides.

The effect on the stereochemistry depends primarily on the methodology to purify the compounds (Table 9). Additionally, the backbone of the molecule and the substituents at the phosphorus can have an impact, too.

It is noteworthy, that derivatives which were separated by crystallisation did not alter at all (Table 9, Entries 1, 3, 4, 7, 11 and 12) independent from their backbone and their substituents. Even after 3 years of storage at room temperature no changes could be determined (Table 9, Entry 12).

Comparing the separation methods crystallisation *versus* column chromatography, column chromatography can be a reason for deterioration of the optical purity of the tested di(triaryl phosphines). The DMXphos derivative with 2-naphthyl substituents was synthesised and purified with both separation methods and stored for circa two years. The batch which was

separated by crystallisation did not alter at all, whereas the one separated by column chromatography lost its purity under the same conditions (storage under inert atmosphere at room temperature; Table 9, Entries 1 and 2).

In case of separation via column chromatography, the phosphines seem to alter rather rapidly. The chiral/achiral-ratio of the DBFphos derivative decreased within 4 months from 95/5 to 71/29 (Table 9, Entry 15). Rigid backbones with smaller bite angles like *P*-chirogenic Xantphos derivatives seem to deteriorate slower (Table 9, Entries 5 and 6). The DMXphos derivative bearing a 2-EtOPh substituent changed within 3 months from 97/3 to 90/10 (chiral/achiral). The ratio chiral/achiral of the *t*Bu-DMXphos derivative with 1-naphthyl substituent decreased within 4 months from 100/0 to 94/6.

It can be concluded that di(triaryl phosphines), especially those with flexible backbones like DPEphos and wide-bite-angle backbones like DBFphos derivatives, epimerise more readily than those with rigid backbones with smaller bite angles like *P*-chirogenic Xantphos derivatives.

The differences in configurational stability between the different separation methods can be explained by small acidic traces from the silica gel of the column remaining in the product after the separation procedure.^{75b} Epimerisation of phosphines is accelerated by acidic catalysis.

The epimerisation of the di(triaryl phosphines) could be suppressed by the storage at 0 °C.

The racemisation behaviour is not only of interest regarding the storage of the compounds but also with respect to the enhanced temperatures of the catalytic reactions in which the phosphines are used as ligands. If di(triaryl phosphines) epimerise during the catalytic reaction, the stereoselective outcome of the reaction will be affected. Therefore, it is significant to know the stability of the phosphines at enhanced temperatures.

2.2.5.1 Long-Term Temperature NMR Stability Tests of Di(triaryl phosphines)

The stability of triaryl phosphines at enhanced temperatures was investigated by long-term temperature NMR stability tests.

It is known, that the rate of the epimerisation depends on the temperature. To get deeper insights into the stability of di(triaryl phosphines), (1*S*,1'*S*)-(2,7-di-*t*butyl-9,9-dimethyl-9H-xanthene-

4,5-diyl)di((2-ethoxy)-phenyl phosphine) (**66a**)⁷⁵ was used as model compound for a qualitative long-term temperature NMR stability test.

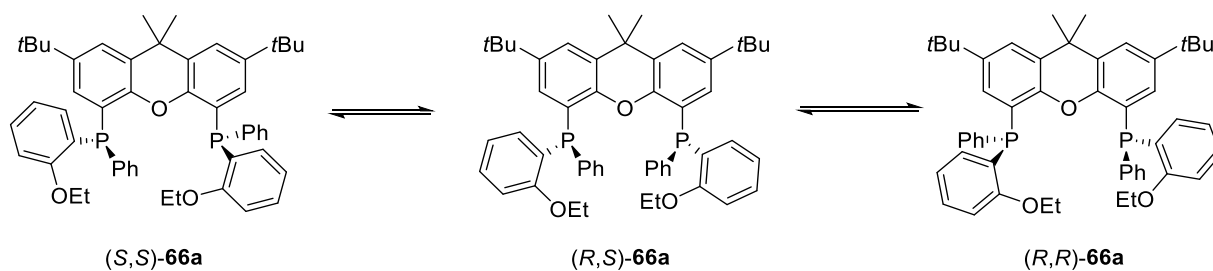


Figure 11: Epimerization of (1*S*,1'*S*)-(2,7-di-*t*-butyl-9,9-dimethyl-9*H*-xanthene-4,5-diyl)di((2-ethoxy)-phenyl phosphine) (**66a**).

Compound **66a** was dissolved in toluene-*d*₈ and placed into an NMR tube under inert atmosphere. The tube was heated to 313 K or 333 K. Over a period of nearly 10 hours, ¹H- and ³¹P NMR spectra were measured.

Table 10: NMR Investigations on temperature dependency of inversion at the *P*-centre of di(triaryl phosphines).

Entry	t [h]	T [K]	$\delta_{\text{chiral-66a}}$ [ppm]	I* chiral- 66a :	$\delta_{\text{achiral-66a}}$ [ppm]	I* achiral- 66a :
1	0.0	297	-23.9	92.4	-24.1	7.6
2	0.3	313	-23.7	92.4	-23.9	7.6
3	1.2	313	-23.7	92.1	-23.9	7.9
4	2.1	313	-23.7	91.8	-23.9	8.2
5	2.4	333	-23.4	91.7	-26.6	8.3
6	3.4	333	-23.4	90.1	-26.6	9.9
7	4.4	333	-23.4	88.6	-26.6	11.4
8	5.4	333	-23.4	86.8	-26.6	13.2
9	7.1	333	-23.4	84.4	-26.6	15.6
10	8.2	333	-23.4	82.6	-26.6	17.4
11	9.2	298	-23.9	82.1	-24.1	17.9

* Integral of the relevant peak in ^{31}P NMR spectroscopy.

The specific signals in the quantitative ^{31}P NMR belonging to (*S,S*)- or (*R,R*)-**66a** (chiral-**66a**) and (*R,S*)-**66a** (achiral-**66a**) show a change in regard to the integrals of the signals (Table 10). By rising the temperature, the amount of achiral-**66a** increases (Table 10). This trend is shown by the ^{31}P NMR spectra of **66a** (Figure 12).

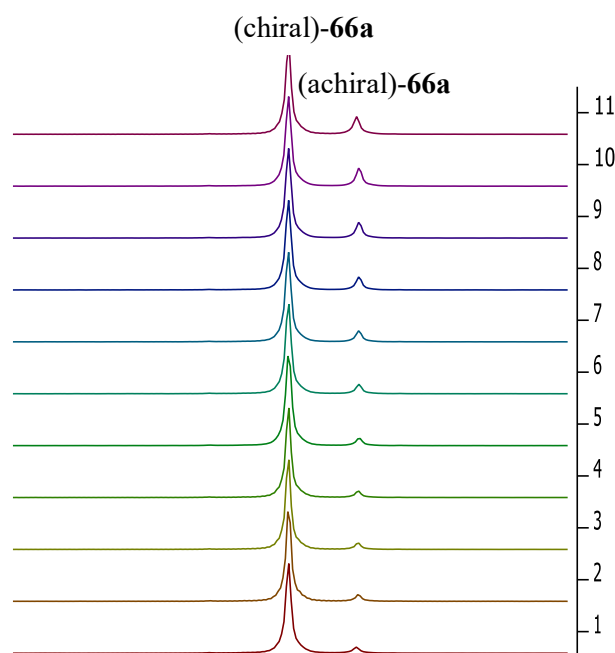


Figure 12: ^{31}P NMR Spectra of **66a** (CDCl_3) recorded at different temperatures (Table 10).

The signals are aligned due to better visualisation. The signals corresponding to (chiral)-**66a** are normalised to $I = 1$. It can be seen that the signal corresponding to (*R,S*)-**66a** increases due to the temperature influence.

In the ^1H NMR spectra of **66a**, the triplet corresponding to OCH_2CH_3 (^1H NMR: $\delta = 0.9$ ppm for chiral-**66a**; $\delta = 0.9$ ppm for achiral-**66a**) doubles with increasing temperature and time which gives proof for the transformation of the chiral **66a** into the achiral compound (Figure 13). The signals are aligned due to better visualisation. The signals corresponding to chiral-**66a** are normalised to $I = 1$. It can be seen that the signal corresponding to (*R,S*)-**66a** increases due to the temperature impact.

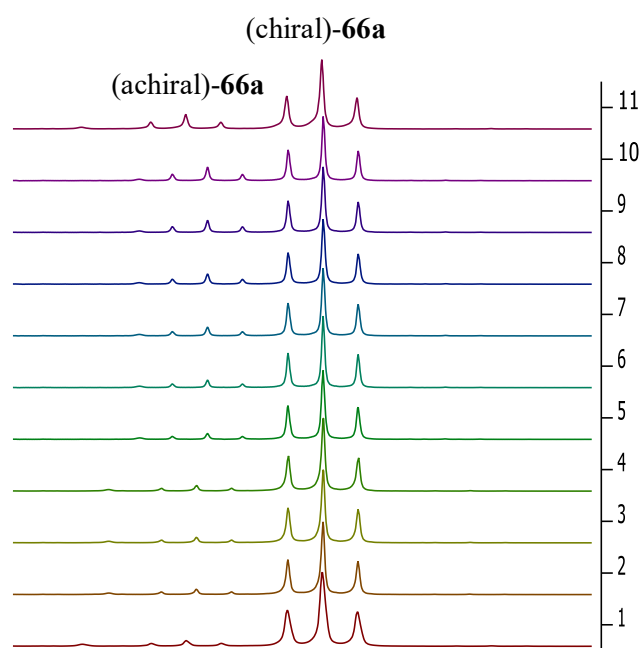


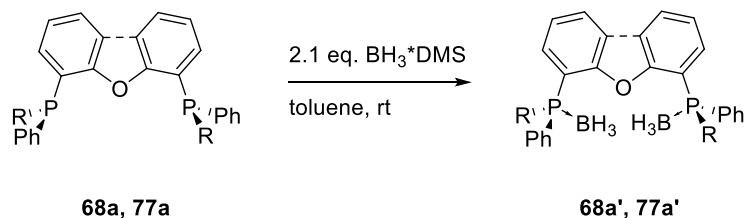
Figure 13: ^1H NMR spectra of **66a** (CDCl_3) recorded at different temperatures (Table 10).

It was shown qualitatively that due to temperature effects epimerisation takes place. It could be proved, that only reactions at temperatures up to 40 °C can be performed to assure that no epimerisation occurs during the reaction. Therefore, applications such as the asymmetric hydrogenation of isophorone at 40 °C or the asymmetric allylation of dimethyl malonate at -20 °C - room temperature are probably appropriate.

For the successful and broad application of the di(triaryl phosphines) in asymmetric catalysis it is also necessary to ensure their stereochemical integrity for long-term storage as usually requested for industrial laboratories.

To safeguard customer's satisfaction, a solution to assure easy long-term storage of the di(triaryl phosphines) without loss of stereochemistry was investigated. Even if it is necessary to remove the BH_3 -protection group first before the two phosphinite units were incorporated into the backbone (Scheme 32 and 36), it could be proved, that the di(triaryl phosphines) can be protected with borane-groups by reacting with $\text{BH}_3 \cdot \text{SMe}_2$. It was found that the Xantphos derivatives permit the introduction of only one BH_3 -unit, probably due to the small distance between the P-atoms of e. g. 4.2 Å for the $\text{Ar} = 2\text{-EtPh}$ derivative. We speculate that in contrast, the flexible backbone of DPEphos derivatives and the wide bite angle of DBFphos derivatives

provide enough space between the *P*-centres (in **77a**, 5.6/5.9 Å; in **68** R = 2-EtPh, 4.9/5.4 Å) to coordinate a BH₃-group at each P-atom.^{75b}



Scheme 38: Protection of DPEphos- and DBFphos derivatives with BH₃-groups.

The phosphines **68a** and **77a** could be transformed into their bis-borane adducts **68a'** and **77a'** by reacting with 2.1 equivalents of BH₃*DMS in toluene at room temperature. The ³¹P NMR spectra showed the typical broad signals for the P-borane adducts (³¹P NMR: δ = 17.4 ppm and 16.1 ppm for **68a'**; δ = 15.8 ppm for **77a'**). The reactions proceeded with complete conversion.

Surprisingly, the ³¹P NMR spectrum of **68a'** was characterised by two broad signals in a ratio of 57/43. Also in the ¹H NMR spectrum (Figure 14) two signals corresponding to OCH₂CH₃ (δ = 1.0 ppm (t, J = 7.0 Hz, 3H), 0.9 ppm (t, J = 6.9 Hz, 2H)) could be determined in the same ratio. Furthermore, the aromatic protons between 6.0-8.0 ppm partly split up in separate signals.

To exclude that an epimerisation took place during the reaction with BH₃*SMe₂, the borane groups were removed again with DABCO from **68a'**. The ³¹P NMR showed one sharp signal of **68a** at δ = -24.4 ppm and no hint for the existence of the *meso*-derivative was found.

The observed effects of doubled signals in the ¹H and ³¹P NMR spectra were also found in other DPEphos derivatives such as Ar = 3-EtPh, 2-MeOPh, but this accounts only for DPEphos.

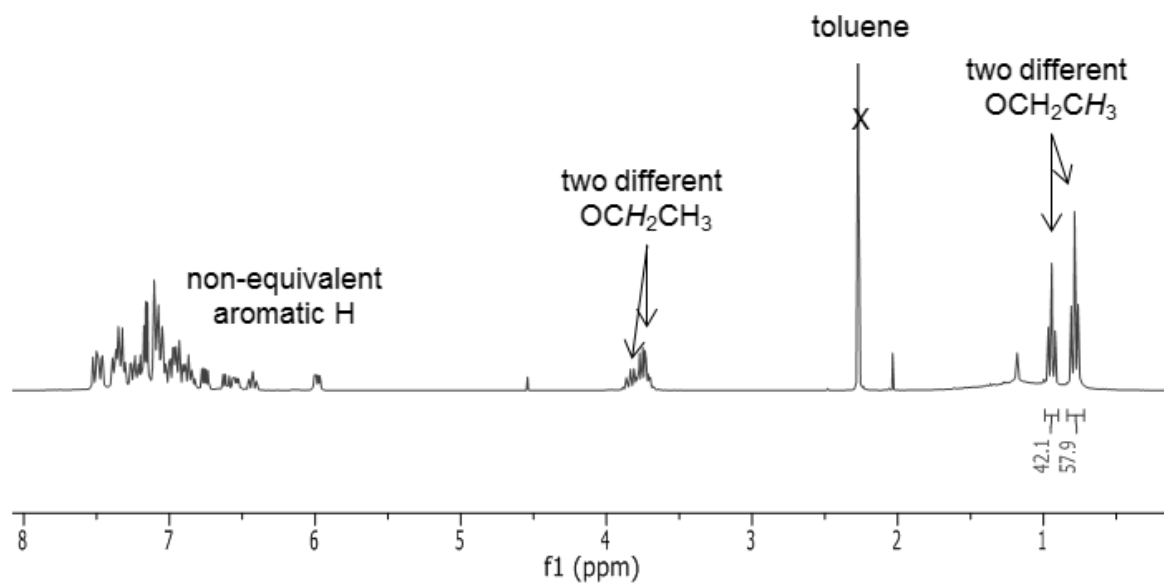


Figure 14: ^1H NMR of **68a'** (CDCl_3).

To investigate if these two signals are in relation (conversion of conformation), the NMR measurements were carried out at different temperatures (328-213 K). Usually an increasing temperature will force epimerisation (Figure 15).

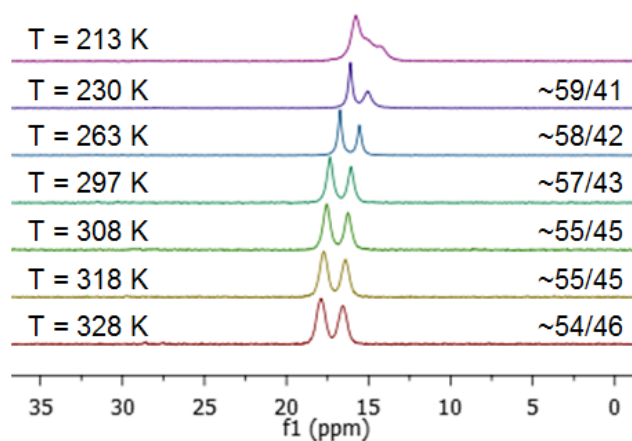


Figure 15: Temperature ^{31}P NMR study of **68a'** (CDCl_3).

It could be shown, that changes of the ratio between the signals occurring due to temperature changes were only moderate (see Table 12). At enhanced temperatures, the signals broadened, whereas the signals became sharper at lower temperatures. It is noteworthy that the ^{31}P NMR spectrum at 213 K showed a significant change of the signals. The signal at $\delta = 15.0$ ppm split into two signals at $\delta = 15.0$ ppm and 14.3 ppm.

Table 11: Ratio of **68a'** isomers at different temperatures determined by quantitative ^{31}P NMR.

Entry	T [K]	δ_{A} [ppm]	% of A	δ_{B} [ppm]	% of B
1	213	15.8	61	^a	39
2	230	16.1	59	15.0	41
3	263	16.7	58	15.6	42
4	297	17.4	57	16.1	43
5	308	17.5	55	16.3	45
6	318	17.7	55	16.4	45
7	328	17.9	54	16.6	46

^aThe signal split into two different ones ($\delta = 15.0$ ppm, 14.3 ppm).

The observed results can be explained taking into consideration different effects such as dynamic effects or effects of coordination.

It can be assumed, that the bis-borane adduct was formed in two symmetrical conformers due to the bulkiness of the *o*-substituents at the phosphorus. The free rotation of the molecule units is restricted and two species can be therefore observed in the NMR.

Compound **68a'** is supposed to possess centres with different dynamics which can trigger the appearance of different species in the NMR. Highly probable, also the rotation of the C-P-bonding of the aryl group can be hindered due to the bulkiness of the substituent.

Another probability is the restricted rotation of the C-P-bonding between the DPE-backbone and the P-unit. Without the borane coordinating to the P-atom, the P-units can rotate freely and only one signal can be observed in the ^{31}P NMR spectrum. If the phosphorus is coordinated to the borane group, the rotation is hindered and two symmetric species are stabilised.

Another dynamic centre could be the ether group of the backbone. Its free rotation could also be restricted due to the bulkiness of the phosphorus units.

During these temperature NMR studies, a total point of coalescence could not be found. Apparently, the point of coalescence occurs at higher temperatures but due to the solvent (CDCl_3) and due to an assumed cleavage of the P-B bond and epimerisation at P-atoms at high temperatures (Figure 17), no NMR spectra could be measured at temperatures higher than 328 K.

Another effect which could cause two signals in the ^{31}P NMR could be due to different coordination modes of the borane to the DPEphos derivative. The supposed structures are shown in Figure 16.

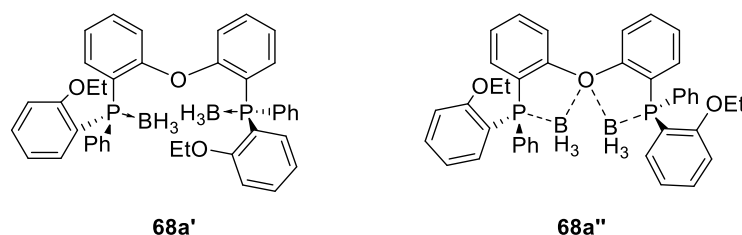
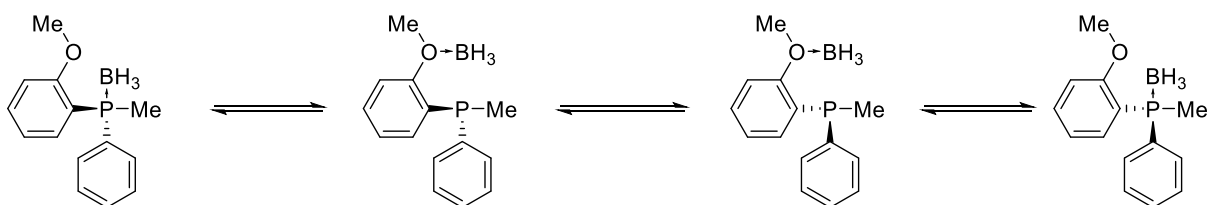


Figure 16: Plausible coordination modes of borane to **60a**.

The most likely structure is supposed to be **68a'**. According to the mass spectroscopy and HRMS (ESI) measurement, two borane groups were found (see experimental part). Since resonances of two symmetric species could be found in the NMR spectra, it can be assumed, that other coordination modes were built, e.g. **68a''**. The structure in Figure 16 shows two borane groups which coordinate to either the free electrons of the phosphorus or to that of the oxygen of the ether group. A similar phenomenon was first described by Imamoto and his working group in 1990 (Scheme 39).⁸³ In their example, (*S*)-*o*-anisylmethylphenyl phosphine-borane, the borane group migrated between P and O and the symmetry of the *P*-centre reversed while BH_3 coordinated to the oxygen of the ether group.



Scheme 39: Migration of the borane group in (*S*)-*o*-anisylmethylphenyl phosphine-borane found by Imamoto and working group.

Transferring this phenomenon on structure **68a''**, the alternation of both borane units takes place fast enough, so that the free and the protected phosphorus species cannot be detected separately in the NMR, so that only one signal of a symmetric DPEphos species (additional to the one of **68a'**) could be determined. In contrast to the situation described by Imamoto, in case of **68a'**, no epimerisation took place, even under the assumption that the BH₃-unit migrates (see above).

Due to the limited data available it could not be unambiguously concluded whether dynamic effects or different coordination modes are responsible for our observations. To explain the incident more in detail, more experiments would be required. Since these phenomena were not the central subject of the thesis, no further experiments were carried out.

Since the aim of the protection of the di(triaryl phosphines) was to investigate their behaviour at enhanced temperatures, long-term temperature studies were implemented.

NMR tubes with a solution of compounds **68a** and **68a'** were heated at 55 °C during a long period in an oil bath. The quantitative ³¹P NMR measurement was carried out at 25 °C. The spectra were compared in relation to the upcoming *meso*-compounds.

The NMR spectra show, that compound **68a** alters due to the temperature impact. At the starting point, the ratio of chiral-/achiral-**68a** is 90/10 ($\delta = -24.9$ ppm (2x P_{chiral}), -25.3 ppm (2xP_{achiral})). After 24 h, the ratio changes to 81/19. With increasing time, the relative amount of achiral-**68a** increases up to 40 % after 120 h (Figure 17).

The bis-borane-complex **68a'** was treated in the same manner like **68a**. It was found, that no epimerisation took place over the time. The only effect which could be observed was the partial loss of the borane groups. After 72 h, the relative amounts of 8 % of the relevant mono-borane adduct ($\delta = +14.5$ ppm (1x P*BH_{3,mono}), -27.2 ppm (1x P_{mono})) and 4 % of the free phosphine ($\delta = -24.9$ ppm (2x P_{chiral})) are detected (Figure 17). After 120 h, small signals (approximately 2 %) between 29 and 27 ppm occur corresponding to upcoming oxides.

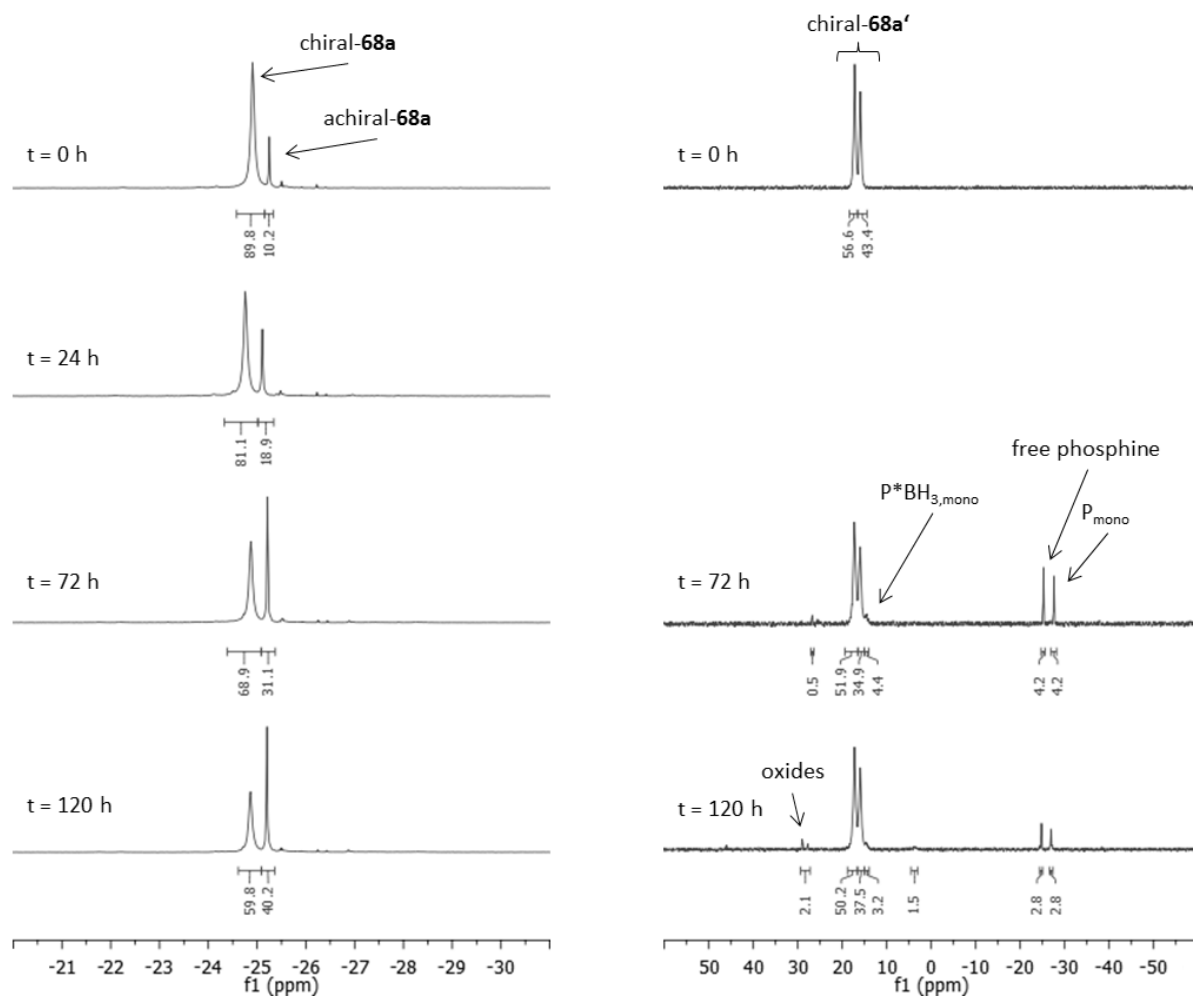


Figure 17: ^{31}P NMR spectra (CDCl₃) of **68a** and **68a'** after thermal treatment (55 °C).

It could be proved, that the protection of the phosphorus with the borane is useful to suppress the epimerisation during long-term storage at room temperature. Even higher temperatures up to 55 °C do not affect the bis-borane-adduct **68a'**.

To prove also the stability of the compounds **77a** and **77a'**, they were also investigated as shown above at 50 °C over a period of 96 hours.

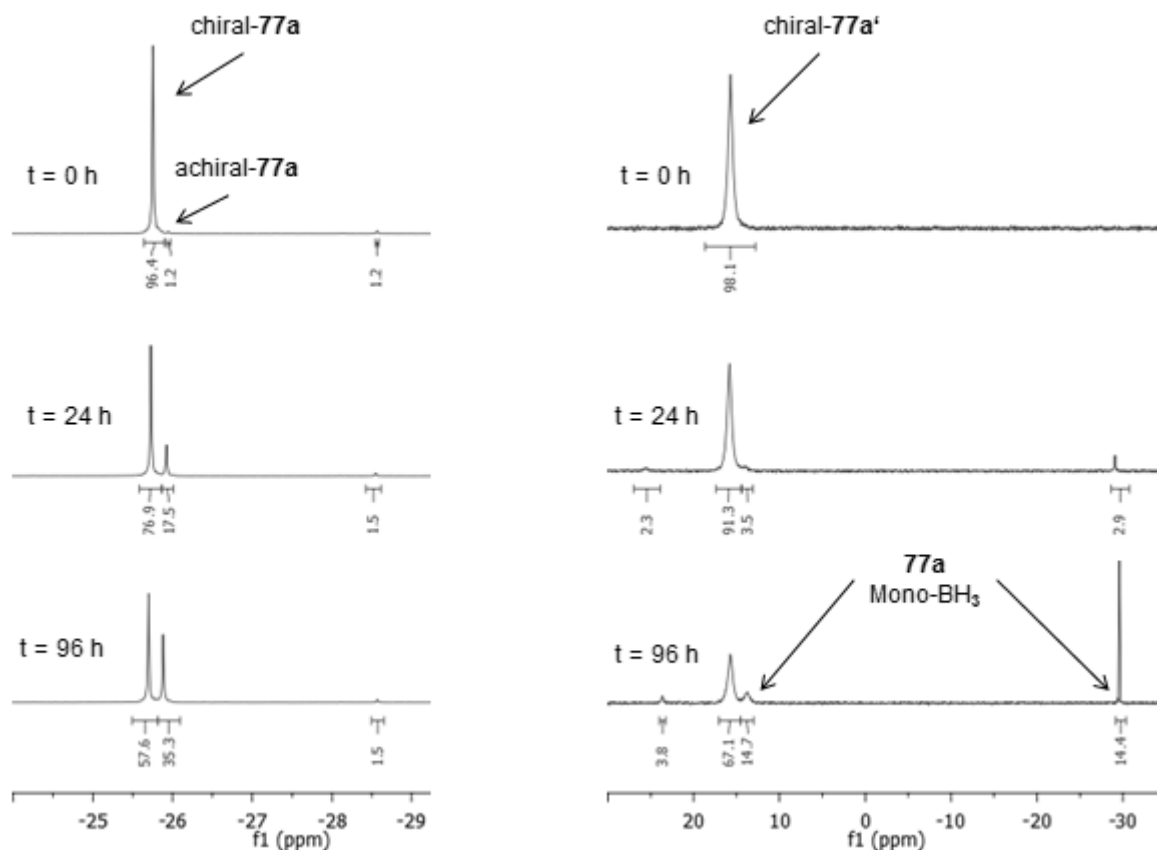


Figure 18: ^{31}P NMR spectra (CDCl₃) of **77a** and **77a'** after thermal treatment (50 °C).

It was found that chiral-**77a** ($\delta = -25.7$ ppm ($2 \times P_{\text{chiral}}$)) changes due to the thermal treatment (Figure 18, left-hand side). At -28.6 ppm the resonance of the residue of the monosubstituted derivative **77** can be seen. After 24 hours 17.5 % of the achiral-compound ($\delta = -25.9$ ppm ($2 \times P_{\text{achiral}}$)) is formed by epimerisation. Furthermore, the relative amount of achiral-**77a** increases under progression of time. After 96 hours of thermal treatment the amount of achiral-**77a** increases further to 35.3 %.

For comparison, by storage of the bis-borane adduct (*S,S*)-**77a'** at 50 °C, the major effect, which is observed, is the loss of one borane (Figure 18, right-hand side). The NMR signals corresponding to the mono-borane occur at $\delta = +13.8$ ppm ($1 \times P^* \text{BH}_{3,\text{mono}}$), -29.6 ppm ($1 \times P_{\text{mono}}$). The signal corresponding to chiral-**77a'** is located at $\delta = +15.7$ ppm ($2 \times P^* \text{BH}_{3,\text{di}}$). Whereas the relative quantity of (*S,S*)_{mono}-**77a'** amounts circa 6 % after 24 hours, it increases to circa 30 % after 96 hours.

In comparison to compound **77a** with circa 35 % *meso*-compound, the borane adduct alters more slowly and demonstrates clearly the advantage of the borane-protection of P-atoms for the long-term storage of DBFphos derivatives.

2.2.5.2 Rh-Catalysed Asymmetric Hydrogenation with Borane-Protected Di(triaryl phosphines)

Since the herein presented di(triaryl phosphines) should be applied in asymmetric catalysis, it was interesting to see, whether the borane-protected compounds are suitable for the direct use in asymmetric reactions to avoid the deprotection of the phosphines prior to the catalytic reaction.

Like shown above, **65a,b** gave the best results in asymmetric hydrogenation of isophorone,⁷⁵ so they provide a good standard to compare the free phosphines and their protected version. It is noteworthy to remind, that Xantphos derivatives **65** permit the introduction of only one BH₃-unit (Figure 19); the NMR spectrum displays unprotected phosphines and their corresponding borane-adducts, respectively.

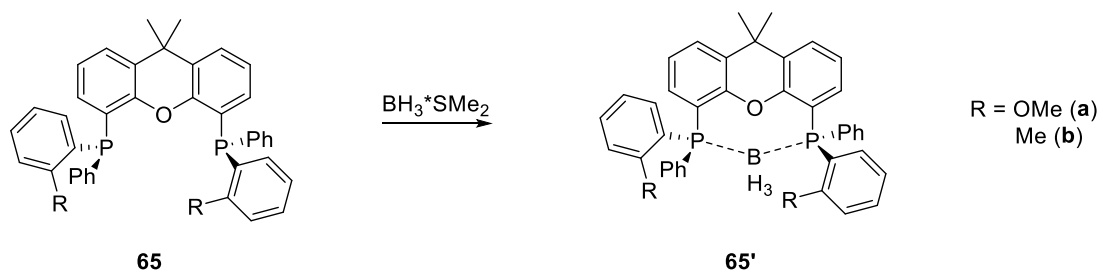


Figure 19: Reaction of (1*S*,1'*S*)-(9,9-dimethyl-9H-xanthene-4,5-diyl)di(arylphenyl phosphine) (**65**) with BH₃.

The application of (1*S*,1'*S*)-(9,9-dimethyl-9H-xanthene-4,5-diyl)di(phenyl(*o*-tolyl) phosphine) (**65a**), (1*S*,1'*S*)-(9,9-dimethyl-9H-xanthene-4,5-diyl)di(phenyl(*o*-anisyl) phosphine) (**65b**) and their borane adducts **65'a,b** were compared in the Rh-catalysed asymmetric hydrogenation.

The reduction of isophorone was performed at 40 °C at 50 bar hydrogen pressure for 15 hours in thf. Rh(acac)(CO)₂ was used as Rh-source due to the knowledge, that it provided the best results in this reaction. Three different scenarios were created: The hydrogenation proceeds either with the addition of “free” phosphine **65**, the addition of the BH₃-protected phosphine

65' or the BH₃-protected phosphine **65'** and additional DABCO to deprotect the phosphines *in situ*.

Table 12: Results of the asymmetric hydrogenation of isophorone^a in dependence on the protection of the phosphorus with BH₃.

		65		65'		65' and DABCO	
	65	conversion [%] ^b	%ee ^c	conversion [%] ^b	%ee ^c	conversion [%] ^b	%ee ^c
a	2-MeO-Ph	100	84	4	32	77	95
b	2-Me-Ph	95	96	11	71	100	84

^aConditions: 1 mmol of isophorone, 5 μmol of [Rh], 6 μmol of ligand (and 6 μmol of DABCO for the *in situ*-deprotection), 3 ml thf, 40 °C, 50 bar. ^bDetermined by NMR. ^cEstimated by GC.

Table 12 shows clearly, that the protected phosphines **65'** only gave poor conversion and enantioselectivities as assumed due to the blockade of P-atoms as donor group to the Rh-central atom. Interestingly, when DABCO was added to the catalytic system, the phosphines of type **65'** were deprotected *in situ*. The catalysis proceeded similar to the hydrogenation with unprotected **65**. Excellent conversion rates and enantioselectivities were observed. The presence of DABCO did not influence the rate and enantioselectivity significantly.

2.3 Conclusion

The synthesis of several di(triaryl phosphines) with DPE- (**68**) or DBF-backbone (**77**) were discussed in this chapter. The new compounds were synthesised *via* the well-known (-)-ephedrine methodology pioneered by Jugé and co-workers.

The yielded DPEphos- and DBFphos-type di(triaryl phosphines) were tested in asymmetric catalysis such as the Rh-catalysed asymmetric hydrogenation and the Pd-catalysed asymmetric allylation.

In general, the DPEphos derivatives **68** provided superior results in asymmetric catalysis compared to DBFphos derivatives **77**. Obviously, the smaller P-P-distance in the former offered a significant advantage. In dependence of the substitution pattern at the aryl group, DPEphos derivatives induced up to 100 % conversion and enantioselectivity up to 59 % (R = 2-MOPh) in the asymmetric hydrogenation of isophorone. The same di-phosphine **68** assisted as co-catalyst in the asymmetric allylation of dimethyl malonate with a yield of 89 % and an

enantioselectivity of 82 %ee. For the same reactions, DBFphos derivatives (Ar = 2-EtOPh) enabled in the asymmetric hydrogenation of isophorone a conversion of 75 % with an enantioselectivity of 24 %ee and for the asymmetric allylation of dimethyl malonate a yield of 78 % with an enantioselectivity of 11 %ee.

It was shown that DBFphos derivatives possess apparently an inappropriate P-P-distance of 5.6/5.9 Å in **77a** to build a mononuclear complex which can transmit stereoselectivity in asymmetric catalysis. The crystal structure of the $\text{Pd}_2(\mu_2\text{-Cl})_2(\mu_2\text{-77a})$ -complex showed unexpectedly, that the DBFphos ligand formed a dinuclear complex with palladium. This could explain why the stereoselectivity of the product **71** or **75** were inferior with DBFphos ligands **77** compared to those achieved with Xantphos derivatives **65**.

Another challenge was to investigate the epimerisation of such di(triaryl phosphines). It was found, that the phosphines altered during long-term storage when they were processed before with column chromatography. Especially phosphines with configurationally flexible backbones like DPE or large bite angles such as DBF seemed to be affected easier.

To assure the stereochemical integrity over a long time, the phosphines should be protected with BH_3 -groups to suppress epimerisation reactions. It could be observed, that with di-phosphines based on DMX-backbones (**65**) only a single borane unit coordinates, whereas DPE- (**68**) and DBFphos derivatives (**77**) are able to accommodate two borane-groups. The stereochemical integrity was investigated employing long-term temperature studies which proved the strong stability of the borane adducts in contrast to the unprotected di-phosphines.

Two borane protected phosphines **65a,b** were tested in the asymmetric hydrogenation to demonstrate their benefit. The borane group could be removed *in situ* with DABCO. In the result the catalytic reaction proceeded in same manner like using the “free” phosphines. It was confirmed, that DABCO had no impact on the performance of the reaction and both conversion and stereochemistry were as good as in the hydrogenation with unprotected phosphines.

3. Synthesis of *P*-Chirogenic Di(triaryl phosphines) with Additional Axial Chirality

3.1 Aim of the investigations

Since the second half of the 20th century, the importance of homogenous catalysts based upon chiral phosphine co-catalysts coordinated to transition metals increased enormously in stereoselective catalysis. Chirality of the ligands can be incorporated by different elements of chirality into the metal complex chirogenic carbon centres or axial chirality. A particular challenge faces the generation of *P*-chirogenic centres. Considering the great variety of such ligands, numerous hybrid ligands containing chirogenic phosphorus and carbon centres can be found in the literature. In contrast ligands possessing both *P*-chirogenic centres as well as axial chirality are rare.¹⁹

At the beginning of the 21st century, chemists started to investigate these kinds of ligands. By combining different symmetry elements in a single compound, they hoped to affect more efficiently the asymmetric catalytic system which could lead to an increase of enantiomeric excess and turnover frequencies. Furthermore, it could contribute to develop a better comprehension of important factors in ligand design.

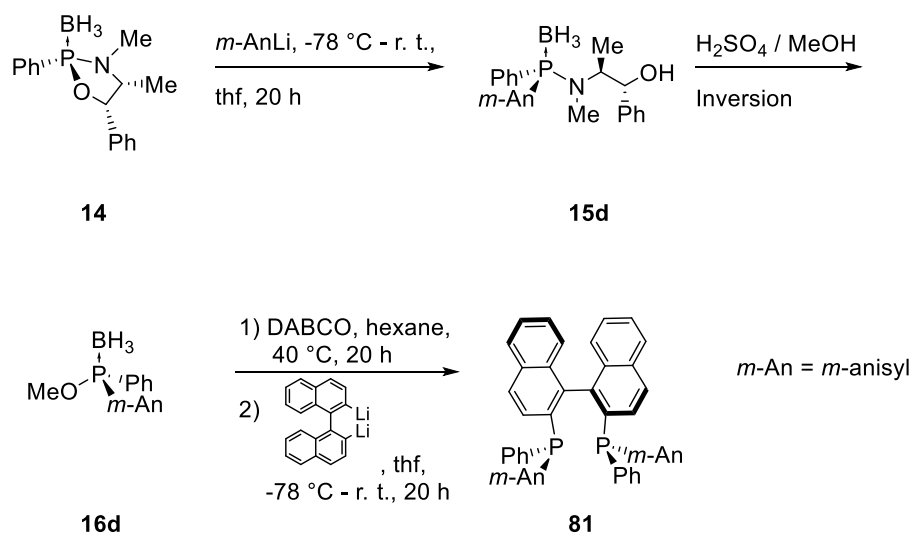
In 1980, Noyori and his working group published the synthesis of enantiomerically pure BINAP.⁸⁴ Today, BINAP is one of the most applied ligands for catalysis, because of its universal operation. Especially in several asymmetric hydrogenation reactions, BINAP displays exceptionally high activity and enantioselectivity. Therefore, this ligand is employed in many industrial processes like Takasago menthol process.⁸⁵ In literature, there are various examples for the synthesis and use of BINAP and its derivatives, but there are only few examples for BINAP decorated with asymmetric *P*-centres. A methodology to access this BINAP-type ligand with two additional chirogenic *P*-centres is investigated in this dissertation.

To receive such rare hybrid ligands, the Ullmann coupling represents an auspicious method for the synthesis and is the method of choice considered herein. The above cited synthetic route of atropisomeric biaryl diphosphines published by Pietrusiewicz is used as a starting point for our studies.⁷¹ The method to synthesise *P*-chirogenic compounds is already well investigated. Moreover, the described separation of diastereomers can be avoided by using Jugé's (-)-ephedrine method to create a range of enantiopure tertiary triarylphosphines **21** with chiral *P*-centres.^{25,75}

3.2 Results and Discussion

Synthesis of Bidentate Tertiary *P*-Chirogenic Triarylphosphines with Additional Axial Chirality

The first impetus of how to produce BINAP-type ligands with two additional chirogenic *P*-centres, is the well-established (-)-ephedrine methodology as described in Chapter 1.3.2.5.1. (Scheme 40). The first step was the stereoselective ring opening of (2*R*,4*S*,5*R*)-3,4-dimethyl-2,5-diphenyl-1,3,2-oxazaphospholidine-*P*-borane adduct (**14**) by aryl lithium. Subsequently, the ephedrine group was cleaved by the acidic methanolysis reaction, where inversion of the steric centre occurred. With the assistance of DABCO, the phosphorus centre had to be deprotected, before the introduction into the dilithiated binaphthyl backbone could take place.



Scheme 40: Envisaged synthesis of BINAP-Derivatives **81** with the (-)-ephedrine methodology.

Unfortunately, in the final synthetic step compound **81** could not be obtained: After the reaction of **16d** (Ar = 3-MeOPh) with 2,2'-dilithiated binaphthyl a mixture of three species (**82**, **83** and **84**) resulted. After column chromatography, the species shown in Figure 20 could be identified by NMR and mass spectroscopy.

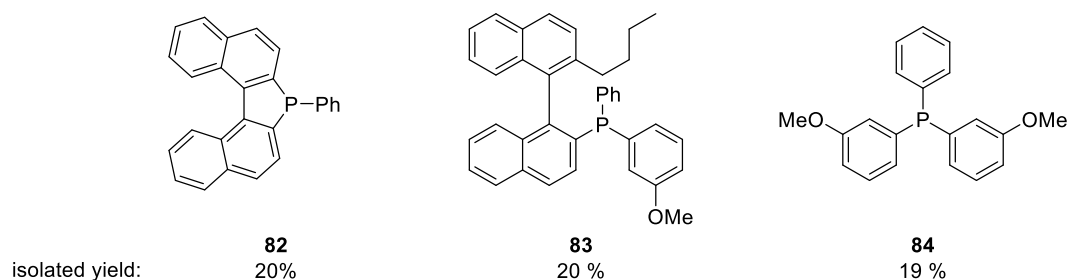
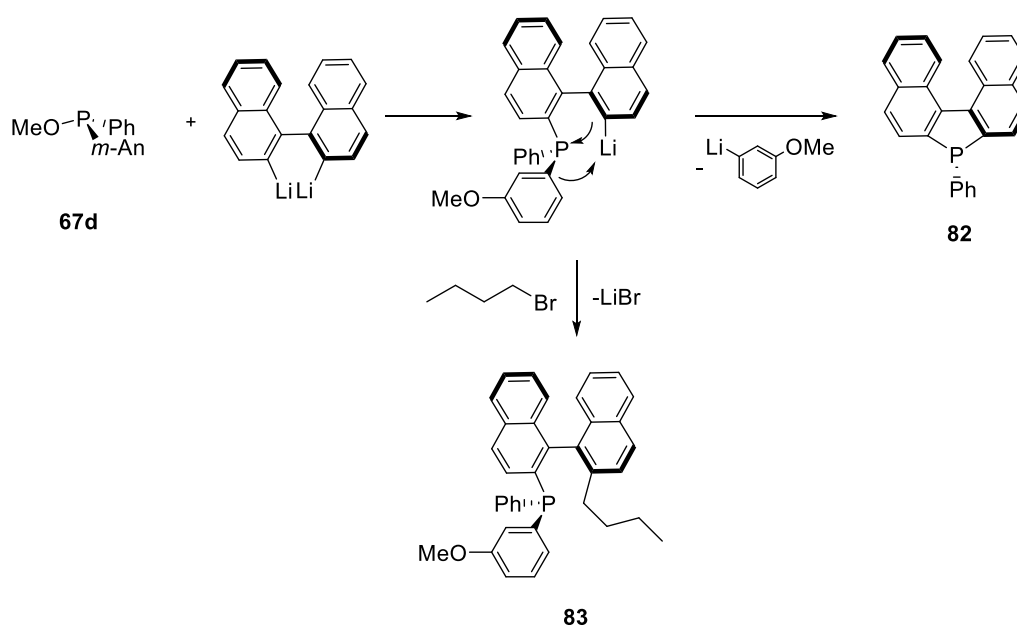


Figure 20: Products after the reaction of **16d** with 2,2'-dilithiated binaphthyl.

The compounds **82**, **83** and **84** are atypical for this kind of reaction. As described in Chapter 2, phosphine groups can be introduced into various backbones like dimethyl xanthene, di-*n*-butyldimethyl xanthene, dibenzofuran and diphenyl ether.

Stephan and his working group published in 2007 similar results; however, they tried to introduce a 2,2'-dilithio-1,1'-biarene at the level of the stereoselective ring opening of **14**.⁸⁶ In this manner they could access derivatives of **82**.

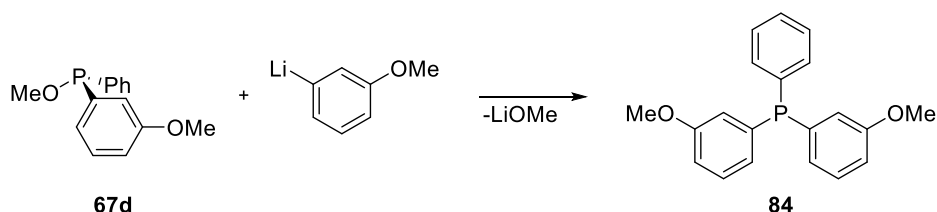
It is postulated, that, after the attack of the first naphthyl anion at the phosphorus atom, the ring closure with a simultaneous displacement of the *m*-anisyl group of the unprotected phosphinite **67d** is favoured (**82**) in comparison to a second substitution due to the physical proximity of the second naphthyl lithium group to phosphorus (Scheme 41).⁸⁶



Scheme 41: Postulated mechanism of the formation of **82** and **83**.

Simultaneously to the lithiation of binaphthyl with BuLi butyl bromide is formed. Butyl bromide can prevent the ring closure by reacting with the lithiated aryl to **83**. The driving force of the C-C-coupling is the formation of LiBr which seems to be as energetically beneficial like the ring closure (Scheme 41).

Compound **84** could result from the reaction of **67d** with the displaced *m*-anisyl group.

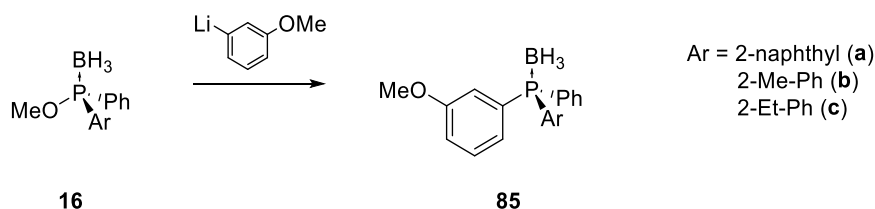


Scheme 42: Postulated mechanism of the formation of **84**

Regarding these results, a new synthetic route must be found *via* the synthesis of *P*-chirogenic (aryl)(1-iodonaphthalene-2-yl)(phenyl) phosphine oxide which can be subjected to Ullmann coupling to receive BINAP-derivatives with two additional chirogenic *P*-centres.

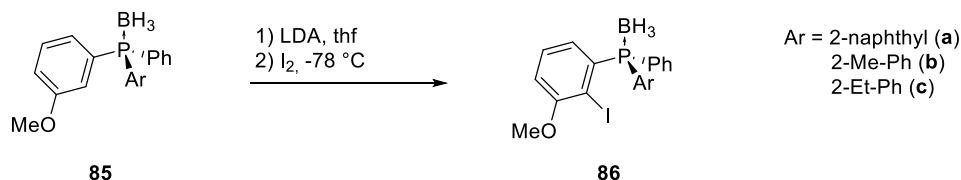
Following the idea of Ullmann coupling a tertiary *P*-chirogenic compound should be created bearing a 2-iodoaryl group and which is stable enough to realise the coupling procedure at around 140 °C.⁷¹

Since borane is a common protecting group for phosphorus compounds and it stabilises the phosphines at higher temperatures, the enantiopure triaryl phosphine was produced according to Jugé's (-)-ephedrine methodology (Scheme 43). It was assumed, that the P-borane bond will not survive the Ullmann coupling at 140 °C due to the instability of the P-B bond. After deprotection of **85** the selective oxidation should be necessary.



Scheme 43: Synthesis of enantiopure *m*-anisylarylphenyl phosphine (**85**).

In the next step, the iodine should be introduced into the 2-position of the *m*-anisyl unit. Therefore, the 2-position should be lithiated selectively by reaction with LDA, before iodine is added (Scheme 44).

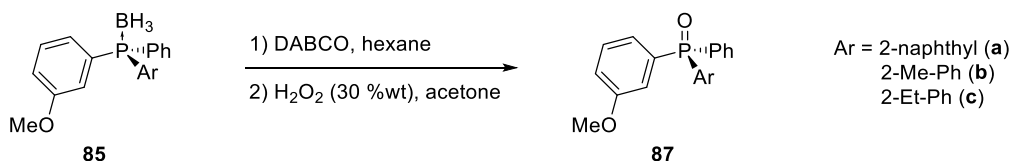


Scheme 44: Synthesis of aryl(2-iodo-3-methoxyphenyl)(phenyl)phosphine borane (**86**).

Unfortunately, the iodination of the borane phosphines did not proceed successfully. Either no conversion took place or the borane-free species of **85** was obtained. This phenomenon is according to the study of Imamoto in 1996.⁸⁷ The iodine can attack the borane group of the phosphines. After quenching the reaction with water, they received the borane-free phosphine.

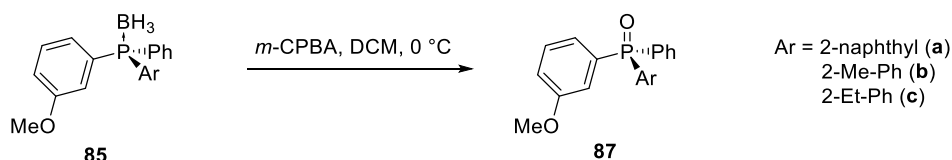
Obviously, the phosphine borane adducts are not applicable for the selective *ortho*-lithiation of the anisyl unit.

Therefore, we switched to the synthesis of *P*-chirogenic phosphine oxides with the goal to introduce the iodine in the 3-anisyl group. There are two methodologies available to produce the phosphine oxides. For the first one, the BH₃ is removed with DABCO. The unprotected phosphine is subsequently reacted with H₂O₂ in acetone to yield **87** (Scheme 45).



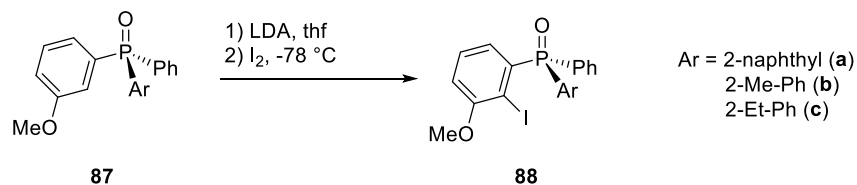
Scheme 45: Synthesis of enantiopure *m*-anisylarylphenylphosphine oxide (**87**) using H₂O₂.

By this procedure the optical purity dropped slightly. Better results were obtained by the direct oxidation of the borane compound **85** with *m*-CPBA following the protocol of Imamoto.⁸⁷ Therefore, compound **85** was treated with *m*-CPBA. The phosphine oxide **87** could be obtained in high yields and with retention of configuration (Scheme 46).



Scheme 46: Synthesis of enantiopure *m*-anisylarylphenylphosphine oxide (**23**) using *m*-CPBA.

Three 3-anisyl-aryl-phenylphosphine oxides **87** were tested in the iodination reaction. Following Pietrusiewicz' protocol, compound **87** was first lithiated with LDA and then reacted with iodine (Scheme 47).⁷¹



Scheme 47: Synthesis of aryl(2-iodo-3-methoxyphenyl)(phenyl)phosphine oxide (**24**).

The conversion of 3-anisyl-2-naphthyl-phenylphosphine oxide (**87a**) into the corresponding iodo compound **88a** was only about 24 %, however the completed lithiation of the anisyl group with LDA was confirmed by quenching with D₂O (Figure 21). Also the variation of the LDA concentration did not improve the conversion.

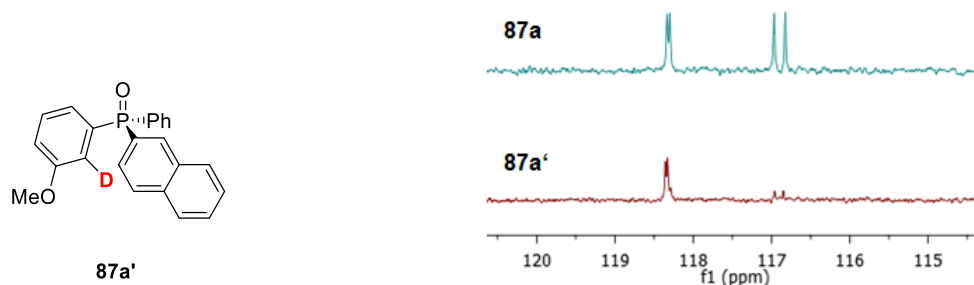


Figure 21: Comparison of ¹³C NMR spectra of **87a** and **87a'**(CDCl₃).

Both ^{13}C NMR spectra in Figure 21 display the CH-signal at $\delta = 116.8$ ppm. A significant reduction of the intensity of the CH-signal in the NMR spectrum of **87a'** proves the incorporation of deuterium at the 2-position of the 3-anisyl moiety. Also in the ^1H NMR spectrum a significant reduction of the aromatic H-signal at $\delta = 7.31$ ppm was found which underlines the introduction of deuterium, too. According to Pietrusiewicz' protocol the iodination should proceed smoothly but this observation we could not verify in our case.

Also the iodination of the *P*-chirogenic phosphine oxides **87b,c** failed. The lithiation with LDA took place at the side chains of these aryl substituents which could also be proved by quenching with D_2O after lithiation. The ^{13}C NMR spectra in Figure 22 illustrates the partially split signals of CH-couplings of the corresponding CH_3 - (*o*-tolyl; $\delta = 21.4$ ppm) and CH_2 -groups (*o*-ethyl phenyl; $\delta = 27.0$ ppm) which give evidence, that the lithiation took place at the side chains of *o*-tolyl and *o*-ethyl phenyl instead at the 2-position of the *m*-anisyl ring.

Obviously, the attack at the C-H acidic *ortho*-H-atom in the 3-anisyl group (adjacent electron-withdrawing groups) is blocked by steric hindrance and the benzylic H-atoms can be removed easier by LDA.

It is noteworthy, that despite a lithiation takes place, no iodination could be determined at the side chains.

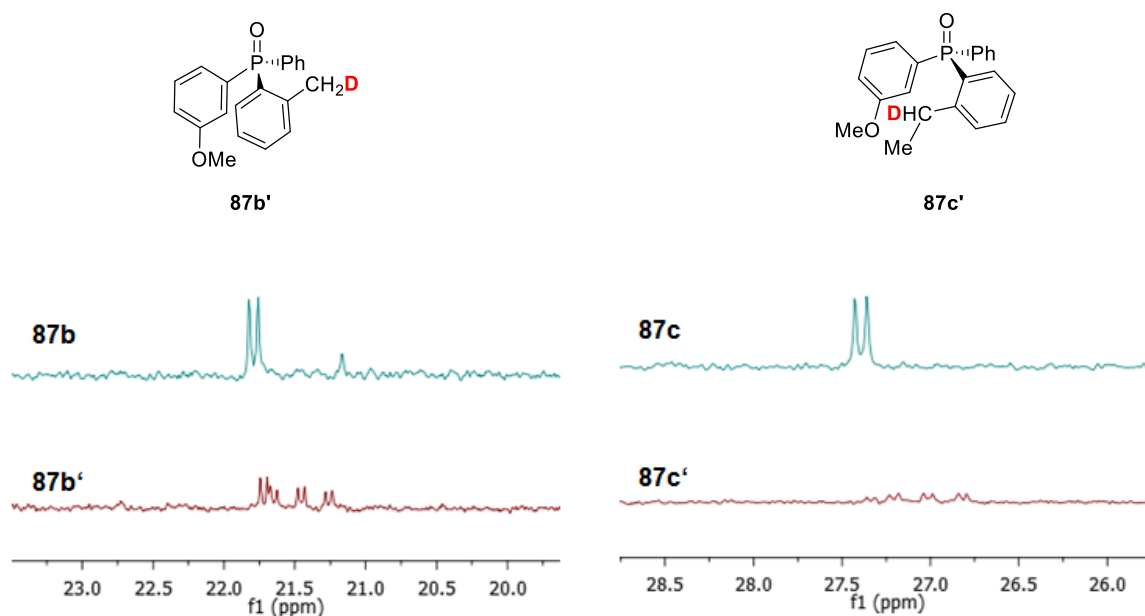
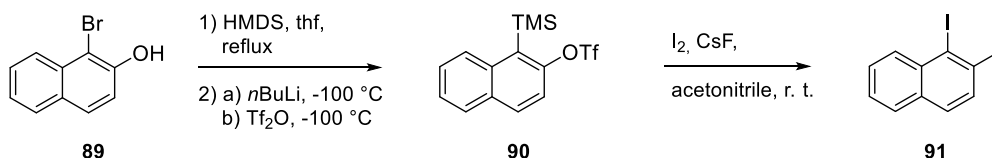


Figure 22: ^{13}C NMR (CDCl_3) of **87b,c**.

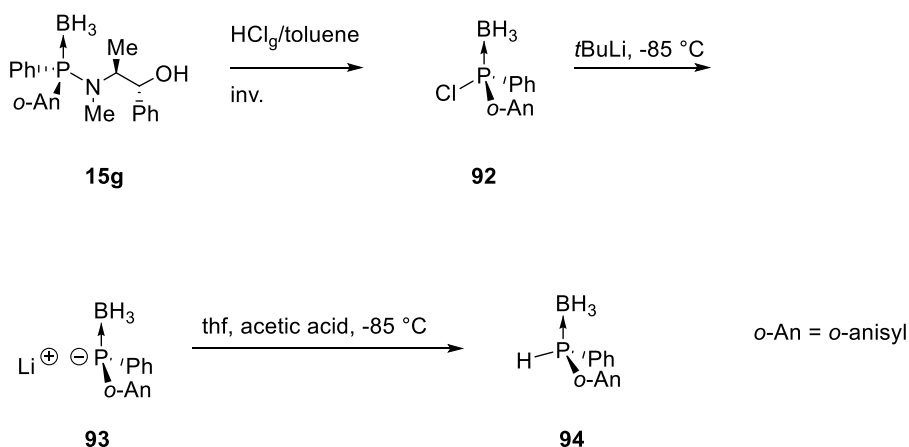
Since the introduction of iodine into the enantiomerically pure phosphine borane-complex **85** or oxide **87**, which is necessary for Ullmann coupling, failed, another procedure was investigated: Thus, a diiodonated naphthyl derivative was synthesised according to the protocols of Guitián and co-workers.⁸⁸



Scheme 48: Synthesis of 1,2-diiodo naphthalene (**91**).

In the first step, 1-bromo-2-naphthol (**89**) was reacted with hexamethyldisiloxane (HMDS). After removing the excess of HMDS the resulted 1-bromo-2-trimethylsilylnaphthalene was treated with *n*BuLi and triflic anhydride, subsequently. The reaction proceeded smoothly and yielded compound **90** with 92 %. The iodine was introduced in **90** with the assistance of CsF (78 % yield).

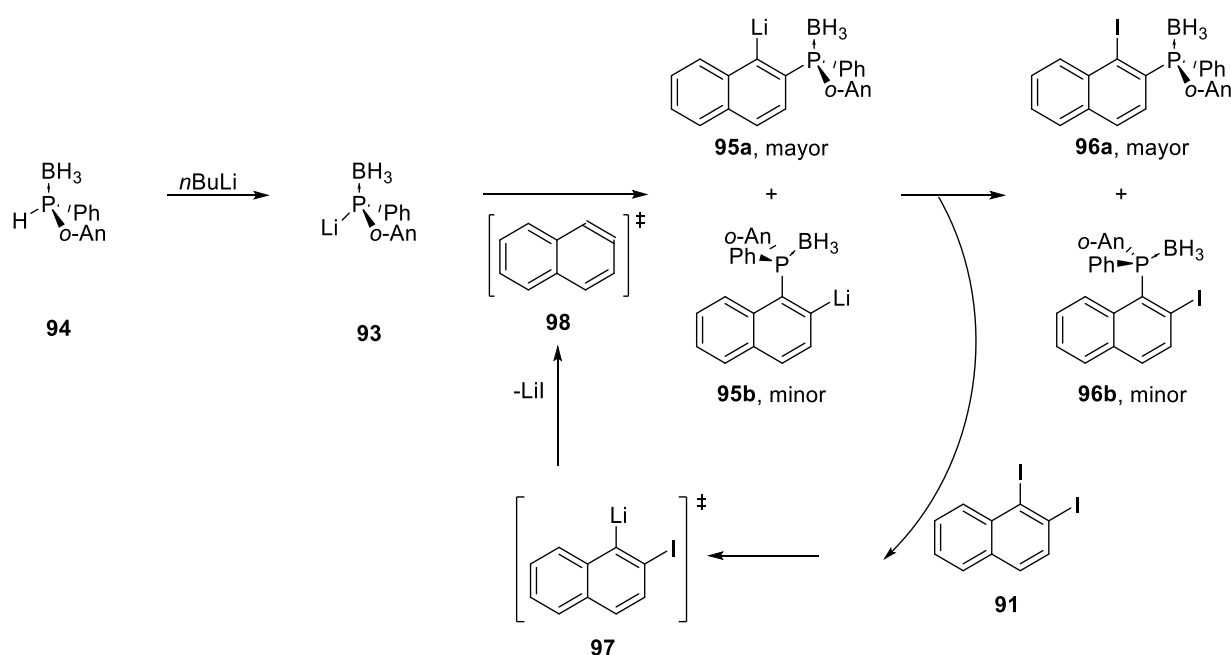
Subsequently, a secondary phosphine was synthesised employing the protocol of Jugé and his working group.⁴⁵ After the ring opening in the 1,3,2-oxoazaphospholidine **14**, the ephedrine unit was substituted by chlorine by treatment with HCl-gas dissolved in toluene. Chlorophosphine **92** was then treated with *t*BuLi and acetic acid subsequently in thf (Scheme 49).



Scheme 49: Synthesis of 2-anisylphenyl phosphine borane (**94**).

The reaction proceeded with conversion of nearly 100 % and under inversion of the configuration at the stereocentre. It was absolutely necessary to perform the reaction of the chlorophosphine at lower temperatures than -85 °C because with increasing temperatures the chiral *P*-centre can racemise. In consideration of these peculiarities, an enantiomeric excess by up to 95 %ee could be achieved.

The next synthetic step was the introduction of the diiodonaphthalene group into the secondary phosphine **94** which is based on aryne chemistry developed by Jugé and co-workers (Scheme 50).⁸⁹ The secondary phosphine borane **94** was deprotonated with *n*BuLi yielding the phosphinide **93**. The excess of 0.2 equivalents of *n*BuLi promoted the halogen-metal exchange with the 1,2-diiodo naphthalene **91**. Consequently, the anion **97** was generated. By elimination of LiI, the aryne **98** was formed, which reacted with the phosphinide borane **93** to yield the *ortho*-lithiated phosphine borane **95**. Finally, a second halogen-metal exchange occurred between the phosphine borane **95** and the 1,2-diiodo naphthalene **91** to result on the one hand the *ortho*-iodonated phosphine borane **96** and the anion **97** to generate a new aryne **98** on the other hand.



Scheme 50: Synthesis of (*R*)-(1-iodonaphthalen-1-yl)(2-methoxyphenyl)(phenyl)phosphine borane (**96a**) and its regioisomer **96b**.

The phosphinide **93** can attack both iodoaryl positions of **91** and thus two different regioisomers were obtained. The desired compound **96a** (^{31}P NMR: $\delta = 15.5$ ppm) was formed as the major product (Figure 23). Additionally, the other regioisomer **96b** (^{31}P NMR: $\delta = 18.6$ ppm) was formed. Moreover, parts of the borane free phosphines **99a,b** (^{31}P NMR: $\delta = 2.3$ ppm for **99a**, $\delta = 12.9$ ppm for **99b**) could be found. The amounts of the different products varied from reaction to reaction.

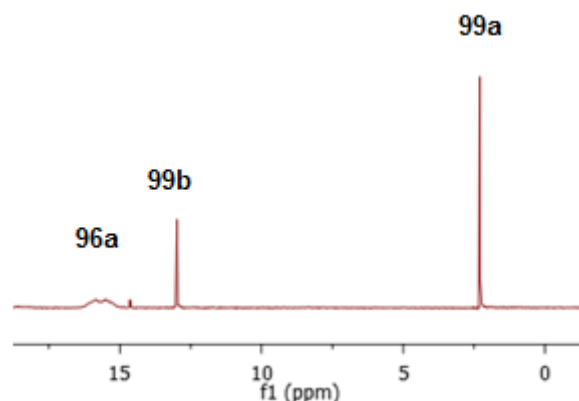
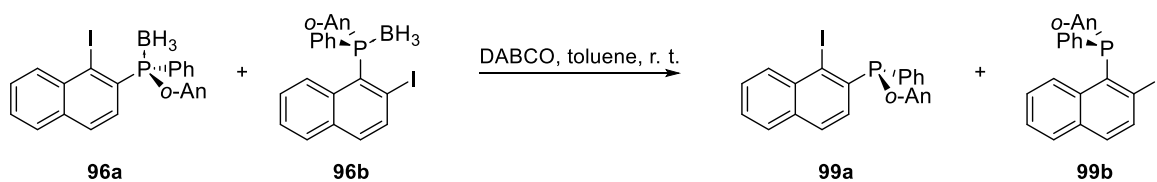


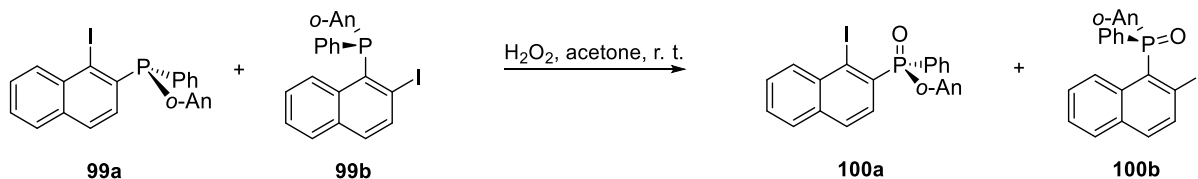
Figure 23: ^{31}P NMR spectrum (CDCl_3) of the raw product of the synthesis of (*R*)-(1-iodonaphthalen-1-yl)(2-methoxyphenyl)-(phenyl)phosphine borane (**96**).

The separation of the products was hard to realise by column chromatography or crystallisation due to similar polarities. Because the borane-free derivatives **99** were needed for the oxidation step, the crude product was treated with DABCO without further purification (Scheme 51).

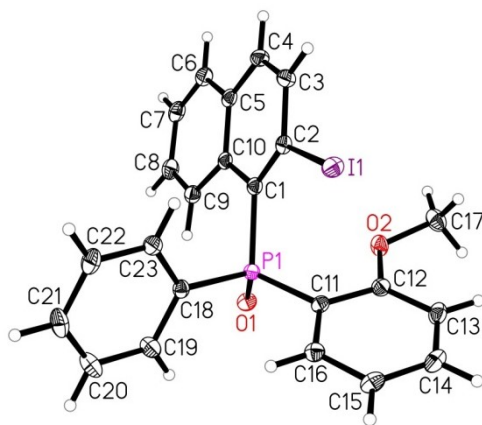


Scheme 51: Removal of the borane group from derivatives **96**.

After removing of $\text{DABCO} \cdot \text{BH}_3$ and solvent, the oxidation was conducted without separation of **99a,b** (Scheme 52).

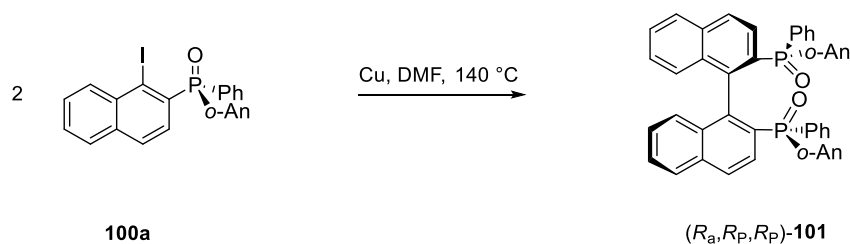
**Scheme 52:** Oxidation of **27**.

For the oxidation, the compounds **99a,b** were dissolved in acetone and oxidised with H_2O_2 . The purification was realised by column chromatography with a yield of **100a** of 25% (overall yield from **15f**) and 87% ee.

**Figure 24:** Molecular structure of the “wrong” isomer **100b** in the solid state.

Only one molecule of the asymmetric unit is depicted. Displacement ellipsoids correspond to 30 % probability.

From derivative **100b** crystals could be isolated which were investigated by x-ray structural analysis (Figure 24). By this way the structure of derivative **100b** could be determined possessing the chiral P-group in 1- and the iodine group in 2-position. By this reason the derivative **100b** was identified as minor product which is not suitable for the coupling reaction. Therefore, **100a** as the other regioisomer was applied.



Scheme 53: Application of **100a** for the Ullmann coupling.

Compound **100a** was coupled in the presence of activated copper powder at $140\text{ }^{\circ}\text{C}$ (Scheme 53). By crystallisation in DCM/ethyl acetate, the pure compound **101** was obtained in 36 % yield. To ensure, that compound **101** was diastereomerically pure, a ^{31}P NMR spectrum was recorded which showed only one P-signal. Probably only one diastereomer of compound **101** was formed, otherwise there would be an additional signal for the (S_a, R_p, R_p) -**101** in regard to the different magnetic environment around the phosphorus atoms. To show the absolute configuration, an x-ray structural analysis was carried out (Figure 25). It shows, the (R_a, R_p, R_p) -isomer of **101**.

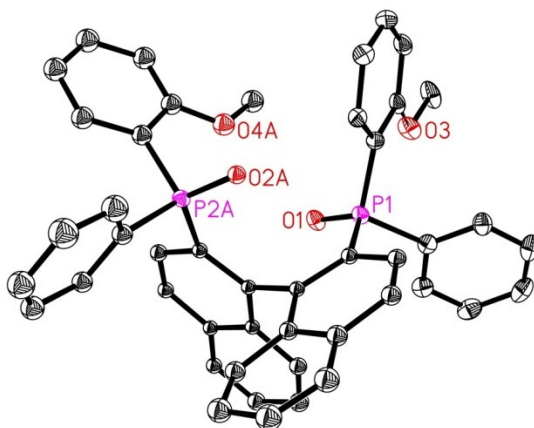


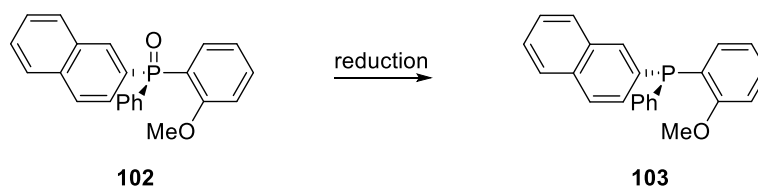
Figure 25: Molecular structure of **101** in the solid state.

Displacement ellipsoids correspond to 30 % probability. Large parts of the molecule are disordered over two sites with occupancies of 0.554(6): 0.446(6). Lower occupancy sites and hydrogen atoms are omitted for clarity.

The configuration of the *P*-centres of **101** is already defined in the configuration of the derivative **100a**. To explain why diastereomer (*R*_a,*R*_P,*R*_P)-**101** was obtained as major product during the Ullman coupling, DFT-calculations were done. Our computations show that the (*R*_a,*R*_P,*R*_P)-isomer is much more stable than the (*S*_a,*R*_P,*R*_P)-isomer on the basis of the computed Gibbs free energy difference of about 5.0 kcal/mol. This agrees with the experimental result. In addition, the optimised bond parameters agree also well with those derived from x-ray analysis (Figure 26).

To use **101** as ligand in asymmetric catalysis, it is necessary to reduce the phosphine oxide to the trivalent phosphines with retention of *P*-centre. Different reduction methods were tested (Table 13).

For preliminary investigations, an enantiopure phosphine oxide **102** with a similar structure in comparison to **101** was used to examine the conversion and the configurational stability at the P-atom (Scheme 54).



Scheme 54: Exemplary investigations of the reduction of the *P*-chirogenic compound **101**.

Table 13: Results of the exemplary investigations of the reduction of the *P*-stereogenic compound **102**.

Entry	Reducing agent	T [°C]	Solvent	t [h]	Conv. [%] ^a	%ee ^b
1	6 Eq. BH ₃ *thf	0- r. t.	thf	19	0	-
2	6 Eq. BH ₃ *thf	0-40	thf	19	0	-
3	Diphenyldisiloxane + Add.	r. t.	ea	48	24	-
4	Diphenyldisiloxane + Add.	r. t.	ea	168	2	-
5	Oxalyl chloride/LiBH ₄	r. t. /0	CHCl ₃ / thf	1.5	96	0
6	5 Eq. PMHS, 0,5 Eq. Ti(O <i>i</i> Pr) ₄	r. t.	thf	24	10	-
7	5 Eq. PMHS, 0,5 Eq. Ti(O <i>i</i> Pr) ₄	r. t.	thf	168	12	-
8	5 Eq. PMHS, 0,5 Eq. Ti(O <i>i</i> Pr) ₄	67	thf	1	20	-
9	30 Eq. PMHS, 3 Eq. Ti(O <i>i</i> Pr) ₄	67	thf	2	100	83
10	30 Eq. PMHS, 3 Eq. Ti(O <i>i</i> Pr) ₅	r. t.	thf	96	100	95

^aEstimated with quant. ³¹P NMR. ^bThe free phosphine **103** was protected with BH₃. The optical purity was examined with chiral HPLC.

The first experiment was conducted according to the protocol of Pietrusiewicz and co-workers.⁹⁰ They published in 2015 a methodology to reduce functionalised tertiary phosphine oxides with BH₃. This reaction was tested with the model substance **102**. It was reacted with an excess of BH₃*thf at various temperatures (Table 13, Entry 1 and 2). After 19 hours the conversion was determined by NMR. For both experiments, no conversion was observed (³¹P NMR: δ = 29.9 ppm for **102**).

The same reaction protocol was tested with diphosphine oxide **101** in hand with an excess of BH₃*thf and BH₃*SMe₂ at 0 °C-room temperature. Also in these both cases no conversion was observed.

Another common protocol to reduce tertiary phosphine oxides is the usage of different silicon reagents. A promising protocol was published in 2017 by Aldrich and his working group.⁹¹ The phosphine oxides were reduced with 1,3-diphenyl-disiloxane and di(nitrophenyl)phosphate as additive at room temperature in excellent yields. Following this protocol, **102** was treated for a long period of time (Table 13, Entry 3 and 4). The conversion after 48 hours was only 24 %

(^{31}P NMR: $\delta = -4.1$ ppm for **103**). A second trial with prolonged reaction time of 168 hours was realised to try to achieve full conversions but only 2 % of free phosphine was found.

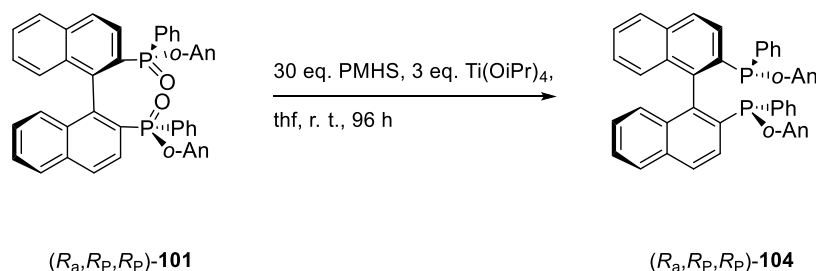
In 2015, Gilheany and co-workers applied lithium borohydride for reductive boronation at phosphorus.⁹² According to their protocol, **102** reacts with oxalyl chloride (Table 13, Entry 5). After removal of the remaining reducing agent, the residue was treated with LiBH_4 . The conversion of this reaction was 96 %, but the HPLC-analysis with a chiral column showed a racemic mixture of (*R*)- and (*S*)-**103**.

Muhammad and his working group carried out the reduction with titanium(IV) as catalyst and polymethylhydrosiloxane (PMHS) as reducing agent and propagated this as an extremely efficient methodology for the reduction of phosphine oxides which takes place under retention of configuration of the phosphorus.⁹³ Following their protocol, only 10 % of free phosphine could be generated (Table 13, Entry 6). Therefore, the reaction was reiterated with a reaction time of 168 hours, which did not raise the conversion significantly (Table 13, Entry 7). To examine whether a higher temperature could increase the conversion, the reaction was carried out at 67 °C (Table 13, Entry 8). Unfortunately, only 20 % of free phosphine could be determined in the ^{31}P NMR. The examination of the optical purity of the product **103** was waived due to the low yields.

In 1997, Hamada and co-workers used a similar protocol to reduce Xantphos derivatives.⁹⁴ According to this protocol, PMHS and $\text{Ti}(\text{O}i\text{Pr})_4$ were added in large excess to the phosphine oxide **102**. The ^{31}P NMR showed full conversion to **103**. The free phosphine was then protected with BH_3 and afterwards examined with chiral HPLC to prove the stereochemistry. It was found, that the phosphine was formed in an enantiomeric excess of 83 %.

To improve the ee-value, the reaction was repeated at room temperature for a longer period of time (Table 13, Entry 10). The conversion was proved to be about 100 %. After the boronation, chiral HPLC was carried out for the separation. The enantiomeric excess was proved to be increased by this protocol to 95 %.

Since the conversion of the phosphine oxide **102** was successful using this protocol, it was applied to reduce compound **101** (Scheme 55).



Scheme 55: Reduction of **101** with PMHS and Ti(OiPr)_4 .

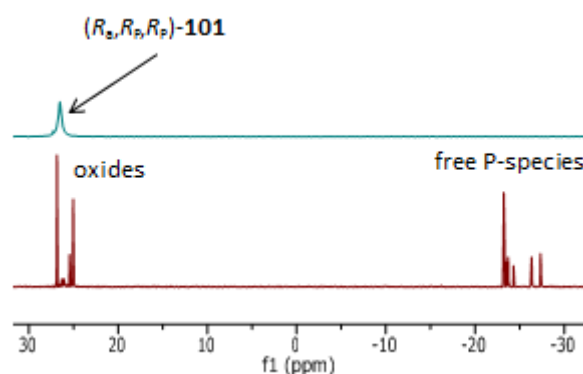


Figure 26: ^{31}P NMR spectrum (CDCl_3) of the raw product (red) after reduction of **101** with PMHS and Ti(OiPr)_4 .

Figure 26 shows the ^{31}P NMR spectrum of the crude product after the reduction of **101**. In the range between 27-24 ppm, where the oxides resonate, still five signals of P-oxides can be detected that means that the reduction was incomplete. There are also 9 signals corresponding to unprotected P-species in the range between 28-23 ppm. It can be assumed, that the reduction did not proceed under retention of the axial and *P*-central chirality, so that due to racemisation different diastereomers were formed. Unfortunately, a separation was not possible.

At this point, the investigations had to be stopped.

3.3 Conclusion

In Chapter 3, the synthesis of a *P*-chirogenic and axial chiral di(triaryl phosphine oxide) with BINAP-backbone **101** could be shown.

First intentions to achieve the synthesis of such di(triaryl phosphines) **81** according to the Jugé method via (-)-ephedrine were not successful.

A new route was developed starting from a *P*-chirogenic secondary phosphine borane **94**. The hydrogen atom of **94** could be substituted by diiodonaphthalene to produce (*R*)-(1-iodonaphthalen-1-yl)(2-methoxyphenyl)(phenyl)phosphine borane (**96**). After the conversion of *P*-chirogenic **96** into its oxide **100** the major phosphine oxide **100a** could be separated by column chromatography.

Subsequently, (*R*)-(1-iodonaphthalen-1-yl)(2-methoxyphenyl)(phenyl)phosphine oxide (**100a**) was coupled via Ullmann coupling.

It was found, that the (*R_a*,*R_P*,*R_P*)-isomer of ([1,1'-binaphthalene]-2,2'-diyl)di((2-methoxy)(phenyl)(phenyl)phosphine oxide (**101**) was the major product.

The reduction of the BINAP-type di(triaryl phosphine oxide) was not successful. Further investigations have to be done to find an appropriate reducing agent and a procedure to realise the reduction with high conversion and constantly high stereoselectivity.

After a successful reduction of **101** to the desired chiral diphosphine **104** this derivative should be tested as ligand in asymmetric reactions. The combination of different symmetry elements in one molecule could lead to an increase of enantiomeric excess and turnover frequencies. Furthermore, it could help to develop a better comprehension of important factors in ligand design.

4. Experimental Data

4.1 General Information

All reactions were carried out under argon atmosphere using standard Schlenk techniques. The used solvents were dried and freshly distilled under argon. Flash chromatography was performed with silica gel 60 (particle size 0.040 - 0.063 mm) with a CombiFlash R_F system (Teledyne ISCO).

Definition of the analytic equipment

The analytic data was examined with the following devices:

GC

The enantiomeric excess of 3,3,5-trimethylcyclohexanone **71** was determined with:

GC HP6890N (Hewlett Packard/Agilent), column: LIPODEX E (25 m), injector volume: 2 µL, temperature program: 90/30-6-180/10

HPLC

The enantiomeric excess of the phosphinite boranes **16a-e** were determined with:

HP 1100 (Hewlett Packard) with DAD, chiralyser and RI-detector

The methods vary in dependence of the compound.

NMR

The NMR spectra were recorded with the following devices:

- **Bruker AVANCE III 500**, at the following frequencies: 500MHz (¹H), 126 MHz (¹³C), 202 MHz (³¹P)
- **Bruker AVANCE 400**, at the following frequencies: 400 MHz (¹H), 100 MHz (¹³C), 161 MHz (³¹P)
- **Bruker AVANCE 300**, at the following frequencies: 300 MHz (¹H), 75 MHz (¹³C), 121 MHz (³¹P)

Chemical shifts of ¹H and ¹³C NMR spectra are reported in ppm downfield from used solvent CDCl₃ as internal standard (7.25 ppm / 77.00 ppm). Chemical shifts of ³¹P NMR spectra are

4. Experimental Data

4.1 General Information

referred to H_3PO_4 as external standard. The spectra were evaluated with the software MestReNova version 8.0.1-10878.

Signals are quoted as s (singlet), d (doublet), t (triplet), q (quartet), m (multiplet) and br (broad).

MS

Mass spectra were recorded on a Thermo Electron MAT 95-XP or an Agilent 1200/6210 Time-of-flight LC-MS.

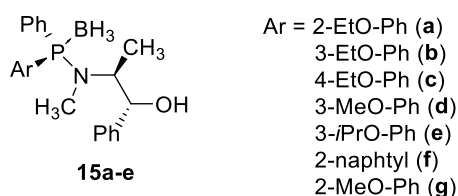
X-ray crystal structure analysis:

Diffraction data were collected on a Bruker Kappa APEX II Duo diffractometer. The structures were solved by direct methods (SHELXS-97⁹⁵) and refined by full-matrix least-squares procedures on F^2 (SHELXL-2014⁹⁶). XP (Bruker AXS) was used for molecular graphics.

4.2 Synthesis and Analytic Data

Compounds **14**, **15a-e** and **16a-e** were synthesised according to known procedures (reference 24).

Synthesis of (1*R*,2*S*)-2-[(*S*)-(Aryl)phenylphosphanyl]methylamino-1-phenylpropane-1-ol-P-borane complex (**15a-e**)



Secondary butyl lithium (20 mmol; 14.3 mL; 1.4 M cyclohexane solution) was placed into a Schlenk-tube and cooled down to 0 °C. Then, the corresponding aryl bromides (20 mmol) were added dropwise. After 1 h stirring, the resulting suspension was diluted with thf until the precipitation is dissolved.

Now, the resulting reagent was added dropwise to a solution of compound **14** (10 mmol; 2.85 g) in thf (10 mL) at -78 °C. After 1 h, the mixture was allowed to warm up to room temperature and stirred overnight.

Then the mixture was quenched with water (5 mL). The organic solvents were evaporated under vacuum before the remaining aqueous residue was extracted with DCM (3x25 mL). Afterwards, the organic layers were combined and dried (MgSO₄). After evaporation of the solvents, the residue was purified by column chromatography.

(1*R*,2*S*)-2-[(*S*)-(2-Ethoxyphenyl)phenylphosphanyl]methylamino-1-phenylpropane-1-ol-P-borane complex (**15a**)

Column chromatography with cyclohexane/AcOEt 19/1 - 4/1; yield: 81 %.

M. p.: 56 °C; colourless solid.

$[\alpha]_D^{23} = +29.7^\circ$ ($c = 1.0$; CHCl₃).

4. Experimental Data

4.2 Synthesis and Analytic Data

¹H NMR (300 MHz, chloroform-*d*) δ = 7.73 (m, 1H; arom. H), 7.46 (m, 1H; arom. H), 7.26 (m, 8H; arom. H), 7.04 (m, 1H; arom. H), 6.86 (m, 1H; arom. H), 4.88 (d, *J* = 5.7 Hz, 1H; CHOH), 4.33 (m, 1H; CH), 3.79 (m, 2H; OCH₂CH₃), 2.59 (d, *J* = 8.1 Hz, 3H; CH₃), 1.95 (s, 1H; OH), 1.23 (d, *J* = 6.8 Hz, 3H; CHCH₃), 0.82 (t, *J* = 7.0 Hz, 3H; OCH₂CH₃), 1.13 (br q, 3H; BH₃).

¹³C NMR (75 MHz, chloroform-*d*) δ = 160.32 (d, *J* = 2.0 Hz; COEt), 142.69 (CC), 135.27 (d, *J* = 11.8 Hz; CH), 133.32 (CH), 132.73 (d, *J* = 72.4 Hz; CP), 130.74 (d, *J* = 10.5 Hz; 2xCH), 129.84 (d, *J* = 2.5 Hz; CH), 128.02 (CH), 128.49 (2xCH), 127.80 (d, *J* = 12.2 Hz; 2xCH), 126.73 (2xCH), 120.76 (d, *J* = 11.1 Hz; CH), 118.28 (d, *J* = 56.9 Hz; CP), 111.89 (d, *J* = 4.4 Hz; CH), 78.93 (d, *J* = 5.7 Hz; CHOH), 63.53 (OCH₂), 58.25 (d, *J* = 10.5 Hz; CH), 30.94 (d, *J* = 3.9 Hz; CH₃), 13.83 (OCH₂CH₃), 13.04 (d, *J* = 2.2 Hz; CHCH₃).

³¹P NMR (122 MHz, chloroform-*d*) δ = +68.96 (m).

MS (EI, 70 eV) *m/z*: 406 (3, [M-H]⁺), 286 (100, [M-BH₃-PhCHOH]⁺), 229 (85, [(2-EtO-Ph)PhP]⁺).

HRMS (ESI) [M+H]⁺: *m/z* calculated C₂₄H₃₁BNO₂P 408.22626, determined 408.22715, [M+H-BH₃]⁺: *m/z* calculated C₂₄H₂₈NO₂P 394.19304, determined 394.19368.

(1*R*,2*S*)-2-[(*S*)-(3-Ethoxyphenyl)phenylphosphanyl]methyldamino-1-phenylpropane-1-ol P-borane complex (**15b**)

Column chromatography with cyclohexane/AcOEt 9/1; yield: 90 %.

M. p.: 95 °C; colourless solid.

$[\alpha]_D^{22} = +40.7^\circ$ (*c* = 1.0; CHCl₃).

¹H NMR (300 MHz, chloroform-*d*) δ = 7.29 (m, 9H; arom. H), 7.08 (m, 4H; arom. H), 6.94 (m, 1H; arom. H), 4.75 (d, *J* = 6.3 Hz, 1H; CHOH), 4.25 (m, 1H; CH), 3.95 (q, *J* = 7.0 Hz, 2H; OCH₂), 2.43 (d, *J* = 7.7 Hz, 3H; CH₃), 1.91 (s, 1H; OH), 1.34 (t, *J* = 7.0 Hz, 3H; OCH₂CH₃), 1.20 (d, *J* = 6.7 Hz, 3H; CHCH₃), 0.97 (br q, 3H; BH₃).

¹³C NMR (75 MHz, chloroform-*d*) δ = 158.85 (d, *J* = 12.6 Hz; COEt), 142.55 (CC), 132.44 (d, *J* = 59.4 Hz; CP), 132.05 (d, *J* = 10.4 Hz; 2xCH), 130.71 (d, *J* = 2.4 Hz; CH), 130.61 (d, *J* = 68.3 Hz; CP), 129.62 (d, *J* = 11.6 Hz; CH), 128.59 (2xCH), 128.33 (d, *J* = 10.5 Hz; 2xCH),

4. Experimental Data

4.2 Synthesis and Analytic Data

127.93 (CH), 126.83 (2xCH), 124.53 (d, $J = 9.6$ Hz; CH), 118.30 (d, $J = 12.1$ Hz; CH), 117.24 (d, $J = 2.1$ Hz; CH), 78.71 (d, $J = 5.8$ Hz; CHOH), 63.66 (OCH₂), 58.20 (d, $J = 10.3$ Hz; CH), 30.57 (d, $J = 3.9$ Hz; CH₃), 14.80 (OCH₂CH₃), 13.59 (d, $J = 2.1$ Hz; CHCH₃).

³¹P NMR (122 MHz, chloroform-*d*) $\delta = +71.44$ (m).

MS (EI, 70 eV) m/z : 392 (1, [M-H-BH₃]⁺), 376 (1, [M-OH-BH₃]⁺), 300 (32, [M-H-BH₃-Ph-CH₃]⁺), 286 (100, M-BH₃-PhCHOH]⁺), 229 (97, [(3-EtO-Ph)PhP]⁺).

HRMS (ESI) [M+Na]⁺: m/z calculated C₂₄H₃₁BNO₂P 430.2082, determined 430.20854, [M+H-BH₃]⁺: m/z calculated C₂₄H₂₈NO₂P 394.19304, determined 394.19411.

(1*R*,2*S*)-2-[(*S*)-(4-Ethoxyphenyl)phenylphosphanyl]methylamino-1-phenylpropane-1-ol P-borane complex (15c)

Column chromatography with cyclohexane/AcOEt 19/1 - 9/1; yield: 71 %.

M. p.: 49 °C; colourless solid.

$[\alpha]_D^{22} = +35.6^\circ$ ($c = 1.0$; CHCl₃).

¹H NMR (300 MHz, chloroform-*d*) $\delta = 7.50$ (m, 5H; arom. H), 7.32 (m, 5H; arom. H), 7.11 (m, 2H; arom. H), 6.93 (m, 2H; arom. H), 4.80 (d, $J = 6.5$ Hz, 1H; CHOH), 4.29 (m, 1H; CH), 4.06 (q, $J = 7.0$ Hz, 2H; OCH₂), 2.45 (d, $J = 7.9$ Hz, 3H CH₃), 1.92 (s, 1H; OH), 1.43 (t, $J = 7.0$ Hz, 3H; OCH₂CH₃), 1.23 (d, $J = 6.7$ Hz, 3H; CHCH₃), 1.00 (br q, 3H; BH₃).

¹³C NMR (75 MHz, chloroform-*d*) $\delta = 161.32$ (d, $J = 2.2$ Hz; COEt), 142.60 (CC), 134.36 (d, $J = 11.5$ Hz; 2xCH), 131.97 (d, $J = 10.2$ Hz; 2xCH), 131.11 (d, $J = 69.5$ Hz; CP), 130.56 (d, $J = 2.4$ Hz; CH), 128.62 (2xCH), 128.31 (d, $J = 10.4$ Hz; 2xCH), 127.96 (CH), 126.91 (2xCH), 121.63 (d, $J = 64.4$ Hz; CP), 114.53 (d, $J = 11.0$ Hz; 2xCH), 78.73 (d, $J = 6.3$ Hz; CHOH), 63.65 (OCH₂), 58.10 (d, $J = 10.1$ Hz; CH), 30.30 (d, $J = 3.8$ Hz; CH₃), 14.83 (OCH₂CH₃), 13.70 (d, $J = 1.9$ Hz; CHCH₃).

³¹P NMR (122 MHz, chloroform-*d*) $\delta = 69.56$ (d, $J = 84.8$ Hz).

MS (EI, 70 eV) m/z : 392 (1, [M-H-BH₃]⁺), 300 (23, [M-H-BH₃-Ph-CH₃]⁺), 286 (100, M-BH₃-PhCHOH]⁺), 229 (97, [(4-EtO-Ph)PhP]⁺), 201 (84, [(4-HO-Ph)PhP]⁺).

4. Experimental Data

4.2 Synthesis and Analytic Data

HRMS (ESI) $[M+Na]^+$: m/z calculated $C_{24}H_{31}BNO_2P$ 430.20820, determined 430.20854, $[M+H-BH_3]^+$: m/z calculated $C_{24}H_{28}NO_2P$ 394.19304, determined 394.19371.

(1*R*,2*S*)-2-[(*S*)-(3-Methoxyphenyl)phenylphosphanyl]methylamino-1-phenylpropane-1-ol P-borane complex (15d)

Column chromatography with cyclohexane/AcOEt 9/1 to 4/1; yield: 93 %.

Yellow syrup.

$[\alpha]_D^{22} = 43.6^\circ$ ($c = 1.0$; $CHCl_3$).

1H NMR (400 MHz, chloroform-*d*) $\delta = 7.29$ (m, 10H; arom. H), 7.08 (m, 3H; arom. H), 6.94 (m, 1H; arom. H), 4.74 (d, $J = 6.2$ Hz, 1H; HOCH), 4.23 (m, 1H; CH), 3.71 (s, 3H; OCH₃), 2.41 (d, $J = 7.7$ Hz, 3H; CH₃), 1.87 (s, 1H; OH), 1.19 (d, $J = 6.8$ Hz, 3H; CHCH₃), 0.94 (br q, 3H; BH₃).

^{13}C NMR (101 MHz, chloroform-*d*) $\delta = 159.43$ (d, $J = 12.7$ Hz; COMe), 142.48 (CC), 132.52 (d, $J = 59.6$ Hz; CP), 132.01 (d, $J = 10.3$ Hz; 2xCH), 130.70 (d, $J = 2.3$ Hz; CH), 130.51 (d, $J = 68.2$ Hz; CP), 129.61 (d, $J = 11.6$ Hz; CH), 128.56 (2xCH), 128.30 (d, $J = 10.5$ Hz; 2xCH), 127.91 (CH), 126.78 (2xCH), 124.62 (d, $J = 9.7$ Hz; CH), 117.78 (d, $J = 12.2$ Hz; CH), 116.60 (d, $J = 2.1$ Hz; CH), 78.68 (d, $J = 5.8$ Hz; HOCH), 58.17 (d, $J = 10.4$ Hz; CH), 55.36 (OCH₃), 30.54 (d, $J = 3.9$ Hz; CH₃), 13.53 (d, $J = 2.1$ Hz; CHCH₃).

^{31}P NMR (162 MHz, chloroform-*d*) $\delta = +71.46$ (m).

MS (EI, 70 eV) m/z : 392 (1, $[M-H]^+$), 378 (2, $[M-H-BH_3]^+$), 286 (92 M-PhCHOH⁺), 272 (100, $[MBH_3-PhCHOH]^+$), 215 (99, $[(3-MeO-Ph)PhP]^+$).

HRMS (ESI) $[M+Na]^+$: m/z calculated $C_{23}H_{29}BNO_2P$ 416.19253, determined 416.19315, $[M+H-BH_3]^+$: m/z calculated $C_{23}H_{26}NO_2P$ 380.17739, determined 380.17790.

(1*R*,2*S*)-2-[(*S*)-(3-Isopropoxyphenyl)phenylphosphanyl]methylamino-1-phenylpropane-1-ol P-borane complex (15e)

Column chromatography with cyclohexane/AcOEt 19/1; yield: 88 %.

Colourless syrup.

$[\alpha]_D^{22} = +39.0^\circ$ ($c = 1.0$; CHCl_3).

^1H NMR (300 MHz, chloroform-*d*) $\delta = 7.30$ (m, 9H; arom. H), 7.08 (m, 4H; arom. H), 6.93 (m, 1H; arom. H), 4.76 (d, $J = 6.2$ Hz, 1H; PhCH), 4.45 (hept, $J = 6.0$ Hz, 1H; OCHMe₂), 4.25 (m, 1H; CH), 2.44 (d, $J = 7.7$ Hz, 3H; CH₃), 1.88 (s, 1H; OH), 1.26 (d, $J = 6.0$ Hz, 3H; OCHCH₃), 1.26 (d, $J = 6.0$ Hz, 3H; OCHCH₃), 1.21 (d, $J = 6.7$ Hz, 3H; CH₃), 0.95 (br q, 3H; BH₃).

^{13}C NMR (75 MHz, chloroform-*d*) $\delta = 157.82$ (d, $J = 12.6$ Hz; CO*i*Pr), 142.56 (CC), 132.39 (d, $J = 59.2$ Hz; CP), 132.07 (d, $J = 10.4$ Hz; 2xCH), 130.71 (d, $J = 2.5$ Hz; CH), 130.66 (d, $J = 68.2$ Hz; CP), 129.65 (d, $J = 11.6$ Hz; CH), 128.61 (2xCH), 128.33 (d, $J = 10.4$ Hz; 2xCH), 127.95 (CH), 126.84 (2xCH), 124.42 (d, $J = 9.6$ Hz; CH), 119.37 (d, $J = 12.1$ Hz; CH), 118.75 (d, $J = 2.0$ Hz; CH), 78.75 (d, $J = 5.7$ Hz; HOCH), 70.14 (OCH), 58.21 (d, $J = 10.3$ Hz; CH), 30.59 (d, $J = 4.0$ Hz; CH₃), 22.05 (OCHCH₃), 21.96 (OCHCH₃), 13.59 (d, $J = 2.1$ Hz; CHCH₃).

^{31}P NMR (122 MHz, chloroform-*d*) $\delta = +71.28$ (m).

MS (EI, 70 eV) m/z : 420 (8, $[\text{M}-\text{H}]^+$), 406 (3, $[\text{M}-\text{H}-\text{BH}_3]^+$), 300 (5, $[\text{M}-\text{BH}_3-\text{PhCHOH}]^+$), 243 (23, $[(2-i\text{PrO}-\text{Ph})\text{PhP}]^+$), 58 (100, $[\text{C}_3\text{H}_6\text{O}]^+$).

HRMS (ESI) $[\text{M}+\text{Na}-\text{BH}_3]^+$: m/z calculated $\text{C}_{25}\text{H}_{30}\text{NO}_2\text{P}$ 430.19064, determined 430.19008, $[\text{M}+\text{Na}]^+$: m/z calculated $\text{C}_{25}\text{H}_{33}\text{BNO}_2\text{P}$ 444.22387, determined 444.22392.

(1*R*,2*S*)-2-(Methyl(*S*)-naphthalene-2-yl(phenyl)phosphanyl)amino)-1-phenylpropane-1-ol P-borane complex (15f)

Column chromatography with cyclohexane/AcOEt 19/1 - 9/1; yield: 87 %.

M. p.: 135-136 °C; yellow solid.

$[\alpha]_D^{23} = +59.8^\circ$ ($c = 1.0$; CHCl_3).

4. Experimental Data

4.2 Synthesis and Analytic Data

¹H NMR (300 MHz, chloroform-*d*) δ = 8.11 (d, 1H; arom. H), 7.87 (m, 3H; arom. H), 7.39 (m, 15H; arom. H), 4.86 (d, *J* = 6.3, 1H; *CHOH*), 4.36 (m, 1H; CH), 2.54 (d, *J* = 7.8, 3H; CH₃), 1.83 (s, 1H; OH), 1.30 (br q, 3H; BH₃), 1.29 (d, *J* = 6.7, 3H; CHCH₃).

¹³C NMR (75 MHz, chloroform-*d*) δ = 142.56 (CC), 134.42 (d, *J* = 2.0; CC), 133.96 (d, *J* = 10.6; CH), 132.70 (d, *J* = 11.2; CC), 132.16 (d, *J* = 10.3; 2xCH), 130.83 (d, *J* = 2.1; CH), 130.72 (d, *J* = 68.5; CP), 128.90 (CH), 128.79 (CP), 128.67 (2xCH), 128.47 (d, *J* = 10.5; 2xCH), 128.22 (d, *J* = 9.8; CH), 128.03 (CH), 128.01 (CH), 127.85 (CH), 127.72 (CH), 126.87 (2xCH), 126.84 (CH), 78.81 (d, *J* = 5.8; *CHOH*), 58.31 (d, *J* = 10.2; CH), 30.67 (d, *J* = 4.0; CH₃), 13.69 (d, *J* = 2.1; CHCH₃).

³¹P NMR (122 MHz, chloroform-*d*) δ = 71.27 (d, *J* = 89.0).

(1*R*,2*S*)-2-[(*S*)-(2-Methoxyphenyl)phenylphosphanyl]methylanino-1-phenylpropane-1-ol P-borane complex (15g)

Crystallisation in hexane/*i*PrOH = 7/3; yield: 73 %.

M. p.: 120 °C; colourless solid.

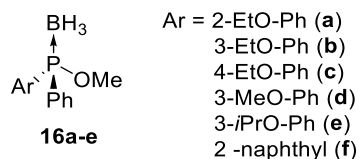
$[\alpha]_D^{23} = +39.4^\circ$ (*c* = 1.0; CHCl₃).

¹H NMR (500 MHz, chloroform-*d*) δ 7.59 (m, 1H; arom. H), 7.49 (m, 3H; arom. H), 7.37 (m, 3H; arom. H), 7.29 (m, 6H; arom. H), 7.04 (m, 1H; arom. H), 6.94 (ddd, *J* = 8.3, 4.1, 1.0 Hz, 1H; arom. H), 4.93 (dd, *J* = 5.6, 2.4 Hz, 1H; *CHOH*), 4.36 (hept, *J* = 12.1, 6.9, 5.6 Hz, 1H; CH), 3.60 (s, 3H; OCH₃), 2.58 (d, *J* = 8.1 Hz, 3H; NCH₃), 1.94 (s, 1H; OH), 1.25 (d, *J* = 6.8 Hz, 3H; CHCH₃) 1.08 (br q, 3H; BH₃).

¹³C NMR (126 MHz, chloroform-*d*) δ 161.26 (d, *J* = 2.7 Hz; COMe), 142.71 (CC), 135.09 (d, *J* = 10.8 Hz; CH), 133.36 (d, *J* = 1.8 Hz; CH), 132.39 (d, *J* = 71.1 Hz; CP), 131.05 (d, *J* = 10.4 Hz; 2xCH), 130.05 (d, *J* = 2.3 Hz; CH), 128.49 (2xCH), 128.07 (d, *J* = 10.5 Hz; 2xCH), 127.73 (CH), 126.68 (2xCH), 120.98 (d, *J* = 10.6 Hz; CH), 118.79 (d, *J* = 56.9 Hz; CP), 111.67 (d, *J* = 4.6 Hz; CH), 79.05 (d, *J* = 5.5 Hz; *CHOH*), 58.24 (d, *J* = 10.7 Hz; NCH), 55.21 (OCH₃), 31.13 (d, *J* = 3.9 Hz; CH₃), 12.65 (d, *J* = 2.3 Hz; CHCH₃).

³¹P NMR (202 MHz, chloroform-*d*) δ 68.63 (d, *J* = 93.6 Hz).

Synthesis of (*R*)-(Aryl)(methoxy)(phenyl)phosphinite P-borane complex (16a-e)



Compound **3** (5.0 mmol) was dissolved in methanol (40 mL) and cooled down to 0 °C. Afterwards, 1 equivalent concentrated H₂SO₄ (5.0 mmol; 0.49 g) was added dropwise. The solution was allowed to warm up to room temperature and stirred for 20 h. After the reaction was complete, water (10 mL) was added and methanol was evaporated under vacuum. The remaining aqueous residue was extracted with DCM (3x25 mL). The organic layers were combined and dried (MgSO₄). After evaporation of the solvents, the residue was purified by column chromatography.

(*R*)-(-)-(2-Ethoxyphenyl)(methoxy)(phenyl)phosphinite P-borane complex (16a)

Column chromatography with cyclohexane/AcOEt 49/1; yield: 79 %.

M. p.: 51 °C, colourless solid.

$[\alpha]_D^{24} = -44.4^\circ$ (c = 1.0; CHCl₃).

¹H NMR (300 MHz, chloroform-*d*) δ = 7.79 (m, 3H; arom. H), 7.45 (m, 4H; arom. H), 7.05 (m, 1H; arom. H), 6.83 (m, 1H; arom. H), 3.87 (m, 2H; OCH₂), 3.73 (d, J = 12.0 Hz, 3H; OCH₃), 1.11 (t, J = 7.0 Hz, 3H; OCH₂CH₃), 1.11 (br q, 3H; BH₃).

¹³C NMR (75 MHz, chloroform-*d*) δ = 160.20 (d, J = 3.7 Hz; COEt), 134.03 (d, J = 1.8 Hz; CH), 133.77 (d, J = 10.4 Hz; CH), 132.28 (d, J = 65.3 Hz; CP), 131.30 (d, J = 3.3 Hz; CH), 131.27 (d, J = 11.4 Hz; 2xCH), 128.09 (d, J = 10.8 Hz; 2xCH), 120.50 (d, J = 10.6 Hz; CH), 119.07 (d, J = 63.8 Hz; CP), 111.87 (d, J = 5.0 Hz; CH), 64.02 (OCH₂), 53.88 (d, J = 2.7 Hz; OCH₃), 14.11 (OCH₂CH₃).

³¹P NMR (122 MHz, chloroform-*d*) δ = 106.24 (m).

MS (EI, 70 eV) *m/z*: 273 (4, [M-H]⁺), 260 (100, [M-BH₃]⁺), 245 (43, [M-BH₃-CH₃]⁺), 229 (20, [MBH₃-OCH₃]⁺).

HRMS (ESI) [M+Na-BH₃]⁺: *m/z* calculated C₁₅H₁₇O₂P 283.08584, determined 283.08632, [M+Na]⁺: *m/z* calculated C₁₅H₂₀BO₂P 297.11890, determined 297.11921.

4. Experimental Data

4.2 Synthesis and Analytic Data

HPLC: Purity >99%ee; column: Chiralcel OD-H (150x4.6 mm), hexane/*i*PrOH 99.75/0.25, 1.25 ml/min, t_R = 8.2 min (*R*)-enantiomer and 9.4 min (*S*)-enantiomer.

(*R*)-(-)-(3-Ethoxyphenyl)(methoxy)(phenyl)phosphinite P-borane complex (16b)

Column chromatography with cyclohexane/AcOEt 9/1; yield: 83 %.

Colourless liquid.

$[\alpha]_D^{24} = -0.4^\circ$ ($c = 1.0$; CHCl₃).

¹H NMR (300 MHz, chloroform-*d*) δ = 7.73 (m, 1H; arom. H), 7.39 (m, 4H; arom. H), 7.02 (m, 2H; arom. H), 4.02 (q, $J = 7.0$ Hz, 2H; OCH₂), 3.73 (d, $J = 12.1$ Hz, 3H; OCH₃), 1.39 (t, $J = 7.0$ Hz, 3H; OCH₂CH₃), 1.02 (br q, 3H; BH₃).

¹³C NMR (75 MHz, chloroform-*d*) δ = 158.96 (d, $J = 13.1$ Hz; COEt), 132.83 (d, $J = 63.0$ Hz; CP), 131.95 (d, $J = 2.4$ Hz; CH), 131.62 (d, $J = 64.2$ Hz; CP), 131.21 (d, $J = 10.9$ Hz; 2xCH), 129.95 (d, $J = 12.2$ Hz; CH), 128.66 (d, $J = 10.5$ Hz; 2xCH), 123.24 (d, $J = 10.9$ Hz; CH), 118.10 (d, $J = 2.2$ Hz; CH), 116.97 (d, $J = 12.8$ Hz; CH). 63.65 (OCH₂), 54.09 (d, $J = 2.5$ Hz; OCH₃), 14.71 (OCH₂CH₃).

³¹P NMR (122 MHz, chloroform-*d*) δ = +107.95(m).

MS (EI, 70 eV) m/z : 273 (1, [M-H]⁺), 260 (100, [M-BH₃]⁺), 245 (94, [M-BH₃-CH₃]⁺), 229 (15, [MBH₃-OCH₃]⁺).

HRMS (ESI) [M+Na-BH₃]⁺: m/z calculated C₁₅H₁₇O₂P 283.08584, determined 283.08591, [M+Na]⁺: m/z calculated C₁₅H₂₀BO₂P 297.11890, determined 297.11927.

HPLC: Purity >98%ee; column: Chiralpak AS-H (150x4.6 mm), hexane/*i*PrOH 99.75/0.25, 1.00 ml/min, t_R = 6.7 min (*S*)-enantiomer and 7.4 min (*R*)-enantiomer.

(R)-(+)-(4-Ethoxyphenyl)(methoxy)(phenyl)phosphinite P-borane complex (16c)

Column chromatography with cyclohexane/AcOEt 49/1; yield: 79 %.

Colourless liquid.

$[\alpha]_D^{24} = +40.5^\circ$ (c = 1.0; CHCl₃).

¹H NMR (300 MHz, chloroform-*d*) δ = 7.72 (m, 4H; arom. H), 7.46 (m, 4H; arom. H), 6.97 (m, 1H; arom. H), 4.06 (q, J = 7.0 Hz, 2H; OCH₂), 3.70 (d, J = 12.1 Hz, 3H; OCH₃), 1.42 (t, J = 7.0 Hz, 3H; OCH₂CH₃), 1.05 (br q, 3H; BH₃).

¹³C NMR (75 MHz, chloroform-*d*) δ = 162.11 (d, J = 2.1 Hz; COEt), 133.53 (d, J = 12.6 Hz; 2xCH), 132.57 (d, J = 64.6 Hz; CP), 131.73 (d, J = 2.6 Hz; 2xCH), 131.12 (d, J = 11.3 Hz; CH), 128.64 (d, J = 10.5 Hz; 2xCH), 122.02 (d, J = 67.8 Hz; CP), 114.78 (d, J = 10.9 Hz; CH), 63.69 (OCH₂), 53.88 (d, J = 2.8 Hz; OCH₃), 14.72 (OCH₂CH₃).

³¹P NMR (122 MHz, chloroform-*d*) δ = 106.92 (m).

MS (EI, 70 eV) *m/z*: 260 (100, [M-BH₃]⁺), 245 (96, [M-BH₃-CH₃]⁺), 229 (37, [M-BH₃-OCH₃]⁺).

HRMS (ESI) [M+Na-BH₃]⁺: *m/z* calculated C₁₅H₁₇O₂P 283.08584, determined 283.08650, [M+Na]⁺: *m/z* calculated C₁₅H₂₀BO₂P 297.11890, determined 297.11923.

HPLC: Purity >99%ee; column: Reprosil 100 (150x4.6 mm), hexane/*i*PrOH 99.75/0.25, 1.25 ml/min, *t*_R = 8.4 min (*R*)-enantiomer and 8.9 min (*S*)-enantiomer.

(R)-(-)-(3-Methoxyphenyl)(methoxy)(phenyl)phosphinite P-borane complex (16d)

Column chromatography with cyclohexane/AcOEt 9/1; yield: 79 %.

Colourless liquid.

$[\alpha]_D^{22} = -3.2^\circ$ (c = 1.0; CHCl₃).

¹H NMR (300 MHz, chloroform-*d*) δ = 7.69 (m, 1H; arom. H), 7.35 (m, 7H; arom. H), 6.99 (m, 1H; arom. H), 3.76 (s, 3H; OCH₃), 3.69 (d, J = 12.1 Hz, 3H; POCH₃), 1.1 (br q, 3H; BH₃).

4. Experimental Data

4.2 Synthesis and Analytic Data

^{13}C NMR (75 MHz, chloroform-*d*) δ = 159.64 (d, J = 13.1 Hz; COMe), 132.98 (d, J = 63.0 Hz; CP), 131.63 (d, J = 63.9 Hz; CP), 132.03 (d, J = 2.4 Hz; CH), 131.30 (d, J = 11.4 Hz; 2xCH), 130.01 (d, J = 12.2 Hz; CH), 128.73 (d, J = 10.5 Hz; 2xCH), 123.49 (d, J = 11.0 Hz; CH), 117.78 (d, J = 2.2 Hz; CH), 116.40 (d, J = 12.8 Hz; CH), 55.45 (OCH₃), 54.19 (d, J = 2.6 Hz; OCH₃).

^{31}P NMR (122 MHz, chloroform-*d*) δ = +108.21 (m).

MS (EI, 70 eV) m/z : 246 (100, [M-BH₃]⁺), 231 (93, [M-BH₃-CH₃]⁺), 215 (30, [M-BH₃-OCH₃]⁺).

HRMS (ESI) [M+H-BH₃]⁺: m/z calculated C₁₄H₁₅O₂P 247.08824, determined 247.08866, [M+Na]⁺: m/z calculated C₁₄H₁₈BO₂P 283.10323, determined 283.10354.

HPLC: Purity >98%ee; column: Chiralpak AS-H (150x4.6 mm), hexane/*i*PrOH 99.75/0.25, 1.00 ml/min, t_R = 6.7 min (*S*)-enantiomer and 7.4 min (*R*)-enantiomer.

(*R*)-(+)-(3-Isopropoxyphenyl)(methoxy)(phenyl)phosphinite P-borane complex (16e)

Column chromatography with cyclohexane/AcOEt 9/1; yield: 85 %.

Colourless liquid.

$[\alpha]_D^{22} = +6.3^\circ$ (c = 1.0; CHCl₃).

^1H NMR (400 MHz, chloroform-*d*) δ = 7.69 (m, 2H; arom. H), 7.43 (m, 3H; arom. H), 7.30 (m, 1H; arom. H), 7.22 (m, 2H; arom. H), 6.96 (m, 1H; arom. H), 4.51 (hept, J = 6.0 Hz, 1H; OCH), 3.69 (d, J = 12.0 Hz, 3H; OCH₃), 1.27 (d, J = 6.1 Hz, 6H; OCHCH₃), 0.98 (br q, 3H; BH₃).

^{13}C NMR (101 MHz, chloroform-*d*) δ = 157.97 (d, J = 13.2 Hz; CO*i*Pr), 132.91 (d, J = 62.9 Hz; CP), 131.98 (d, J = 2.4 Hz; CH), 131.73 (d, J = 64.3 Hz; CP), 131.31 (d, J = 11.3 Hz; 2xCH), 130.01 (d, J = 12.2 Hz; CH), 128.71 (d, J = 10.5 Hz; 2xCH), 123.18 (d, J = 10.9 Hz; CH), 119.35 (d, J = 2.2 Hz; CH), 118.33 (d, J = 12.8 Hz; CH), 70.16 (OCH), 54.17 (d, J = 2.5 Hz; OCH₃), 21.98 (OCHCH₃), 21.96 (OCHCH₃).

^{31}P NMR (162 MHz, chloroform-*d*) δ = +108.08 (m).

4. Experimental Data

4.2 Synthesis and Analytic Data

MS (EI, 70 eV) m/z : 288 (2, $[M]^+$), 274 (100, $[M-BH_3]^+$), 259 (96, $[M-BH_3-CH_3]^+$), 243 (57, $[MBH_3-OCH_3]^+$).

HRMS (ESI) $[M+Na-BH_3]^+$: m/z calculated $C_{16}H_{19}O_2P$ 297.10149, determined 297.10111, $[M+Na]^+$: m/z calculated $C_{16}H_{22}BO_2P$ 311.13456, determined 311.13497.

HPLC: Purity 99%*ee*; column: Chiralcel OD-H (150x4.6 mm), hexane, 1.25 ml/min, t_R = 12.2 min (*S*)-enantiomer and 13.2 min (*R*)-enantiomer.

(*R*)-(Methoxy)(naphthalene-2-yl)(phenyl)phosphine P-borane complex (16f)

Column chromatography with cyclohexane/AcOEt 19/1; yield: 89 %.

M. p.: 88-89 °C colourless solid.

$[\alpha]_D^{24} = +44.3^\circ$ ($c = 1.0$; $CHCl_3$).

1H NMR (300 MHz, chloroform-*d*) δ = 8.38 (d, $J = 12.6$, 1H; arom. H), 7.67 (m, 13H; arom. H), 3.79 (dd, $J = 12.1, 0.4$, 3H; OCH_3), 1.22 (br q, 3H; BH_3).

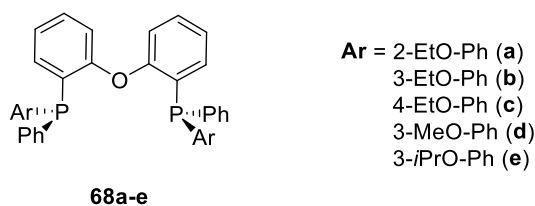
^{13}C NMR (75 MHz, chloroform-*d*) δ = 134.85 (d, $J = 2.2$; CC), 133.59 (d, $J = 13.4$; CH), 132.62 (d, $J = 12.2$; CC), 132.03 (d, $J = 2.4$; CH), 131.84 (d, $J = 64.9$; CP), 131.38 (d, $J = 11.3$; 2xCH), 129.18 (CP), 129.05 (CH), 128.87 (CH), 128.74 (2xCH), 128.61 (CH), 128.38 (CH), 127.94 (CH), 127.07 (CH), 126.10 (CH), 125.97 (CH), 54.27 (d, $J = 2.5$ (OCH_3)).

^{31}P NMR (122 MHz, chloroform-*d*) δ = 107.78 (m).

4. Experimental Data

4.2 Synthesis and Analytic Data

Synthesis of (1*S*,1'*S*)-(Oxybis(2,1-phenylen))di((alkoxyphenyl)(phenyl)-phosphine) (68a-e)



Solution A: In a Schlenk-tube, compound **16** (3.3 mmol) was dissolved in hexane (10 mL), before DABCO (6.6 mmol; 0.74 g) was added. The solution was stirred overnight at 40 °C.

Solution B: Diphenyl ether (1.5 mmol; 0.49 g) and 2.5 equivalents TMEDA (3.8 mmol; 0.44 g) were dissolved in diethyl ether (10 mL). *n*Butyl lithium (2.4 mL, 1.6 M in cyclohexane) was added dropwise at room temperature. The solution was stirred overnight.

After 20 h solution A was filtered off from the precipitate (DABCO·BH₃) and simultaneously added dropwise to solution B at -45 °C. After further 20 h stirring at room temperature the reaction was quenched with water (10 mL) and the organic solvents were evaporated under vacuum. The remaining aqueous residue was extracted with DCM (3x25 mL) and the organic layers were combined and dried (MgSO₄). After evaporation of the solvents the residue was purified by column chromatography.

(1*S*,1'*S*)-(Oxybis(2,1-phenylen))di((2-ethoxyphenyl)(phenyl)phosphine) (68a)

Attempts for purification by column chromatography and/or crystallisation failed. Only a mixture of **68a** and its mono-substituted derivative **69a** was obtained (ratio 90/10 in ³¹P NMR: -24.44 ppm/-25.31 ppm).

¹H NMR (300 MHz, chloroform-*d*) δ = 7.26 (m, 14H; arom. H), 6.94 (m, 4H; arom. H), 6.76 (m, 8H; arom. H), 3.94 (m, 4H; OCH₂CH₃), 1.12 (t, J = 7.0 Hz, 6H; OCH₂CH₃).

¹³C NMR (75 MHz, chloroform-*d*) δ = 160.23 (d, J = 2.9 Hz; 2xCO), 160.02 (d, J = 5.5 Hz; 2xCO), 136.30 (d, J = 10.7 Hz; 2xCP), 134.52 (2xCH), 134.25 (d, J = 2.3 Hz; 4xCH), 133.69 (d, J = 3.0 Hz; 2xCH), 130.16 (2xCH), 129.67 (2xCH), 128.55 (d, J = 14.8 Hz; 2xCH), 128.33 (2xCH), 128.14 (m; 2xCP), 128.11 (d, J = 7.7 Hz; 4xCH), 125.58 (d, J = 12.4 Hz; 2xCP), 123.39 (2xCH), 120.81 (2xCH), 118.66 (2xCH), 110.95 (2xCH), 63.86 (OCH₂CH₃), 14.59 (OCH₂CH₃).

4. Experimental Data

4.2 Synthesis and Analytic Data

^{31}P NMR (122 MHz, chloroform-*d*) δ = -24.44.

MS (EI, 70 eV) m/z : 626 (10, $[\text{M}]^+$), 625 (14, $[\text{M}-\text{H}]^+$), 581 (7, $[\text{M}-\text{OC}_2\text{H}_5]^+$), 549 (20, $[\text{M}-\text{Ph}]^+$), 505 (21, $[\text{M}-(2\text{-EtO-Ph})]^+$), 398 (93, $[\text{M}-\text{PPh}(2\text{-EtO-Ph})+\text{H}]^+$), 397 (100, $[\text{M}-\text{PPh}(2\text{-EtO-Ph})]^+$).

HRMS (ESI) $[\text{M}+\text{H}]^+$: m/z calculated $\text{C}_{40}\text{H}_{36}\text{O}_3\text{P}_2$ 627.22124, determined 627.22092.

(1*S*,1'*S*)-(Oxybis(2,1-phenylen))di((3-ethoxyphenyl)(phenyl)phosphine) (68b)

Attempts for purification by column chromatography and/or crystallisation failed. Only a mixture of **68b** and its mono-substituted derivative **69b** was obtained (ratio 94/6 in ^{31}P NMR: -15.58 ppm/-15.20 ppm).

^1H NMR: δ = 7.28-7.13 (14H, m, arom. H), 6.94 (2H, m, arom. H), 6.84-6.74 (8H, m, arom. H), 6.67 (2H, ddd, J = 8.1, 4.5, 0.9 Hz, arom. H), 3.90 (4H, q, J = 7.0 Hz, 2xOCH₂), 1.34 (6H, t, J = 7.0 Hz, 2xCH₃).

^{13}C NMR: δ = 159.1 (d, J = 18.4 Hz, 2xCO), 158.6 (m, 2xCOEt), 138.0 (d, J = 12.1 Hz, 2xCP), 136.4 (d, J = 11.5 Hz, 2xCP), 133.9 (2xCH), 133.9 (d, J = 21.0 Hz, 4xCH), 130.1 (2xCH), 129.2 (m, 2xCH), 128.9 (d, J = 16.0 Hz, 2xCP), 128.4 (2xCH), 128.2 (m, 4xCH), 126.1 (d, J = 9.9 Hz, 2xCH), 123.5 (2xCH), 119.4 (d, J = 22.6 Hz, 2xCH), 118.0 (2xCH), 114.8 (2xCH), 63.2 (2xOCH₂), 14.8 (2xCH₃).

^{31}P NMR: δ = -15.6.

MS (EI, 70 eV) m/z : 626 (1, $[\text{M}]^+$), 625 (19, $[\text{M}-\text{H}]^+$), 549 (1, $[\text{M}-\text{Ph}]^+$), 505 (1, $[\text{M}-(3\text{-EtO-Ph})]^+$), 398 (73, $[\text{M}-\text{PPh}(3\text{-EtO-Ph})+\text{H}]^+$), 397 (100, $[\text{M}-\text{PPh}(3\text{-EtO-Ph})]^+$).

HRMS (ESI) $[\text{M}+\text{H}]^+$: m/z calculated $\text{C}_{40}\text{H}_{36}\text{O}_3\text{P}_2$ 627.22124, determined 627.22134.

(1*S*,1'*S*)-(Oxybis(2,1-phenylen))di((4-ethoxyphenyl)(phenyl)phosphine) (68c)

Attempts for purification by column chromatography and/or crystallisation failed. Only a mixture of **68c** and its mono-substituted derivative **69c** was obtained (ratio 97/3 in ^{31}P NMR: 17.84 ppm/-17.62 ppm).

4. Experimental Data

4.2 Synthesis and Analytic Data

¹H NMR (300 MHz, chloroform-*d*) δ = 7.13 (m, 16H; arom. H), 6.85 (m, 2H; arom. H), 6.72 (m, 6H; arom. H), 6.59 (m, 2H; arom. H), 3.93 (q, J = 7.0 Hz, 4H; OCH₂CH₃), 1.33 (t, J = 6.9 Hz, 6H; OCH₂CH₃).

¹³C NMR (75 MHz, chloroform-*d*) δ = 159.63 (2xCO), 159.28 (d, J = 17.6 Hz; 2xCO), 137.41 (d, J = 11.6 Hz; 2xCP), 135.80 (d, J = 22.5 Hz; 4xCH), 133.91 (2xCH), 133.63 (d, J = 20.1 Hz; 4x CH), 130.12 (2xCH), 129.62 (d, J = 16.0 Hz; 2xCP), 128.31 (2xCH), 128.23 (4xCH), 126.96 (d, J = 8.6 Hz; 2xCP), 123.59 (2xCH), 118.18 (2xCH), 114.56 (m; 4xCH), 63.40 (OCH₂CH₃), 14.98 (OCH₂CH₃).

³¹P NMR (122 MHz, chloroform-*d*) δ = -17.84.

MS (EI, 70 eV) m/z : 626 (6, [M]⁺), 625 (10, [M-H]⁺), 549 (8, [M-Ph]⁺), 398 (81, [M-PPh(4-EtO-Ph)+H]⁺), 397 (100, [M-PPh(4-EtO-Ph)]⁺).

HRMS (ESI) [M+H]⁺: m/z calculated C₄₀H₃₆O₃P₂ 627.22124, determined 627.22094.

(1*S*,1'*S*)-(Oxybis(2,1-phenylen))di((3-methoxyphenyl)(phenyl)phosphine) (**68d**)

Attempts for purification by column chromatography and/or crystallisation failed. Only a mixture of **68d** and its mono-substituted derivative **69d** was obtained (ratio 94/6 in ³¹P NMR: 15.60 ppm/-15.27 ppm).

¹H NMR (300 MHz, chloroform-*d*) δ = 7.33 (m, 14H; arom. H), 7.06 (m, 2H; arom. H), 6.91 (m, 8H; arom. H), 6.78 (m, 2H; arom. H), 3.77 (s, 6H; OCH₃).

¹³C NMR (75 MHz, chloroform-*d*) δ = 159.29 (m; 4xCO), 138.24 (d, J = 12.6 Hz; 2xCP), 136.51 (d, J = 11.9 Hz; 2xCP), 134.12 (d, J = 9.6 Hz; 4xCH), 133.91 (2xCH), 130.29 (2xCH), 129.35 (m; 2xCH), 128.95 (d, J = 16.4 Hz; 2xCP), 128.58 (2xCH), 128.35 (m; 4xCH), 126.27 (d, J = 19.7 Hz; 2xCH), 123.69 (2xCH), 119.04 (d, J = 23.1 Hz; 2xCH), 118.10 (2xCH), 114.29 (2xCH), 55.17 (OCH₃).

³¹P NMR (122 MHz, chloroform-*d*) δ = -15.60.

MS (EI, 70 eV) m/z : 598 (10, [M]⁺), 597 (19, [M-H]⁺), 521 (20, [M-Ph]⁺), 491 (21, [M-(3-MeOPh)]⁺), 384 (95, [M-PPh(3-MeO-Ph)+H]⁺), 383 (100, [M-PPh(3-MeO-Ph)]⁺).

HRMS (ESI) [M+H]⁺: m/z calculated C₃₈H₃₂O₃P₂ 599.18994, determined 599.18978.

(1*S*,1'*S*)-(Oxybis(2,1-phenylen))di((3-isopropoxyphenyl)(phenyl)phosphine) (68e)

Attempts for purification by column chromatography and/or crystallisation failed. Only a mixture of **68e** and its mono-substituted derivative **69e** was obtained (ratio 96/4 in ^{31}P NMR: 15.74 ppm/-15.16 ppm).

^1H NMR (300 MHz, chloroform-*d*) δ = 7.16 (m, 14H; arom. H), 6.90 (m, 2H; arom. H), 6.76 (m, 8H; arom. H), 6.61 (m, 2H; arom. H), 4.36 (p, J = 6.1 Hz, 2H; OCH), 1.21 (d, J = 5.0 Hz, 6H, OCHCH₃), 1.19 (d, J = 5.0 Hz, 6H; OCHCH₃).

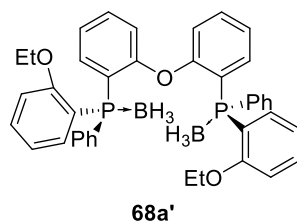
^{13}C NMR (75 MHz, chloroform-*d*) δ = 159.31 (d, J = 18.1 Hz; 2xCO), 157.73 (m; 2xCO), 138.24 (d, J = 12.2 Hz; 2xCP), 136.57 (d, J = 11.9 Hz; 2xCP), 134.11 (2xCH), 133.95 (d, J = 17.7 Hz; 4xCH), 130.22 (2xCH), 129.41 (m; 2xCH), 129.14 (d, J = 16.4 Hz; 2xCP), 128.49 (2xCH), 128.31 (m; 4xCH), 126.30 (d, J = 20.6 Hz; 2xCH), 123.65 (2xCH), 121.00 (d, J = 22.4 Hz; 2xCH), 118.10 (2xCH), 116.42 (2xCH), 69.77 (OCH), 22.16 (OCHCH₃), 22.11 (OCHCH₃).

^{31}P NMR (122 MHz, chloroform-*d*) δ = -15.74.

MS (EI, 70 eV) m/z : 577 (1, [M-Ph]⁺), 519 (1, [M-(3-*i*PrO-Ph)]⁺), 412 (16, [M-PPh(3-*i*PrOPh)+H]⁺), 411 (47, [M-PPh(3-*i*PrO-Ph)]⁺), 165 (66, [C₉H₁₁OP]⁺), 59 (100, [C₃H₇O]⁺).

HRMS (ESI) [M+H]⁺: m/z calculated C₄₂H₄₀O₃P₂ 655.25254, determined 655.25212.

Synthesis of (1*S*,1'*S*)-(Oxybis(2,1-phenylen))di((2-ethoxyphenyl)(phenyl)phosphine)-borane complex (68a')



Compound **68a** (0.24 mmol; 0.15 g) was dissolved in toluene (3 mL). 2.4 equivalents BH₃*SMe₂ (0.3 mL; 2 M in toluene) were added at room temperature. The solution was stirred for 20 h at room temperature. Afterwards, the solvent was evaporated under vacuum and the residue was crystallised in DCM/hexane (0.5 mL/5 mL).

4. Experimental Data

4.2 Synthesis and Analytic Data

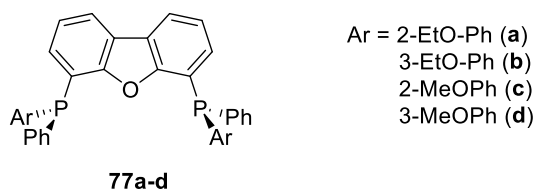
The ^{31}P NMR spectrum of **68a'** shows two broad signals in a ratio of 57 % ($\delta = 17.4$ ppm) to 43 % ($\delta = 16.1$ ppm). It could not be determined, which species occurred.

^{31}P NMR (122 MHz, chloroform-*d*) $\delta = 17.4$ (br s), 16.1 (br s).

MS (EI, 70 eV) m/z : 652 (1, $[\text{M}-2\text{H}]^+$), 626 (2, $[\text{M}-2\text{BH}_3]$), 597 (1, $[\text{M}-2\text{BH}_3-\text{Et}]^+$), 511 (1, $[\text{M}-2\text{BH}_3-2(\text{OEt}-\text{Ph})]^+$).

HRMS (ESI) $[\text{M}+\text{Na}]^+$: m/z calculated $\text{C}_{40}\text{H}_{42}\text{B}_2\text{O}_3\text{P}_2$ 677.27007, determined 677.26948.

Synthesis of 4,6-Di((*S*)-(alkoxyphenyl)(phenyl)phosphanyl)dibenzo[b,d]furan (**77a-d**)



Solution A: Compound **16** (3.3 mmol) was dissolved in hexane (10 mL), before DABCO (6.6 mmol; 0.74 g) was added. The solution was stirred overnight at 40 °C.

Solution B: 4,6-Dibromodibenzofuran (synthesised according to the protocol of Schwartz et al.⁹⁷) (1.5 mmol; 0.49 g) was dissolved in thf (10 mL) and 2.2 equivalents of *n*butyl lithium (2.1 mL, 1.6 M in cyclohexane) were added dropwise at -78 °C. The solution was stirred for 3 h, while the temperature increases to -20 °C.

After 20 h solution A was filtered off from the precipitate ($\text{DABCO} \cdot \text{BH}_3$) and simultaneously added dropwise to solution B at -78 °C. After additional 20 h stirring at room temperature, the reaction was quenched with water (10 mL) and the organic solvents were evaporated under vacuum. The remaining aqueous residue was extracted with DCM (3x25 mL). The organic layers were combined and dried (MgSO_4). After evaporation of the solvents, the residue was purified by column chromatography.

4,6-Di((S)-(2-ethoxyphenyl)(phenyl)phosphanyl)dibenzo[b,d]furan (77a)

Column chromatography with cyclohexane/AcOEt 99/1 and **crystallisation** from DCM/hexane yield: 90 % (99 % purity).

M. p.: 130 °C, colourless solid.

$[\alpha]_D^{22} = -33.4^\circ$ (c = 1.0; CHCl₃).

¹H NMR (300 MHz, chloroform-*d*) δ = 7.93 (dd, J = 7.6, 1.3 Hz, 2H; arom. H), 7.32 (m, 3H; arom. H), 7.22 (m, 11H; arom. H), 7.09 (m, 2H; arom. H), 6.78 (m, 2H; arom. H), 6.65 (m, 4H; arom. H), 3.91 (m, 4H; OCH₂CH₃), 1.02 (t, J = 7.0 Hz, 6H; OCH₂CH₃).

¹³C NMR (75 MHz, chloroform-*d*) δ = 160.41 (d, J = 14.8 Hz; 2xCO), 158.32 (d, J = 13.9 Hz; 2xCO), 135.77 (d, J = 10.2 Hz; 2xCP), 134.31 (d, J = 21.5 Hz; 4xCH), 133.44 (d, J = 2.9 Hz; 2xCH), 132.47 (d, J = 9.7 Hz; 2xCH), 130.01 (2xCH), 128.60 (2xCH), 128.23 (d, J = 7.6 Hz; 4xCH), 125.97 (m; 2xCP), 123.56 (m; 2xCC), 122.96 (d, J = 3.3 Hz; 2xCH), 121.25 (d, J = 19.3 Hz; 2xCP), 121.19 (2xCH), 120.99 (2xCH), 111.32 (2xCH), 64.12 (2xOCH₂CH₃), 14.50 (2xOCH₂CH₃).

³¹P NMR (122 MHz, chloroform-*d*) δ = -25.73.

MS (EI, 70 eV) *m/z*: 624 (100, [M]⁺), 657 (50, [M-Ph]⁺), 519 (17, [M-Ph-C₂H₄]⁺), 503 (13, [M-(2-EtO-Ph)]⁺).

HRMS (ESI) [M+H]⁺: *m/z* calculated C₄₀H₃₄O₃P₂ 625.20559, determined 625,20528.

4,6-Di((S)-(3-ethoxyphenyl)(phenyl)phosphanyl)dibenzo[b,d]furan (77b)

Column chromatography with cyclohexane/AcOEt 19/1; yield: 76 % (96 % purity).

M. p.: 63-64 °C, colourless solid.

$[\alpha]_D^{22} = -31.4^\circ$ (c = 1.0; CHCl₃).

¹H NMR (300 MHz, chloroform-*d*) δ = 7.92 (dd, J = 7.7, 1.3 Hz, 2H; arom. H), 7.27 (m, 12H; arom. H), 7.13 (m, 2H; arom. H), 7.04 (m, 2H; arom. H), 6.80 (m, 6H; arom. H), 3.90 (q, J = 7.0 Hz, 4H; OCH₂CH₃), 1.33 (t, J = 7.0 Hz, 6H; OCH₂CH₃).

4. Experimental Data

4.2 Synthesis and Analytic Data

¹³C NMR (75 MHz, chloroform-*d*) δ = 158.81 (d, *J* = 9.1 Hz; 2xCO), 158.03 (d, *J* = 14.2 Hz; 2xCO), 137.29 (d, *J* = 10.7 Hz; CP), 135.69 (d, *J* = 10.7 Hz; CP), 133.94 (d, *J* = 20.5 Hz; 4xCH), 132.02 (d, *J* = 7.1 Hz; 2xCH), 129.46 (d, *J* = 7.7 Hz; 2xCH), 128.83 (2xCH), 128.42 (d, *J* = 7.1 Hz; 4xCH), 126.06 (d, *J* = 18.7 Hz; 2xCH), 123.57 (m; 2xCC), 123.22 (d, *J* = 2.0 Hz; 2xCH), 121.54 (2xCH), 121.53 (d, *J* = 19.0 Hz; 2xCP), 119.44 (d, *J* = 23.1 Hz; 2xCH), 115.20 (2xCH), 63.34 (2xOCH₂CH₃), 14.92 (2xOCH₂CH₃).

³¹P NMR (122 MHz, chloroform-*d*) δ = -16.32.

MS (EI, 70 eV) *m/z*: 624 (80, [M]⁺), 609 (100, [M-CH₃]⁺), 565 (13, [M-CH₃-OC₂H₅+H]⁺), 396 (95, [M-(3-EtO-Ph)PhP+H]⁺).

HRMS (ESI) [M+H]⁺: *m/z* calculated C₄₀H₃₄O₃P₂ 625.20559, determined 625.20543.

4,6-Di((*S*)-(2-methoxyphenyl)(phenyl)phosphanyl)dibenzo[*b,d*]furan (77c)

Crystallisation from DCM/hexane; yield: 70 % (98 % purity).

M. p.: 105 °C, colourless solid.

$[\alpha]_D^{22}$ = -12.1 ° (*c* = 1.0; CHCl₃).

¹H NMR (300 MHz, chloroform-*d*) δ = 7.83 (dd, *J* = 7.7 Hz, 1.3, 1H, arom. H), 7.15 (m, 9H, arom. H), 6.90 (m, 1H, arom. H), 6.74 (m, 1H, arom. H), 6.57 (m, 1H, arom. H), 3.60 (s, 3H; OCH₃).

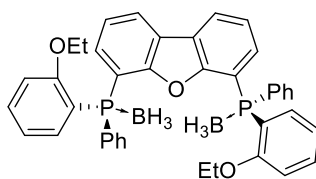
¹³C NMR (75 MHz, chloroform-*d*) δ = 161.19 (d, *J* = 15.6 Hz; 2xCO), 158.18 (d, *J* = 14.8 Hz; 2xCO), 135.44 (d, *J* = 10.6 Hz; 2xCP), 134.04 (d, *J* = 21.2 Hz; 4xCH), 133.61 (2xCH), 132.15 (d, *J* = 7.9 Hz; 2xCH), 130.17 (2xCH), 128.54 (2xCH), 128.18 (d, *J* = 7.4 Hz; 4xCH), 124.38 (d, *J* = 12.4 Hz; 2xCP), 123.49 (2xCC), 122.96 (d, *J* = 2.6 Hz; 2xCH), 121.12 (2xCH), 121.08 (d, *J* = 19.4 Hz; 2xCP), 121.07 (2xCH), 110.36 (2xCH), 55.77 (OCH₃).

³¹P NMR (122 MHz, chloroform-*d*) δ = -27.25.

MS (EI, 70 eV) *m/z*: 596 (56 %, [M]⁺), 595 (24 %, [M-H]⁺), 519 (64, [M-Ph]⁺), 489 (14, [M-(2-MeOPh)]⁺), 237 (100).

HRMS (ESI) [M+H]⁺: *m/z* calculated C₃₈H₃₀O₃P₂ 596.16647, determined 596.16530.

Synthesis of 4,6-Di((*S*)-(2-ethoxyphenyl)(phenyl)phosphanyl)dibenzo[*b,d*]furan borane complex (77a')



77a'

Compound **77a** (0.24 mmol; 0.15 g) was dissolved in toluene (3 mL). At room temperature, 2.4 equivalents BH₃*SMe₂ (0.3 mL; 2 M in toluene) were added. The solution was stirred for 20 h at room temperature. Afterwards, the solvent was evaporated under vacuum and the residue was crystallised in DCM/hexane (0.5 mL/5 mL).

Crystallisation from DCM/hexane; yield: 97 %.

¹H NMR (300 MHz, chloroform-*d*) δ = 8.13 (m, 2H; arom. H), 7.79 (m, 4H; arom. H), 7.39 (m, 14H; arom. H), 6.96 (m, 2H; arom. H), 6.79 (m, 2H; arom. H), 3.78 (m, 4H; 2xOCH₂CH₃), 1.09 (br q, 6H; 2xBH₃) 0.74 (t, *J* = 7.0 Hz, 6H; 2xOCH₂CH₃).

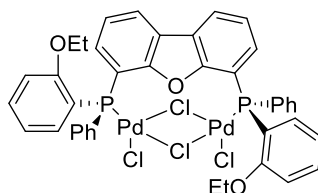
¹³C NMR (75 MHz, chloroform-*d*) δ = 160.46 (2xCO), 156.93 (2xCO), 135.15 (d, *J* = 12.3 Hz; 2xCH), 133.65 (d, *J* = 10.2 Hz; 4xCH), 133.48 (2xCH), 132.56 (d, *J* = 8.9 Hz; 2xCH), 130.89 (d, *J* = 2.6 Hz; 2xCH), 129.16 (CH), 128.49 (d, *J* = 10.5 Hz; 4xCH), 125.41 (CH), 124.20 (d, *J* = 5.1 Hz; 2xCP), 123.22 (d, *J* = 3.6 Hz; 2xCH), 123.14 (d, *J* = 4.3 Hz; 2xCH), 121.13 (d, *J* = 11.9 Hz; 2xCH), 115.83 (d, *J* = 27.8 Hz; 2xCP), 115.06 (d, *J* = 26.2 Hz; 2xCP), 112.03 (d, *J* = 4.7 Hz; 2xCH), 63.62 (2xOCH₂CH₃), 13.85 (2xOCH₂CH₃).

³¹P NMR (122 MHz, chloroform-*d*) δ = 15.71 (br s).

MS (EI, 70 eV) *m/z*: 652 (1, [M]⁺), 624 (100, [M-2BH₃]), 595 (5, [M-2BH₃-Et]⁺), 580 (2, [M-2BH₃-OEt]⁺).

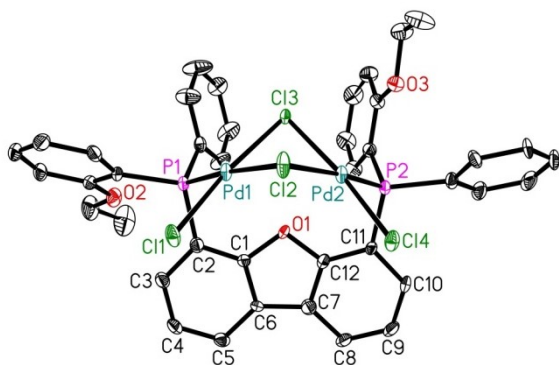
HRMS (ESI) [M+H]⁺: *m/z* calculated C₄₀H₄₂B₂O₃P₂ 675.25442, determined 675.25365.

Synthesis of $\text{Pd}_2(\mu_2\text{-Cl})_2(\mu_2\text{-77a})$ -complex



$\text{Pd}_2(\mu_2\text{-Cl})_2(\mu_2\text{-77a})$ -complex

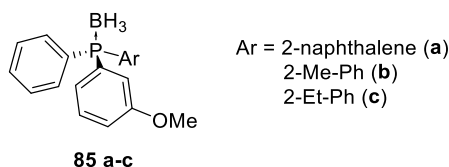
$\text{Pd}(\text{NMe})_2\text{Cl}_2$ (0.2 mmol, 50 mg) and compound **77a** (0.2 mmol, 119 mg) were dissolved in DCM and stirred for ten minutes at room temperature. The solvent was evaporated under vacuum. The $\text{Pd}_2(\mu_2\text{-Cl})_2(\mu_2\text{-77a})$ -complex crystallised from DCM/diethyl ether.



Molecular structure of $\text{Pd}_2(\mu_2\text{-Cl})_2(\mu_2\text{-77a})$ -complex in the solid state. Displacement ellipsoids correspond to 30 % probability. Crystals of $\text{Pd}_2(\mu_2\text{-Cl})_2(\mu_2\text{-77a})$ contained co-crystallised solvent (CH_2Cl_2). Contributions of further co-crystallised solvent molecules were removed from the diffraction data with PLATON/ SQUEEZE.⁹⁸ Hydrogen atoms and co-crystallised solvent were omitted for clarity.

Chemical formula	$\text{C}_{41}\text{H}_{36}\text{Cl}_6\text{O}_3\text{P}_2\text{Pd}_2$
Formula weight	1064.14
Crystal system	monoclinic
Space group	$I1P2_1$
a [Å]	10.8345(2)
b [Å]	18.5236(3)
c [Å]	11.8168(2)
α [deg]	90
β [deg]	99.3088(6)
γ [deg]	90
V [Å ³]	2340.33(7)
Wavelength [Å]	0.71073
T [K]	150(2)
Z	2
μ [mm ⁻¹]	1.213
Calculated density	1.510
[g·cm ⁻³]	
Reflections collected	57699
Independent reflections	10195
Parameters	441
R_{int}	0.0186
R_1 ($I > 2\sigma(I)$)	0.0328
wR_2 (all data)	0.1000
Goodness-of-fit on F^2	1.073
Flack parameter	0.011(10)

Synthesis of (Aryl)(3-methoxyphenyl)(phenyl)phosphine P-borane complex (85)



A solution of bromo aryl (3.3 mmol) in diethyl ether (10 mL) was cooled down to 0 °C. Now, secondary butyl lithium (3.3 mmol; 2.4 mL; 1.4 M cyclohexane solution) was added dropwise.

After stirring for 1 h, the solution was added *via* cannula to a solution of compound **16** (3.0 mmol) in diethyl ether (10 mL) at -78 °C.

After additional 20 h stirring at room temperature, the reaction was quenched with water (10 mL) and the organic solvents were evaporated under vacuum. The remaining aqueous residue was extracted in DCM (3x25 mL). The organic layers were combined and dried (MgSO₄). After evaporation of the solvents, the residue was purified by column chromatography.

(S)-(3-Methoxyphenyl)(naphthalene-2-yl)(phenyl)phosphine P-borane complex (85a)

Column chromatography with cyclohexane/AcOEt 99/1; yield: 53 %.

Colourless oil.

$[\alpha]_D^{23} = -12.26^\circ$ (c = 1.0; CHCl₃).

¹H NMR (300 MHz, chloroform-*d*) δ = 7.92 (m, 3H; arom. H), 7.60 (m, 10H; arom. H), 7.24 (m, 2H; arom. H), 7.10 (m, 1H; arom. H), 3.83 (s, 3H; OCH₃), 1.40 (br q, 3H; BH₃).

¹³C NMR (75 MHz, chloroform-*d*) δ = 159.77 (d, J = 13.0 Hz; CO), 135.02 (d, J = 10.6 Hz; CH), 134.43 (d, J = 2.1 Hz; CC), 133.34 (d, J = 9.7 Hz; CH), 132.80 (d, J = 11.7 Hz; CC), 131.43 (d, J = 2.5 Hz; CH), 130.66 (d, J = 57.5 Hz; CP), 130.07 (d, J = 11.7 Hz; CH), 129.59 (d, J = 57.0 Hz; CP), 128.99 (CH), 128.85 (CH), 128.84 (2xCH), 128.63 (d, J = 9.8 Hz; CH), 128.21 (CH), 128.17 (d, J = 9.3 Hz; CH), 127.89 (CH), 127.01 (CH), 126.30 (d, J = 58.1 Hz; CP), 125.58 (d, J = 8.7 Hz; CH), 118.64 (d, J = 11.7 Hz; CH), 117.08 (d, J = 2.4 Hz; CH), 55.44 (OCH₃).

³¹P NMR (122 MHz, chloroform-*d*) δ = 22.00 (d, J = 66.0 Hz).

4. Experimental Data

4.2 Synthesis and Analytic Data

MS (EI, 70 eV) m/z : 356 (1, $[M]^+$), 342 (100, $[M-BH_3]^+$), 327 (4, $[M-BH_3-CH_3]^+$), 311 (3, $[M-BH_3-OMe]^+$), 265 (15, $[M-BH_3-Ph]^+$).

HRMS (ESI) $[M+Na]^+$: m/z calculated für $C_{23}H_{22}BOP$ 379.13977, determined 379.13907.

HPLC: purity >99%ee; column: Reprosil 100 (150x4.6 mm), hexane/*i*PrOH 99.75/0.25, 2.00 ml/min, t_R = 15.1 min (*R*)-enantiomer und 16.8 min (*S*)-enantiomer.

(*S*)-(3-Methoxyphenyl)(phenyl)(*o*-tolyl)phosphine P-borane complex (85b)

Column chromatography with cyclohexane/AcOEt 99/1; yield: 72 %.

Colourless oil.

$[\alpha]_D^{23} = -3.50^\circ$ ($c = 1.0$; $CHCl_3$).

1H NMR (400 MHz, chloroform-*d*) δ = 7.65 (m, 2H; arom. H), 7.43 (m, 5H; arom. H), 7.20 (m, 4H; arom. H), 7.04 (m, 2H; arom. H), 3.78 (s, 3H; OCH_3), 2.30 (s, 3H; CH_3).

^{13}C NMR (75 MHz, chloroform-*d*) δ = 159.79 (d, $J = 12.9$ Hz; CO), 143.00 (d, $J = 10.7$ Hz; CC), 134.21 (d, $J = 8.5$ Hz; CH), 133.31 (d, $J = 9.4$ Hz; 2xCH), 131.95 (d, $J = 9.0$ Hz; CH), 131.39 (dd, $J = 7.9$ Hz, 2.4 Hz; 2xCH), 130.53 (d, $J = 57.8$ Hz; CP), 130.06 (d, $J = 12.0$ Hz; CH), 129.07 (d, $J = 57.4$ Hz; CP), 128.94 (d, $J = 10.1$ Hz; 2xCH), 127.66 (d, $J = 55.1$ Hz; CP), 125.96 (d, $J = 9.5$ Hz; CH), 125.51 (d, $J = 8.4$ Hz; CH), 118.59 (d, $J = 11.7$ Hz; CH), 116.97 (d, $J = 2.2$; CH), 55.42 (OCH_3), 22.61 (d, $J = 4.9$ Hz; CH_3).

^{31}P NMR (122 MHz, chloroform-*d*) δ = 21.35 (br d, $J = 65.0$).

MS (EI, 70 eV) m/z : 320 (3, $[M]^+$), 306 (100, $[M-BH_3]^+$), 291 (30, $[M-BH_3-CH_3]^+$), 275 (4, $[M-BH_3-OMe]^+$), 199 (11, $[M-BH_3-C_6H_4OMe]^+$).

HPLC: purity >99%ee; column: Chiralpak AD-H (150x4.6 mm), hexane/*i*PrOH 98/2, 1.00 ml/min, t_R = 6.8 min (*S*)-enantiomer und 9.3 min (*R*)-enantiomer.

(S)-(2-Ethylphenyl)(3-methoxyphenyl)(phenyl)phosphine P-borane complex (85c)

Column chromatography with cyclohexane/AcOEt 99/1; yield: 92 %.

Colourless oil.

$[\alpha]_D^{23} = -4.20^\circ$ ($c = 1.0$; CHCl_3).

^1H NMR (300 MHz, chloroform-*d*) $\delta = 7.63$ (m, 2H; arom. H), 7.46 (m, 4H; arom. H), 7.36 (m, 2H; arom. H), 7.16 (m, 5H; arom. H), 7.03 (m, 2H; arom. H), 3.78 (s, 3H; OCH_3), 2.68 (m, 2H; CH_2), 1.40 (br q; BH_3), 1.03 (t, $J = 7.4$ Hz, 3H; CH_3).

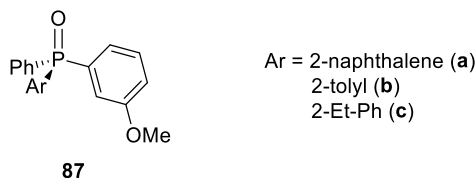
^{13}C NMR (75 MHz, chloroform-*d*) $\delta = 159.75$ (d, $J = 12.8$ Hz; CO), 149.10 (d, $J = 10.8$ Hz; CC), 134.24 (d, $J = 8.6$ Hz; CH), 133.31 (d, $J = 9.4$ Hz; 2xCH), 131.62 (d, $J = 2.5$ Hz; CH), 131.27 (d, $J = 2.5$ Hz; CH), 131.09 (d, $J = 57.1$ Hz; CP), 130.07 (CH), 129.94 (d, $J = 3.4$ Hz; CH), 129.64 (d, $J = 57.5$ Hz; CP), 128.89 (d, $J = 10.2$ Hz; 2xCH), 127.18 (d, $J = 55.6$ Hz; CP), 125.89 (d, $J = 9.5$ Hz; CH), 125.54 (d, $J = 8.4$ Hz; CH), 118.56 (d, $J = 11.5$ Hz; CH), 116.93 (d, $J = 2.4$ Hz; CH), 55.41 (OCH_3), 27.88 (d, $J = 5.8$ Hz; CH_2), 15.16 (CH_3).

^{31}P NMR (122 MHz, chloroform-*d*) $\delta = 21.06$ (br m).

MS (EI, 70 eV) m/z : 334 (1, $[\text{M}]^+$), 320 (100, $[\text{M}-\text{BH}_3]^+$), 305 (12, $[\text{M}-\text{BH}_3-\text{CH}_3]^+$), 291 (3, $[\text{M}-\text{BH}_3-\text{Et}]^+$), 275 (1, $[\text{M}-\text{BH}_3-\text{OEt}]^+$).

HPLC: purity >99%ee; column: Chiralpak AD-H (150x4.6 mm), hexane/*i*PrOH 99/1, 1.00 ml/min, $t_R = 8.4$ min (*S*)-enantiomer und 9.6 min (*R*)-enantiomer.

Synthesis of (Aryl)(3-methoxyphenyl)(phenyl)phosphine oxide (87)



Method A: Compound **85** (0.56 mmol) dissolved in hexane (5 mL). DABCO (0.62 mmol; 0.07 g) was added to the solution and the mixture was stirred for 20 h at room temperature. After separation of the solution from the $\text{DABCO} \cdot \text{BH}_3$ complex, H_2O_2 (30 %wt; 1.68 mmol) was added dropwise to the solution. After additional 20 h stirring at room temperature, water

4. Experimental Data

4.2 Synthesis and Analytic Data

(10 mL) was added to the solution and the organic solvents were evaporated under vacuum. The remaining aqueous residue was extracted in DCM (3x25 mL). The organic layers were combined and dried (MgSO₄). After evaporation of the solvents, the residue was purified by crystallisation.

Method B: Compound **85** (3.5 mmol) was dissolved in DCM (10 mL) and cooled down to 0 °C. To this solution, *m*-CPBA (15.4 mmol; 2.66 g) was added slowly. After stirring for 2 h 0.25 M Na₂SO₃ solution was added to the suspension. The phases were separated. The aqueous layer was extracted with ethyl acetate (4x25 mL). The organic layers were combined and washed with saturated NaHCO₃ solution and brine before they were dried (Na₂SO₄). After filtration, the solvents were evaporated under vacuum. The remaining residue was purified by column chromatography.

(*R*)-(3-Methoxyphenyl)(naphthalene-2-yl)(phenyl)phosphine oxide (87a)

¹H NMR (300 MHz, chloroform-*d*) δ = 8.33 (m, 1H; arom. H), 7.92 (m, 3H; arom. H), 7.60 (m, 10H; arom. H), 7.23 (m, 1H; arom. H), 7.12 (m, 1H; arom. H), 3.83 (s, 3H; OCH₃).

¹³C NMR (75 MHz, chloroform-*d*) δ = 159.69 (d, *J* = 14.9 Hz; CO), 134.79 (d, *J* = 2.4 Hz; CC), 134.08 (d, *J* = 9.4 Hz; CH), 133.96 (d, *J* = 103.5 Hz; CP), 132.58 (d, *J* = 104.5 Hz; CP), 132.49 (d, *J* = 13.1 Hz; CC), 132.21 (d, *J* = 10.2 Hz; 2xCH), 132.12 (d, *J* = 3.7 Hz; CH), 129.80 (d, *J* = 14.4 Hz; CH), 129.59 (d, *J* = 104.4 Hz; CP), 129.06 (CH), 128.63 (d, *J* = 12.2 Hz; 2xCH), 128.38 (d, *J* = 11.9 Hz; CH), 128.35 (CH), 127.92 (CH), 127.04 (CH), 126.92 (d, *J* = 10.8 Hz; CH), 124.50 (d, *J* = 10.1 Hz; CH), 118.32 (d, *J* = 2.7 Hz; CH), 116.90 (d, *J* = 10.8 Hz; CH), 55.53 (OCH₃).

³¹P NMR (122 MHz, chloroform-*d*) δ = 29.93 (s).

MS (EI, 70 eV) *m/z*: 358 (61, [M]⁺), 357 (100, [M-H]⁺), 343 (1, [M-CH₃]⁺), 281 (2, [M-Ph]⁺), 251 (15, [M-C₆H₄OMe]⁺).

HRMS (ESI) [M+H]⁺: *m/z* berechnet für C₂₃H₁₉O₂P 359.11954, gemessen 359.11957, [M+Na]⁺: *m/z* berechnet für C₂₃H₁₉O₂P 381.10149, gemessen 381.10150.

(*R*)-(3-Methoxyphenyl)(phenyl)(*o*-tolyl)phosphine oxide (87b)

Column chromatography with cyclohexane/AcOEt 1/1; yield: 50 %.

Colourless oil.

$[\alpha]_D^{23} = -5.7^\circ$ ($c = 1.0$; CHCl₃).

¹H NMR (300 MHz, chloroform-*d*) δ = 7.65 (m, 2H; arom. H), 7.41 (m, 7H; arom. H), 7.05 (m, 4H; arom. H), 3.79 (s, 3H; OCH₃), 2.45 (m, 3H; CH₃).

¹³C NMR (75 MHz, chloroform-*d*) δ = 159.77 (d, $J = 14.7$; CO), 143.47 (CC), 134.06 (d, $J = 102.6$ Hz; CP), 133.59 (d, $J = 12.9$ Hz; CH), 132.56 (d, $J = 103.6$ Hz; CP), 132.25 (d, $J = 2.8$ Hz; CH), 131.99 (d, $J = 10.0$ Hz; 4xCH), 131.96 (CH), 130.67 (d, $J = 103.5$ Hz; CP), 129.79 (d, $J = 14.3$ Hz; CH), 128.66 (d, $J = 12.1$ Hz; 2xCH), 125.28 (d, $J = 12.9$ Hz; CH), 124.22 (d, $J = 10.0$ Hz; CH), 118.19 (d, $J = 2.7$ Hz; CH), 116.64 (d, $J = 10.6$ Hz; CH), 55.53 (OCH₃), 21.79 (d, $J = 4.8$ Hz; CH₃).

³¹P NMR (122 MHz, chloroform-*d*) δ = 32.76 (s).

HPLC: purity >98%*ee*; column: Chiralpak AD-H (150x4.6 mm), hexane/*i*PrOH 92/8, 1.25 ml/min, t_R = 12.6 min (*R*)-enantiomer und 13.9 min (*S*)-enantiomer.

(*R*)-(2-Ethylphenyl)-(3-Methoxyphenyl)(phenyl)phosphine oxide (87c)

Column chromatography with cyclohexane/AcOEt 1/1; yield: 61 %.

Yellow oil.

$[\alpha]_D^{23} = -6.0^\circ$ ($c = 1.0$; CHCl₃).

¹H NMR (300 MHz, chloroform-*d*) δ = 7.66 (m, 2H; arom. H), 7.47 (m, 4H; arom. H), 7.34 (m, 3H; arom. H), 7.06 (m, 4H; arom. H), 3.79 (s, 3H; OCH₃), 2.91 (m, 2H; CH₂), 1.06 (t, $J = 7.5$ Hz, 3H; CH₃).

¹³C NMR (75 MHz, chloroform-*d*) δ = 159.66 (d, $J = 14.7$ Hz; CO), 149.51 (d, $J = 8.4$ Hz; CC), 134.68 (d, $J = 102.5$ Hz; CP), 133.51 (d, $J = 13.3$ Hz; CH), 133.21 (d, $J = 103.3$ Hz; CP), 132.28 (d, $J = 2.7$ Hz; CH), 131.94 (d, $J = 9.7$ Hz; 2xCH), 131.77 (d, $J = 2.8$ Hz; CH), 130.47 (d, $J = 103.4$ Hz; CP), 129.99 (d, $J = 10.4$ Hz; CH), 129.64 (d, $J = 14.4$ Hz; CH), 128.53 (d, $J = 12.1$

4. Experimental Data

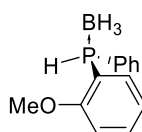
4.2 Synthesis and Analytic Data

Hz; 2xCH), 125.11 (d, $J = 13.7$ Hz; CH), 124.23 (d, $J = 9.9$ Hz; CH), 118.00 (d, $J = 2.6$; CH), 116.60 (d, $J = 10.4$ Hz; CH), 55.46 (OCH₃), 27.31 (d, $J = 5.0$ Hz; CH₂), 15.02 (CH₃).

³¹P NMR (122 MHz, chloroform-*d*) $\delta = 32.30$ (s).

HPLC: purity >99%ee; column: Chiralpak AD-H (150x4.6 mm), hexane/*i*PrOH 92/8, 1.25 ml/min, $t_R = 8.6$ min (*R*)-enantiomer und 9.9 min (*S*)-enantiomer.

Synthesis of (2-Methoxyphenyl)(phenyl)phosphine P-borane complex (94)



94

Compound **15g** (2.5 mmol) was dissolved in freshly made solution of HCl_g in toluene (0.3 M; 10.2 mmol; 33.9 mL) at 0 °C and stirred for 1.5 h while the temperature was allowed to reach room temperature. The solution was filtered to separate it from the resulting ephedrine hydrochloride precipitate. The yielded solution was treated with some vacuum-argon-cycles to eliminate the hydrogen chloride and was cooled down to -85 °C (bath of ethanol and addition of nitrogen). Tertiary butyl lithium solution (1.7 M in pentane, 5.1 mmol; 3.0 mL) was added dropwise under powerful stirring. After five minutes thf (3 mL) was added dropwise. The colour of the solution changes to yellow. After one minute acidic acid (1.3 mL) was added fast. The solution was stirred a further minute. At the end of the reaction 25 mL of water was added under intensive stirring.

After completion of the reaction 20 mL of ethyl acetate was added. The two phases were separated and the aqueous phase was extracted again 3 times with ethyl acetate. The combined organic phases were dried over MgSO₄ and the solvent was evaporated after filtration.

Data according to reference ⁹⁹.

Crystallisation from CH₂Cl₂ and petrol ether, yield: 92 %.

$[\alpha]_D^{21} = -58.6^\circ$ ($c = 1.0$; CHCl₃).

4. Experimental Data

4.2 Synthesis and Analytic Data

^1H NMR (500 MHz, chloroform-*d*) δ = 7.75 (m, 1H; arom. H), 7.68 (m, 2H; arom. H), 7.44 (m, 4H; arom. H), 7.06 (m, 1H; arom. H), 6.93 (m, 1H; arom. H), 6.44 (dq, J = 394.6 Hz, J = 6.8 Hz, 1H; PH), 3.84 (s, 3H; OCH₃), 1.08 (br q, 3H; BH₃).

^{13}C NMR (126 MHz, chloroform-*d*) δ = 160.63 (CO), 135.00 (d, J = 13.6 Hz; CH), 133.96 (d, J = 2.2 Hz; CH), 132.89 (d, J = 9.7 Hz; 2xCH), 131.18 (d, J = 2.6 Hz; CH), 128.77 (d, J = 10.5 Hz; 2xCH), 126.91 (d, J = 58.8 Hz; CP), 121.44 (d, J = 12.2 Hz; CH), 114.58 (d, J = 55.9 Hz; CP), 110.87 (d, J = 4.2 Hz; CH), 55.85(OCH₃).

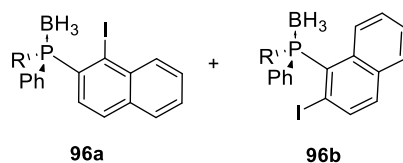
^{31}P NMR (202 MHz, chloroform-*d*) δ = -16.49 (d, J = 67.5 Hz).

MS (EI, 70 eV) m/z : 230 (5, [M]⁺), 229 (36, [M-H]⁺), 216 (100, [M-BH₃]⁺), 215 (11, [M-BH₃-H]⁺), 201 (1, [M-BH₃-Me]⁺).

HRMS (ESI) [M-H]⁺: m/z calculated C₁₃H₁₅BOP 229.09481, determined 229.09483; [M+Na]⁺: m/z calculated C₁₃H₁₆BOP+Na 253.09240, determined 253.09219.

HPLC: purity 95%ee; column: lux (5 μ m) Cellulose-1 (250x4.6 mm), hexane/*i*PrOH 98/2, 1.00 ml/min, t_R = 10.9 min (*R*)-enantiomer and 11.6 min (*S*)-enantiomer.

Synthesis of (Iodonaphthalene-2-yl)(2-methoxyphenyl)(phenyl)phosphine P-borane complex (96)



Compound **94** (2.1 mmol) was dissolved in thf (5 mL) and cooled down to -78 °C. Then, *n*butyl lithium (2.1 mmol, 1.05 mL, 2.0 M in cyclohexane) was added dropwise to the solution. Afterwards, the solution was stirred for 1 h at -78 °C. Compound **91** (2.9 mmol; 1.11 g) was dissolved in thf (3 mL) and added dropwise to the lithiated phosphine. After one hour stirring at -78 °C, water (5 mL) was added and the mixture was allowed to warm up until room temperature. Now the phases were separated and the aqueous phase was extracted with DCM (3x25mL). The combined organic phases were dried (MgSO₄), filtrated and evaporated under vacuum. Due to the fact, that parts of **96** lose their borane group during the reaction, the next step (deprotection of the phosphine **96**) was started without further purification.

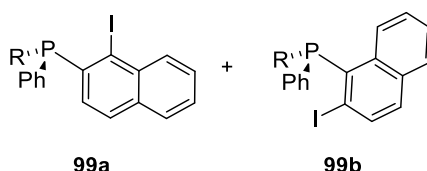
(1-Iodonaphthalene-2-yl)(2-methoxyphenyl)(phenyl)phosphine P-borane complex (96a)

^{31}P NMR (202 MHz, chloroform-*d*) δ 15.5.

(2-Iodonaphthalene-2-yl)(2-methoxyphenyl)(phenyl)phosphine P-borane complex (96b)

^{31}P NMR (202 MHz, chloroform-*d*) δ 18.6.

Synthesis of (Iodonaphthalene-2-yl)(2-methoxyphenyl)(phenyl)phosphine (99)



Compound **96** (2.0 mmol) and DABCO (3.0 mmol; 0.34 g) were dissolved in toluene and stirred for 20 h at room temperature. Then the solvent was evaporated under vacuum and the excess of DABCO and its borane adduct were separated from the phosphine **99** by column chromatography.

Both regioisomers **99** were hard to separate. This was why the next step (oxidation of the phosphine **99**) was started without further separation.

Column chromatography with Petrolether/DCM 2/1

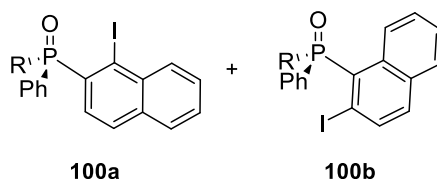
(1-Iodonaphthalene-2-yl)(2-methoxyphenyl)(phenyl)phosphine P-borane complex (96a)

^{31}P NMR (202 MHz, chloroform-*d*) δ 2.3.

(2-Iodonaphthalene-2-yl)(2-methoxyphenyl)(phenyl)phosphine P-borane complex (96b)

^{31}P NMR (202 MHz, chloroform-*d*) δ 12.9.

Synthesis of (Iodonaphthalene-2-yl)(2-methoxyphenyl)(phenyl)phosphine oxide (100)



Compound **99** (1.0 mmol) was dissolved in acetone (15 mL) and 1.5 equivalents H_2O_2 (30 % in H_2O ; 0.17 g) were added slowly. The mixture was stirred for 20 h before the acetone was evaporated under vacuum. The remaining residue was extracted with DCM (3x25mL). The organic phases were dried (Na_2SO_4), filtrated and evaporated. The regioisomers **100a,b** were separated by column chromatography.

(*R*)-(1-Iodonaphthalene-2-yl)(2-methoxyphenyl)(phenyl)phosphine oxide (100a)

Column chromatography with ethyl acetate, yield: 47 % (over all yield from secondary phosphine **94**: 23 %).

M. p.: 128.8 °C; brown solid.

^1H NMR (500 MHz, chloroform-*d*) δ 8.07 (m, 1H; arom. H), 7.68 (m, 1H; arom. H), 7.51 (m, 2H; arom. H), 7.43 (m, 2H; arom. H), 7.24 (m, 3H; arom. H), 7.12 (m, 2H; arom. H), 6.99 (m, 1H; arom. H), 6.81 (m, 1H; arom. H), 6.59 (m, 1H; arom. H), 3.14 (s, 3H; OCH_3).

^{13}C NMR (126 MHz, chloroform-*d*) δ 160.50 (d, $J = 3.3$ Hz; CO), 136.13 (d, $J = 110.2$ Hz; CP), 135.57 (d, $J = 6.7$ Hz; CH), 135.36 (d, $J = 10.8$ Hz; CC), 134.72 (d, $J = 2.4$ Hz; CC), 134.35 (d, $J = 2.1$ Hz; CH), 133.85, 132.70 (d, $J = 109.5$ Hz; CP), 132.52 (d, $J = 10.1$ Hz; 2xCH), 131.58 (d, $J = 2.8$ Hz; CH), 130.34 (d, $J = 13.5$ Hz; CH), 128.49 (CH), 128.35 (d, $J = 7.5$ Hz; 2xCH), 128.26 (d, $J = 12.7$ Hz; 2xCH), 128.07 (d, $J = 12.3$ Hz; CH), 121.43 (d, $J = 11.8$ Hz; CH), 120.46 (d, $J = 106.2$ Hz; CP), 111.49 (d, $J = 6.6$ Hz; CH), 107.79 (d, $J = 6.2$ Hz; CI), 55.36 (OCH_3).

^{31}P NMR (202 MHz, chloroform-*d*) δ 32.79.

MS (EI, 70 eV) m/z : 484 (43, $[\text{M}]^+$), 483 (60, $[\text{M}-\text{H}]^+$), 453 (100, $[\text{M}-\text{OMe}]^+$), 357 (46, $[\text{M}-\text{I}]^+$), 326 (13, $[\text{M}-\text{OMe}-\text{I}]^+$).

4. Experimental Data

4.2 Synthesis and Analytic Data

FTMS (ESI) $[M+H]^+$: m/z calculated $C_{23}H_{18}IO_2P+H$ 485.01619, determined 485.01632; $[M+Na]^+$: m/z calculated $C_{23}H_{18}IO_2P+Na$ 506.99813, determined 506.99722.

HPLC: purity >83%ee; column: lux (5 μ m) Cellulose-1 (250x4.6 mm), hexane/*i*PrOH 80/20, 1.00 ml/min, t_R = 11.1 min (*S*)-enantiomer and 14.6 min (*R*)-enantiomer.

In analogy, the opposite enantiomer was synthesised from oxazaphospholidine **14** with (+)-ephedrine.

HPLC: purity >86%ee; column: lux (5 μ m) Cellulose-1 (250x4.6 mm), hexane/*i*PrOH 80/20, 1.00 ml/min, t_R = 11.1 min (*S*)-enantiomer and 14.6 min (*R*)-enantiomer.

(*R*)-(2-Iodonaphthalene-2-yl)(2-methoxyphenyl)(phenyl)phosphine oxide (100b)

Column chromatography with ethyl acetate, yield: 7 % (over all yield from secondary phosphine **94**: 3 %).

M. p.: 131.5 °C; brown solid.

1H NMR (500 MHz, chloroform-*d*) δ 8.70 (m, 1H; arom. H), 8.04 (m, 1H; arom. H), 7.84 (m, 2H; arom. H), 7.78 (m, 1H; arom. H), 7.64 (m, 1H; arom. H), 7.51 (m, 3H; arom. H), 7.43 (m, 3H; arom. H), 7.26 (m, 1H; arom. H), 7.04 (m, 1H; arom. H), 6.84 (m, 1H; arom. H), 3.45 (s, 3H; OCH₃).

^{13}C NMR (126 MHz, chloroform-*d*) δ 161.31 (d, J = 2.4 Hz; CO), 139.58 (d, J = 10.8 Hz; CH), 136.45 (d, J = 8.7 Hz; CC), 134.27 (d, J = 4.5 Hz; CH), 134.23 (d, J = 1.9 Hz; CH), 133.59 (d, J = 107.2 Hz; CP), 133.21 (d, J = 8.2 Hz; CC), 132.72 (d, J = 2.9 Hz; CH), 132.60 (d, J = 10.2 Hz; 2xCH), 132.36 (d, J = 106.3 Hz; CP), 131.81 (d, J = 2.8 Hz; CH), 128.53 (CH), 128.50 (d, J = 12.7 Hz; 2xCH), 127.46 (d, J = 5.4 Hz; CH), 126.51 (d, J = 4.2 Hz; 2xCH), 123.00 (d, J = 107.6 Hz; CP), 121.29 (d, J = 12.6 Hz; CH), 111.56 (d, J = 6.5 Hz; CH), 100.12 (d, J = 6.0 Hz; CI), 55.60 (OCH₃).

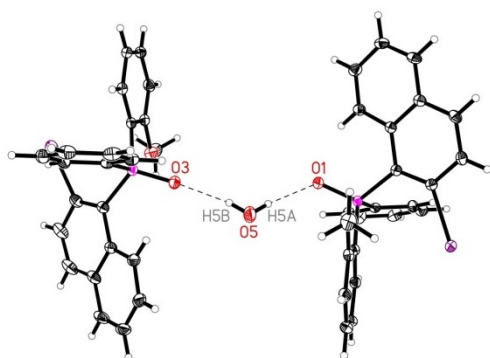
^{31}P NMR (202 MHz, chloroform-*d*) δ 31.83.

4. Experimental Data

4.2 Synthesis and Analytic Data

MS (EI, 70 eV) m/z : 484 (6, $[M]^+$), 483 (5, $[M-H]^+$), 453 (1, $[M-OMe]^+$), 357 (100, $[M-I]^+$), 326 (13, $[M-OMe-I]^+$).

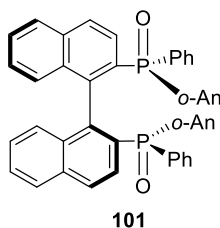
HRMS (ESI) $[M+H]^+$: m/z calculated $C_{23}H_{18}IO_2P+H$ 485.01619, determined 485.01589; $[M+Na]^+$: m/z calculated $C_{23}H_{18}IO_2P+Na$ 506.99813, determined 506.99755.



Both molecules of the asymmetric unit of **100b** together with co-crystallised solvent (H_2O) showing intermolecular O-H...O hydrogen bonds as dashed lines (O5-H5A...O1: O5...O1 2.776(5) Å, O5-H5A...O1 163(5)°; O5-H5B...O3: O5...O3 2.783(5) Å, O5-H5B...O3 167(5)°). Displacement ellipsoids correspond to 30 % probability.

Chemical formula	$C_{46}H_{38}I_2O_5P_2$
Formula weight	986.50
Crystal system	triclinic
Space group	$P1$
a [Å]	12.0298(5)
b [Å]	13.3673(5)
c [Å]	14.1899(6)
α [deg]	105.3268(10)
β [deg]	110.8027(10)
γ [deg]	100.9758(10)
V [Å ³]	1952.26(14)
Wavelength [Å]	0.71073
T [K]	150(2)
Z	2
μ [mm ⁻¹]	1.741
Calculated density [g·cm ⁻³]	1.678
Reflections collected	71321
Independent reflections	7678
Parameters	506
R_{int}	0.0345
R_1 ($I > 2\sigma(I)$)	0.0294
wR_2 (all data)	0.0720
Goodness-of-fit on F^2	1.032

Synthesis of (1*R*,1'*R*)-[1,1'-Binaphthalene]-2,2'-diyl-di((2-anisyl)(phenyl)phosphine oxide) (101)



Compound **100a** (0.6 mmol, 0.28 g) and activated Cu-powder (1.8 mmol; 0.11 g) were placed into a Schlenk-tube. After DMF was added the suspension was heated up to 140 °C for four hours. Then the mixture was allowed to cool down before the solvent was evaporated under vacuum. The residue was treated with boiling DCM and the organic phases were separated by filtration from the insoluble material. The organic phases were combined and washed with saturated NH₄CL-solution and dried (MgSO₄). After filtration the solvent was evaporated under vacuum and the pure product **101**, could be obtain by crystallisation (DCM/AcOEt).

Crystallisation from DCM/ethyl acetate.

Decomposition temperature: 281 °C; colourless crystals.

$[\alpha]_D^{21} = -179.1^\circ$ (c = 1.0; CHCl₃).

¹H NMR (300 MHz, chloroform-*d*) δ 7.81 (m, 4H; arom. H), 7.67 (m, 2H; arom. H), 7.35 (m, 16H; arom. H), 7.07 (m, 4H; arom. H), 6.67 (m, 4H), 3.37 (s, 6H; 2xOCH₃).

¹³C NMR (75 MHz, chloroform-*d*) δ 161.72 (d, J = 2.1 Hz; 2xCO), 143.43 (d, J = 106.19 Hz; 2xCP), 136.73 (d, J = 10.0 Hz; 2xCH), 134.65 (d, J = 11.8 Hz; 2xCC), 133.76 (d, J = 2.3 Hz; 2xCC), 133.44 (2xCH), 130.88 (d, J = 9.4 Hz; 4xCH), 130.31 (d, J = 2.9 Hz; 2xCH), 128.14 (d, J = 117.9 Hz; 2xCP), 127.83 (d, J = 12.35 Hz; 2xCH), 127.81 (d, J = 12.72 Hz; 2xCH), 127.57 (d, J = 2.8 Hz ; 4xCH), 127.08 (d, J = 12.62 Hz, 2xCH), 127.06 (2xCH), 125.78 (2xCH), 120.93 (d, J = 100.74 Hz; 2xCP), 120.12 (d, J = 12.6 Hz; 2xCH), 110.46 (d, J = 6.1 Hz; 2xCH), 55.09 (2xOCH₃).

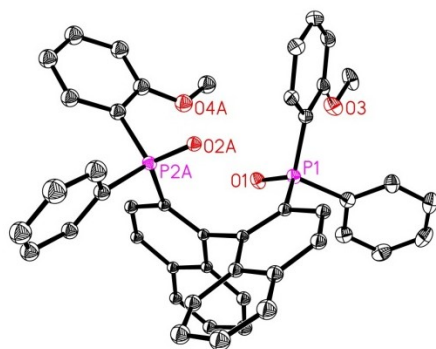
³¹P NMR (122 MHz, chloroform-*d*) δ 26.52.

MS (EI, 70 eV) *m/z*: 714 (1, [M]⁺), 713 (1, [M-H]⁺), 483 (99, [M-P(O)(C₆H₅)(C₆H₄OCH₃)]⁺).

4. Experimental Data

4.2 Synthesis and Analytic Data

HRMS (ESI) $[M+H]^+$: m/z calculated $C_{46}H_{36}IO_4P_2+H$ 715.21616, determined 715.21565;
 $[M+Na]^+$: m/z calculated $C_{46}H_{36}IO_4P_2+Na$ 737.19810, determined 737.19745.



Molecular structure of **101** in the solid state. Displacement ellipsoids correspond to 30 % probability. Large parts of the molecule were disordered over two sites with occupancies of 0.554(6): 0.446(6). Lower occupancy sites and hydrogen atoms were omitted for clarity.

Chemical formula	$C_{46}H_{36}O_4P_2$
Formula weight	714.69
Crystal system	orthorhombic
Space group	$XPP2_12_12_1$
a [Å]	9.7304(5)
b [Å]	10.5685(5)
c [Å]	35.7215(17)
α [deg]	90
β [deg]	90
γ [deg]	90
V [Å ³]	3673.4(3)
Wavelength [Å]	1.54178
T [K]	130(2)
Z	4
μ [mm ⁻¹]	1.430
Calculated density [g·cm ⁻³]	1.292
Reflections collected	29391
Independent reflections	6488
Parameters	397
R_{int}	0.0275
R_1 ($I > 2\sigma(I)$)	0.0500
wR_2 (all data)	0.1303
Goodness-of-fit on F^2	1.033
Flack parameter	0.021(5)

5. Abbreviations

Word abbreviations

add.	additive
arom.	aromatic
aq.	aqueous
br q	broad quartet
- <i>d</i>	deuterated
e. g.	for example
EI	electron ionisation
ESI	electro spray ionisation
et al.	and further
eq.	equivalents
GC	gas chromatography
G	gaseous
HPLC	high performance liquid chromatography
HRMS	high resolution mass spectrometry
inv.	inversion
L	ligand
Mp.	melting point
MS	mass spectrometry
<i>n</i>	linear
NMR	nuclear magnetic resonance
rac-	racemic
r. t.	room temperature
<i>s</i>	secondary
<i>t</i>	tertiary
quant.	quantitative
wt	weight

Chemicals and Elements

acac	acetyl acetate
AcOEt	ethyl acetate
Ar	aryl
BH ₃ *SMe ₂	dimethylsulfide-borane complex
BINAP	2,2'-di(diphenylphosphino)-1,1'-binaphthyl
BuLi	butyl lithium
CAMP	<i>o</i> -anisylcyclohexylmethylphenylphosphine
cod	1,5-cyclooctadiene
CPME	Cyclopentyl methyl ether
Cy	cyclohexane
DABCO	1,4-diazabicyclo[2.2.2]octane
dba	dibenzylideneacetone
DBF	dibenzofuran
DCM	dichloro methane

5. Abbreviations

Units and Symbols

DIOP	O-isopropyliden-2,3-dihydroxy-1,4-di(diphenylphosphino)-butane
DIPAMP	di(<i>o</i> -anisylmethylphenylphosphine)
DMF	dimethylformamide
DMX	9,9-dimethylxanthene
DPE	diphenylether
dppb	1,4-di(diphenylphosphino)butane
dppe	di(diphenylphosphino)ethane
E	electrophile
Et	ethyl
HMDS	hexamethyldisiloxane
<i>i</i> Pr	isopropyl
LDA	Lithium diisopropylamide
Me	methyl
<i>m</i> -	<i>meta</i>
<i>m</i> -CPBA	<i>meta</i> -chloroperoxybenzoic acid
<i>o</i> -	<i>ortho</i>
<i>o</i> -An	<i>ortho</i> -anisyl
<i>p</i> -	<i>para</i>
PAMP	<i>o</i> -anisylmethylphenylphosphine
Ph	phenyl
PMHS	polymethylhydrosiloxan
Pr	propyl
R	rest
Sp	sparteine
<i>t</i> Bu	tertiary butyl group
Tf	triflate
TBSOTf	<i>t</i> butyldimethylsilyl triflate
thf	tetrahydrofuran
TMEDA	N,N,N',N'-tetramethylethylenediamine
X	halogene

Units and Symbols

δ	chemical shift in ppm
αD	rotation angle
eV	electron volt
°	degree
°C	degree Celsius
G	gram
H	hour
Hz	Hertz
J	coupling constant
m/z	mass charge ratio
MHz	Megahertz
M	metre
μ L	microlitre
mbar	millibar
mg/L	milligram per litre

5. Abbreviations

Units and Symbols

mL	millilitre
mm	millimetre
mmol	millimol
min	minutes
mol	mol
M	molar
Nm	nanometre
Ppm	parts per million
%	percent
% ee	percent enantiomeric excess

6. References

- [1] W. S. Knowles, M. J. Sabacky, *Chem. Commun.* **1968**, 1445-1446.
- [2] L. Horner, H. Siegel, H. Büthe, *Angew. Chem.* **1968**, 24, 1034-1035.
- [3] T. P. Dang, H. B. Kagan, *Chem. Commun.* **1971**, 481.
- [4] W. Strohmeier, F.-J. Müller, *Chem. Ber.* **1967**, 100, 2812-2821.
- [5] C. A. Tolman, *J. Am. Chem. Soc.* **1970**, 92, 2953-2955.
- [6] C. A. Tolman, *Chem. Rev.* **1977**, 77, 313-348.
- [7] a) C. A. Tolman, *J. Am. Chem. Soc.* **1970**, 92, 2956-2965; b) D. White, N. J. Coville, *Adv. Organomet. Chem.* **1994**, 36, 95.
- [8] C. P. Casey, G. T. Whiteker, *Isr. J. Chem.* **1990**, 30, 299-304.
- [9] P. C. Kamer, P. W. N. M. van Leeuwen, J. N. H. Reek, *Acc. Chem. Res.* **2001**, 34, 895-904.
- [10] C. P. Casey, G. T. Whiteker, M. G. Melville, L. M. Petrovich, J. A. Gavney, Jr., D. R. Powell, *J. Am. Chem. Soc.* **1992**, 114, 5535-5543.
- [11] C. D. Montgomery, *J. Chem. Educ.* **2013**, 90, 661-664.
- [12] C. C. Levin, *J. Am. Chem. Soc.* **1975**, 97, 5649-5655.
- [13] J. N. Murrell, S. F. Kettle, J. M. Tedder, *Valence Theory*, 2nd ed. Wiley, New York, N.Y., 1970, p 59.
- [14] R. D. Baechler, K. Mislow, *J. Am. Chem. Soc.* **1970**, 92, 3090-3093.
- [15] J. Holz, H. Jiao, M. Gandelman, A. Börner, *Eur. J. Org. Chem.* **2018**, 2984-2994.
- [16] a) W. Egan, K. Mislow, *J. Am. Chem. Soc.* **1971**, 93, 1805-1806; b) W. A. Egan, R. Tang, G. Zon, K. Mislow, *J. Am. Chem. Soc.* **1971**, 93, 6205-6216; c) W. A. Egan, R. Tang, G. Zon, K. Mislow, *J. Am. Chem. Soc.* **1970**, 92, 1442-1444; d) M. Widhalm, L. Brecker, K. Mereiter, *Tetrahedron: Asymmetry* **2006**, 17, 1355-1369.

- [17] R. T. Boéré, A. M. Bond, S. Cronin, N. W. Duffy, P. Hazendonk, J. D. Masuda, K. Pollard, T. L. Roemmele, P. Trana and Y. Zhang, *New J. Chem.* **2008**, 32, 214-231.
- [18] C. A. Jolly, F. Chan and D. S. Marynick, *Chem. Phys. Lett.* **1990**, 174, 320-324; S. Rizzo, T. Benincori, V. Bonometti, R. Cirilli, P. R. Mussini, M. Pierini, T. Pilati and F. Sannicoló, *Chem. Eur. J.* **2013**, 19, 182-194.
- [19] For reviews on *P*-chirogenic phosphines compare: a) K. M. Pietrusiewicz, M. Zablocka, *Chem. Rev.* **1994**, 94, 1375-1411; b) T. Imamoto, Synthesis of *P*-stereogenic Phosphines via Enantioselective Alkylation, In *Phosphorus Ligands in Asymmetric Catalysis*, A. Börner (Ed.), Wiley-VCH, 2008, pp 1201-1210; c) C. Darcel, J. Uziel, S. Jugé, Synthesis of *P*-stereogenic phosphorus compounds based on chiral amino alcohols as chiral auxiliary, In *Phosphorus Ligands in Asymmetric Catalysis*, A. Börner (Ed.), Wiley-VCH, 2008, pp 1211-1233; d) A. Grabulosa, *P-Stereogenic Ligands in Enantioselective Catalysis*, RSC Publishing, Cambridge, 2011; e) M. Dutarte, J. Bayardon, S. Jugé, *Chem. Rev.* **2016**, 45, 5771-5794.
- [20] a) L. Horner, *Pure Appl. Chem.* **1964**, 9, 225-244; b) D. B. Denney, J. W. Hanifin, *Tetrahedron Lett.* **1963**, 4, 2177-2180; c) Y. Hamada, F. Maturuta, M. Oku, K. Hatano, T. Shiori, *Tetrahedron Lett.* **1997**, 38, 8961-8964; d) S. Matsukawa, H. Sugama, T. Imamoto, *Tetrahedron Lett.* **2000**, 41, 6461-6465.
- [21] K. M. Pietrusiewicz, M. Zablocka, *Chem. Rev.* **1994**, 94, 1375-1411.
- [22] a) L. Horner, H. Winkler, *Tetrahedron Lett.* **1964**, 5, 455-460; b) J. A. MacKay, E. Vedejs, *J. Org. Chem.* **2006**, 71, 498-503.
- [23] G. Zon, K. E. DeBruin, K. Neumann, K. Mislow, *J. Am. Chem. Soc.* **1969**, 91, 7023-7027.
- [24] T. Imamoto, T. Hoshiki, T. Onozawa, T. Kusumoto, K. Sato, *J. Am. Chem. Soc.* **1990**, 112, 5244-5252.
- [25] S. Jugé, M. Stephan, J. A. Laffitte, J. P. Genêt, *Tetrahedron Lett.* **1990**, 31, 6357-6360.
- [26] T. Imamoto, K. Sugito, Y. Yoshida, *J. Am. Chem. Soc.* **2005**, 127, 11934-11935.
- [27] a) H. Heath, B. Wolfe, T. Livinghouse, S. K. Bae, *Synthesis* **2001**, 2341-2347; b) K. Katagiri, H. Danjo, K. Yamaguchi, T. Imamoto, *Tetrahedron* **2005**, 61, 4701-4707.

- [28] A. Grabulosa, G. Muller, J. I. Ordinas, A. Mezzetti, M. A. Maestro, M. Font-Bardia, X. Solans, *Organometallics* **2005**, *24*, 4961-4973.
- [29] S. Yamago, M. Yanagawa, H. Mukai, E. Nakamura, *Tetrahedron* **1996**, *52*, 5091-5102.
- [30] J. Meisenheimer, L. Lichtenstadt, *Ber. Dtsch. Chem. Ges.* **1911**, *44*, 356-359.
- [31] M. Stankevič, K. M. Pietrusiewicz, *J. Org. Chem.* **2007**, *72*, 816-822.
- [32] a) O. Korpiun, K. Mislow, *J. Am. Chem. Soc.* **1967**, *89*, 4784-4786; b) R. A. Lewis, O. Korpiun, K. Mislow, *J. Am. Chem. Soc.* **1967**, *89*, 4786-4787; c) O. Korpiun, R. A. Lewis, J. Chickos, K. Mislow, *J. Am. Chem. Soc.* **1968**, *90*, 4842-4846.
- [33] A. Nudelman, D. J. Cram, *J. Am. Chem. Soc.* **1968**, *90*, 3869-3870.
- [34] W. S. Knowles, M. J. Sabacky, DE 2123063, **1971**.
- [35] W. S. Knowles, M. J. Sabacky, B. D. Vineyard, *J. Chem. Soc., Chem. Commun.* **1972**, 10-11.
- [36] W. S. Knowles, *Angew. Chem. Int. Ed.* **2002**, *41*, 1998-2007.
- [37] W. S. Knowles, M. J. Sabacky, B. D. Vineyard, D. J. Weinkauff, *J. Am. Chem. Soc.* **1975**, *97*, 2567-2568.
- [38] a) T. H. Chan, *Chem. Comm.* 1968, 895-896, b) A. Grabulosa, J. Granell, G. Muller, *Coord. Chem. Rev.* **2007**, *251*, 25-90.
- [39] B. Wolfe and T. Livinghouse, *J. Am. Chem. Soc.* **1998**, *120*, 5116-5117.
- [40] P. Beak, D. R. Anderson, M. D. Curtis, J. M. Laumer, D. J. Pippel, G. A. Weisenburger, *Acc. Chem. Res.* **2000**, *33*, 715-727
- [41] S. Jugé, M. Stephan, R. Merdès, J. P. Genet, S. Halut-Desportes, *J. Chem. Soc., Chem. Commun.* **1993**, 531-533.
- [42] E. B. Kaloun, R. Merdès, J. P. Genêt, J. Uziel, S. Jugé, *J. Organomet. Chem.* **1997**, *529*, 455-463.

- [43] D. Moulin, S. Bago, C. Bauduin, C. Darcel, S. Jugé, *Tetrahedron: Asymmetry* **2000**, *11*, 3939-3956.
- [44] C. Bauduin, D. Moulin, E. B. Kaloun, C. Darcel, S. Jugé, *J. Org. Chem.* **2003**, *68*, 4293-4301.
- [45] S. Jugé, J. Bayardon, E. Rémond, H. Lauréano, J.-C. Henry, F. Leroux, F. Colobert, WO 2013/007724 A1, **2013**.
- [46] S. Jugé, J. P. Genêt, *Tetrahedron Lett.* **1989**, *30*, 2783-2786.
- [47] E. J. Corey, Z. Chen, G. J. Tanoury, *J. Am. Chem. Soc.* **1993**, *115*, 11000-11001.
- [48] B. D. Vineyard, W. S. Knowles, M. J. Sabacky, G. L. Bachman, D. J. Weinkauff, *J. Am. Chem. Soc.* **1977**, *99*, 5946-5952.
- [49] O. Korpiun, R. A. Lewis, J. Chickos, K. Mislow, *J. Am. Chem. Soc.* **1968**, *90*, 4842-4846.
- [50] T. Imamoto, T. Kusumoto, N. Suzuki, K. Sato, *J. Am. Chem. Soc.* **1985**, *107*, 5301-5303.
- [51] A. R. Muci, K. R. Campos, D. A. Evans, *J. Am. Chem. Soc.* **1995**, *117*, 9075-9076.
- [52] Y. Yamanoi, T. Imamoto, *J. Org. Chem.* **1999**, *64*, 2988-2989.
- [53] K. Nagata, S. Matsukawa, T. Imamoto, *J. Org. Chem.* **2000**, *65*, 4185-4188.
- [54] A. Ohashi, T. Imamoto, *Tetrahedron Lett.* **2001**, *42*, 1099-1101.
- [55] For reviews on chiral ferrocenylphosphines compare: a) C. J. Richards, A. J. Locke, *Tetrahedron: Asymmetry* **1998**, *9*, 2377-2407; b) T. J. Colacot, *Chem. Rev.* **2003**, *103*, 3101-3118; c) L.-X. Dai, T. Tu, S.-L. You, W.-P. Deng, X.-L. Hou, *Acc. Chem. Res.* **2003**, *36*, 659-667; d) P. Barbaro, C. Bianchini, G. Giambastiani, S. L. Parisel, *Coord. Chem. Rev.* **2004**, *248*, 2131-2150.
- [56] A. Togni, C. Breutel, M. C. Soares, N. Zanetti, T. Gerfin, *Inorg. Chim. Acta* **1994**, *222*, 213-224.
- [57] M. Lotz, K. Polborn, P. Knochel, *Angew. Chem., Int. Ed.* **2002**, *41*, 4708-4711.
- [58] J. J. A. Perea, A. Börner, P. Knochel, *Tetrahedron Lett.* **1998**, *39*, 8073-8076.

- [59] T. Sturm, W. Weissensteiner, F. Spindler, *Adv. Synth. Catal.* **2003**, *345*, 160-164.
- [60] M. Sawamura, H. Hamashima, M. Sugawara, R. Kuwano, Y. Ito, *Organometallics* **1995**, *14*, 4549-4558.
- [61] N. W. Boaz, S. D. Debenham, E. B. Mackenzie, S. E. Large, *Org. Lett.* **2002**, *4*, 2421-2424.
- [62] I. R. Butler, W. R. Cullen, S. J. Rettig, *Organometallics* **1986**, *5*, 1320-1328.
- [63] C. Gambs, G. Consiglio, A. Togni, *Helv. Chim. Acta* **2001**, *84*, 3105-3126.
- [64] K. Mikami, K. Aikawa, Y. Yusa, J. J. Jodry, M. Yamanaka, *Synlett* **2002**, *10*, 1561-1578.
- [65] T. Hamada, S. L. Buchwald, *Org. Lett.* **2002**, *4*, 999-1001.
- [66] M. Cereghetti, W. Arnold, E. A. Broger, A. Rageot, *Tetrahedron Letters* **1996**, *37*, 5347-5350.
- [67] W. J. Tang, W. M. Wang, Y. X. Chi, X. M. Zhang, *Angew. Chem. Int. Ed.* **2003**, *42*, 3509-3511.
- [68] M. Rubio, S. Vargas, A. Suárez, E. Álvarez, A. Pizzano, *Chem. Eur. J.* **2007**, *13*, 1821-1833.
- [69] M. Rubio, A. Suárez, E. Álvarez, C. Bianchini, W. Oberhauser, M. Peruzzini, A. Pizzano, *Organometallics* **2007**, *26*, 6428-6436.
- [70] E. Rafter, J. Muldoon, H. M. Bunz, D. G. Gilheany, *Tetrahedron: Asymmetry* **2011**, *22*, 1680-1686.
- [71] K. Dziuba, A. Flis, A. Szmigielska, K. M. Pietrusiewicz, *Tetrahedron: Asymmetry* **2010**, *21*, 1401-1405.
- [72] J. Jia, Z. Ling, Z. Zhang, K. Tamura, I. D. Gridnev, T. Imamoto, W. Zhang, *Adv. Synth. Catal.* **2018**, *360*, 738 –743.
- [73] J. Holz, S. Doerfelt, A. Börner, *Adv. Synt. Catal.* **2017**, *359*, 4379-4387.
- [74] In *Synthese von neuen P-chiralen Bis(triarylphosphin)-Liganden*, K. Rumpel, Universität Rostock, Master Thesis 2015.

- [75] a) A. Börner, J. Holz, K. Rumpel, WO2017/191310 A1, **2017**; b) J. Holz, K. Rumpel, A. Spannenberg, R. Paciello, H. Jiao, A. Börner, *ACS Catal.* **2017**, 7, 6162-6169.
- [76] Unpublished results.
- [77] A. M. Johns, M. Utsunomiya, C. D. Incarvito, J.F. Hartwig *J. Am. Chem. Soc.* **2006**, 128, 1828-1839; F. M. Miloserdov, C. L. McMullin, M. M. Belmonte, J. Benet-Buchholz, V. I. Bakmutov, S.A. Macgregor, V.V. Grushin, *Organometallics* **2014**, 33, 736-752; H. Yu, G. Zhang, H. Huang, *Angew. Chem., Int. Ed.* **2015**, 54, 10912-10916.
- [78] E. M. Vogl, J. Bruckmann, M. Kessler, C. Krüger, M. W. Haenel, *Chem. Ber.* **2006**, 130, 1315-1319.
- [79] S.-M. Kuang, P. E. Fanwick, R. A. Walton, *Inorg. Chem.* **2002**, 41, 405-412.
- [80] M. A. Esteruelas, N. Honczek, M. Oliván, E. Oñate, M. Valencia, *Organometallics*, **2011**, 30, 2468-2471.
- [81] A. R. Browne, N. Deligonul, B. L. Anderson, A. L. Rheingold, T. G. Gray, *Chem. Eur. J.* **2014**, 20, 17552-17564.
- [82] M. Xie, C. Han, J. Zhang, G. Xie, H. Xu, *Chem. Mater.* **2017**, 29, 6606-6610.
- [83] T. Imamoto, T. Oshiki, T. Onozawa, T. Kusumoto, K. Sato, *J. Am. Chem. Soc.* **1990**, 112, 5244-5252.
- [84] A. Miyashita, A. Yasuda, H. Takaya, K. Toriumi, T. Ito, T. Souchi, R. Noyori, *J. Am. Chem. Soc.* **1980**, 102, 7932-7934.
- [85] B. Schäfer, *Chem. Unserer Zeit* **2013**, 47, 174-182.
- [86] M. M. S. Stephan, D. Sýterk, B. Modéc, B. Mohar, *J. Org. Chem* **2007**, 72, 8010-8018.
- [87] T. Imamoto, K. Hirose, H. Amano, *Main Group Chemistry* **1996**, 1, 331-338.
- [88] a) D. Peña, A. Cobas, D. Pérez, E. Guitián, *Synthesis* **2002**, 10, 1454-1458; b) D. Rodríguez-Lojo, A. Cobas, D. Peña, D. Pérez, E. Guitián, *Org. Lett.* **2012**, 14, 1363-1365.
- [89] J. Bayardon, H. Laureano, V. Diemer, M. Dutartre, U. Das, Y. Rousselin, J.-C. Henry, F. Colobert, F. R. Leroux, S. Jugé, *J. Org. Chem.* **2012**, 77, 5759-5769.

- [90] S. Sowa, M. Stankevič, A. Szmigielska, H. Małuszyńska, A. E. Koziół, K. M. Pietrusiewicz *J. Org. Chem.* **2015**, *80*, 1672-1688.
- [91] J. A. Buonomo, C. G. Eiden, C. C. Aldrich, *Chem. Eur. J.* **2017**, *23*, 14434-14438.
- [92] S. S. Al Sulaimi, K. V. Rajendran, D. G. Gilheany, *Eur. J. Org. Chem.* **2015**, 5959-5965.
- [93] T. Coumbe, N. J. Lawrence, F. Muhammad, *Tetrahedron Lett.* **1994**, *35*, 625-628.
- [94] Y. Hamada, F. Matsuura, M. Oku, K. Hatano, T. Shioiri, *Tetrahedron Lett.* **1997**, *38*, 8961-8964.
- [95] G. M. Sheldrick, *Acta Cryst.* **2008**, *A64*, 112-122.
- [96] G. M. Sheldrick, *Acta Cryst.* **2015**, *C71*, 3-8.
- [97] E. B. Schwartz, C. B. Knobler, D. J. Cram, *J. Am. Chem. Soc.* **1992**, *114*, 10775-10784.
- [98] A. L. Spek, *Acta Cryst.* **2015**, *C71*, 9-18.
- [99] Mohamad Jahjah, Rabih Jahjah, Stéphane Pellet-Rostaing, Marc Lemaire, *Tetrahedron: Asymmetry* **2007**, *18*, 1224-1232.